Titre: Title:	Development of Amino Functionalized Graphene Based Polymer Nanofibers for Gas Sensors
Auteur: Author:	Hanan Abdali
Date:	2019
Type:	Mémoire ou thèse / Dissertation or Thesis
Référence: Citation:	Abdali, H. (2019). Development of Amino Functionalized Graphene Based Polymer Nanofibers for Gas Sensors [Thèse de doctorat, Polytechnique Montréal]. PolyPublie. https://publications.polymtl.ca/4110/

POLYTECHNIQUE MONTRÉAL

affiliée à l'Université de Montréal

Development of Amino Functionalized Graphene based Polymer Nanofibers for Gas Sensors

HANAN ABDALI

Département de génie chimique

Thèse présentée en vue de l'obtention du diplôme de *Philosophiae Doctor*

Génie chimique

Novembre 2019

POLYTECHNIQUE MONTRÉAL

affiliée à l'Université de Montréal

Cette thèse intitulée :

Development of Amino Functionalized Graphene based Polymer Nanofibers for Gas Sensors

présentée par **Hanan ABDALI**

en vue de l'obtention du diplôme de *Philosophiae Doctor*

a été dûment acceptée par le jury d'examen constitué de :

Olivier HENRY, président

Abdellah AJJI, membre et directeur de recherche

Ebrahim JALALI DIL, membre

Hani NAGUIB, membre externe

DEDICATION

To God, my beloved parents, brothers, and my beloved husband.

ACKNOWLEDGEMENTS

I would like to express my gratitude to all my colleagues that have become friends and have made my academic life enjoyable and exciting.

I am deeply indebted to my supervisor, Professor Abdellah Ajji, for his support and guidance. His encouragement as an advisor has provided me with the best possible environment in which to work, and the benefit of his insight during my research has been invaluable.

Additionally, I would like to present my thanks to the rest of my thesis committee, namely Professor Olivier Henry, Doctor Ebrahim Jalali Dil and Professor Hani Naguib for accepting the evaluation of my thesis.

Consequently, I would also like to further recognise the efforts of the technical and administrative staff of the Chemical Engineering Department at Polytechnique de Montréal for their help during the course of the experimental work, especially to Claire Cerclé, Matthieu Gauthier, Richard Silverwood, Redouane Boutrouka, Mélina Hamdine, Martine Lamarche, Gino Robin, Anic Desforges, and Sebastien Chenard.

Also, special thanks to the Bentolhoda Heli for her help, advice, and suggestions especially during my research concerning gas detection. I would like to offer my utmost thanks to Fatma Dhieb for her aid in translating my abstract into French.

I further take this opportunity to acknowledge all those who have been part of the electrospinning group meetings, in particular for their advice, suggestions and questions. I sincerely appreciate their input which has been of considerable value and has often served to align the direction of my own research.

A special thanks to my dear friends and colleagues Shiva, Hoda, Hajer, Mounia, Nusrat, Fatma, Nury and Zohreh, whom I have cherished great regard and value in their continued friendship and support in my endeavours.

I am especially grateful to my best friends, Safi Samir and Shatha Mokhtar for their unconditional support, patience and encouragement during my time here in Montreal. I would also like to thank Nicole Sanmuganathan for all her help in developing my articles and thesis and for her patient advice. I warmly acknowledge all my friends and relatives especially Norah Al-Ahmadi, Ohoud Al-Oudah and Afnan Shaikh in Saudi Arabia for their unfailing support and encouragement.

My warm and sincere thanks to my father, Salah Abdali, my mother, Maryam Abdali, my husband Fahad Al-Dossri and all my brothers for their endless encouragement, inspiration and loving support throughout my life. A special word of gratitude to my brother, Murad Abdali, without whom I could not have kept the necessary energy and motivation to complete my postgraduate studies so far away from home. I am indebted to his unceasing love, support and patience.

Finally, I would also like to thank the Saudi Bureau and the Saudi government for without their financial support and endorsement, none of this would have been possible.

بِسْمِ اللَّهِ الرَّحْمَنِ الرَّحِيمِ

In the name of Allah, the Entirely Merciful, the Especially Merciful

(اقْرَأْ بِاسْمِ رَبِّكَ الَّذِي خَلَقَ * خَلَقَ الْإِنْسَانَ مِنْ عَلَقٍ * اقْرَأْ وَرَبُّكَ الْأَكْرَمُ * الَّذِي عَلَّمَ بِالْقَلَمِ * عَلَّمَ الْإِنْسَانَ مَا لَمْ يَعْلَمْ)

(Recite in the name of your Lord who created * Created man from a clinging substance * Recite, and your Lord is the most Generous * Who taught by the pen * Taught man that which he knew not)

[العلق: 1 - 5]

[Al-Alaq:1-5]

((اللَّهُمَّ انْفَعْنِي بِمَا عَلَّمْتَنِي، وَعَلِّمْنِي مَا يَنْفَعُنِي، وَزِدْنِي عِلْمًا))

((O Allah, benefit me by that which You have taught me, and teach me that which will benefit me, and increase me in knowledge))

RÉSUMÉ

Ces dernières années, la préparation d'architectures nanostructurées a été une stratégie importante pour améliorer les performances de détection de gaz. Ces matériaux ont un rapport surface / volume extrêmement élevé et ont des structures avec une nanoporosité élevée, ce qui augmente l'adsorption des gaz. Parmi ces nanomatériaux, le graphène fonctionnalisé a suscité un intérêt considérable pour l'application en détection du fait de sa conductivité variable, ce qui le rend disponible pour les phénomènes de transport d'électrons à très grande mobilité électrique en présence de gaz oxydants et réducteurs. De plus, la polyaniline (PANI) est facilement synthétisée et la structure de sa chaîne moléculaire peut être modifiée de manière pratique par copolymérisation ou dérivations structurelles. Grace à ses propriétés électriques, électrochimiques et optiques uniques, elle peut également être utilisée comme détecteur efficace pour la surveillance de composés organiques et inorganiques.

Les travaux de recherche actuels portent sur la conception et la fabrication du capteur à température ambiante en utilisant du graphène fonctionnalisé avec de la polyaniline en tant que matériaux actifs de détection pour détecter les gaz toxiques tels que le dioxyde de carbone (CO2). La première phase consiste à identifier et à détailler les matériaux primaires et les facteurs du processus nécessaires à la production du graphène amino-fonctionnalité (AmG), puis à étudier la morphologie et la microstructure de l'AmG, ainsi qu'à caractériser la morphologie et les propriétés des composites nanofibres de l'AmG / PANI / Poly (méthacrylate de méthyle) (PMMA). Les résultats des analyses par spectroscopie infrarouge à transformée de Fourier (FTIR), par spectroscopie photoélectronique à rayons X (XPS) et par spectroscopie Raman ont confirmé la fonctionnalisation réussie du graphène avec des groupements amino, tandis que l'observation par microscopie électronique à transmission (TEM) a montré que l'ajout de groupements fonctionnels amino au graphène a moins endommagé la structure graphitique du graphène. Ensuite, les nanofibres AmG / PANI ont été produites en utilisant le procédé d'électrofilage. Les micrographies du microscope électronique à balayage (MEB) ont montré la formation de nanofibres AmG / PANI / PMMA avec un diamètre compris entre 35 et 133 nm, et une épaisseur générale uniforme le long des nanofibres. Ces résultats sont prometteurs pour l'utilisation directe d'AmG et de PANI dans de nombreuses applications telles que les capteurs, les électroniques flexibles, etc.

La deuxième phase décrit la fabrication et la caractérisation des composites de nanofibres AmG / PANI par polymérisation *in situ*, et l'efficacité de ces nanocomposites de nanofibres polymérisés en tant que nouveau matériau pour la détection du gaz CO_2. Par conséquent, la deuxième phase comprend deux stratégies pour concevoir des capteurs de CO_2 à température ambiante et légers basés sur des nanocomposites de nanofibres AmG / PANI. 1) Les surfaces des nanofibres électrofilées de PMMA ont été traitées à la température ambiante par un rayonnement ultraviolet (UV) et ensuite, l'AmG / PANI a été synthétisé par une polymérisation oxydative chimique à la surface des nanofibres de PMMA. Les composites de nanofibres AmG / PANI ont présenté une bonne réponse de résistance électrique au CO_2 à la température ambiante par rapport aux composites de nanofibres PANI / PMMA. En outre, les composites de nanofibres AmG / PANI ont révélé des propriétés de détection du CO_2 améliorées telles qu'une sensibilité élevée (20 ppm) et un temps de réponse plus court (10s), ainsi qu'une bonne stabilité. 2) Le cellulose bactérienne réticulée -amino graphène / polyaniline CLBC-AmG / PANI a été synthétisé par interaction covalente du AmG et du BC via une estérification d'une seule étape, puis le monomère d'aniline a été placé à la surface du CLBC-AmG par polymérisation chimique *in situ*. Le CLBC-AmG a montré un rapport d'intensité I_D / I_G (1.1) supérieur à celui de l'AmG (0.97), ce qui est attribué aux nanofibres de BC intercalées entre les feuilles d'AmG, entrainant une augmentation du désordre dans les feuilles de graphène. De plus, le capteur de CO_2 basé sur le CLBC-AmG / PANI a montré une meilleure flexibilité, une sélectivité élevée et une détection précise des concentrations de CO_2 comprises entre 50 et 2000 ppm. Cet intervalle de concentration couvre suffisamment le besoin de détection du CO_2 pour de nombreuses applications environnementales et industrielles.

ABSTRACT

In recent years, the preparation of nanostructured architectures has been an important strategy for improving gas sensing performance. These materials have an extremely high surface-to-volume ratio and high nanoporous structures, which increases the adsorption of gases. Among these nanomaterials, functionalized graphene has generated considerable interest in sensing applications owing to its variable conductivity, which makes it available for electron transport phenomena with very high electrical mobility in the presence of oxidizing and reducing gases. Additionally, polyaniline (PANI) is easily synthesized and its molecular chain structure can be modified conveniently by copolymerization or structural derivations. Due to its unique electrical, electrochemical, and optical properties, it can also be utilized as efficient sensors for monitoring organic and inorganic compounds.

The current research work focuses on the design and fabrication of the room temperature sensor by using functionalized graphene with polyaniline as sensing active materials to detect toxic gases such as carbon dioxide (CO_2). The first phase focuses on identifying and detailing the primary materials and process factors necessary to produce amino-functionalized graphene (AmG) and then investigating the morphology and microstructure of the AmG, as well as characterizing the morphology and properties of the AmG/PANI/Poly(methyl methacrylate) (PMMA) nanofiber composites. The fourier transform infrared spectroscopy (FTIR), X-ray photoelectron spectroscopy (XPS) and Raman spectroscopy analysis results confirmed the successful functionalization of the graphene with amino groups, while the transmission electron microscopy (TEM) observation demonstrated that the addition of amino-functional groups to graphene generated less damage to the graphitic structure of the graphene. Then, the AmG/PANI nanofibers were produced by using the electrospinning process. The scanning electron microscope (SEM) micrographs showed the formation of AmG/PANI/PMMA nanofibers with a diameter ranging between 35 and 133 nm, with a general uniform thickness along the nanofibers. These results are promising for the direct use of AmG and PANI in many applications such as sensors, flexible electronics, etc.

The second phase describes the fabrication and characterization of AmG/PANI nanofiber composites by *in situ* polymerization, and the efficiency of these polymerized nanofiber nanocomposites as a new material for sensing CO_2 gas. Consequently, the second phase involved two strategies to design lightweight, room temperature CO_2 sensors based on AmG/PANI

nanofiber nanocomposites. 1) The surfaces of the PMMA electrospun nanofibers were treated at room temperature by ultraviolet (UV) radiation and then the AmG/PANI was synthesized by a chemical oxidative polymerization on the surface of the PMMA nanofibers. The AmG/PANI nanofiber composites displayed a good electrical resistance response to CO_2 at room temperature compared with the PANI/PMMA nanofiber composites. In addition, the AmG/PANI nanofiber composites revealed enhanced CO_2 sensing properties such as high sensitivity (20 ppm) and faster response time (10s) along with good stability. 2) The cross-linked bacterial cellulose-amino graphene/polyaniline CLBC-AmG/PANI was synthesized by covalent interaction of AmG and BC via one step esterification and then the aniline monomer was grown on the surface of CLBC-AmG through *in situ* chemical polymerization. The CLBC-AmG exhibited a higher I_D/I_G intensity ratio (1.1) than the AmG (0.97), which is ascribed to BC nanofibers intercalating between the AmG sheets which resulted in increased disorder in the graphene sheets. Moreover, the CO_2 sensor based on the CLBC-AmG/PANI showed superior flexibility, high selectivity, and accurate detection of CO_2 concentrations ranging from 50 to 2000 ppm. This concentration range sufficiently covers the need for CO_2 detection for many environmental and industrial applications.

TABLE OF CONTENTS

LIST OF TABLES

LIST OF FIGURES

LIST OF SYMBOLS AND ABBREVIATIONS

AmG	Amino functionalized graphene
APS	Ammonium persulfate
Al_2O_3	Aluminum oxide
BC	Bacterial cellulose
CLBC-AmG	Cross linked bacterial cellulose/amino functionalized graphene
CO_2	Carbon dioxide
CO	Carbon monoxide
CNT	Carbon nanotube
°C	Degrees celsius
$CHCL_3$	Chloroform
DMF	*N*,*N* dimethylformamide
DI	Deionized water
DCC	N,N′-Dicyclohexylcarbodiimide
EDA	Ethylenediamine
FTIR	Fourier transform infrared spectroscopy
G	Graphene
GO	Graphene oxide
HCSA	Camphor-10-sulfonic acid
H_2	Hydrogen

min	Minutes
mm	Millimeter
MFC	Mass flow controllers
Mw	Molecular weight
NH_3	Ammonia
NBA	π-conjugated amine
nm	Nanometer
PANI	Polyaniline
PMMA	Poly(methyl methacrylate)
ppm	Part per million
PS	Polystyrene
PEI	Polyethylenimine
rGO	Reduced graphene oxide
$R_{air\ or\ N_2}$	The initial resistance in air or nitrogen
R_g	The resistances after exposing to targt gas
RT	Room temperature
RH	Relative humidity
S	Sensitivity
SAED	Electron diffraction patterns

SSA	5-Sulfosalicylic acid dihydrate
SEM	Scanning electron microscope
sec	Seconds
Sb_2O_3	Antimony oxide
TEM	Transmission electron microscopy
TGA	Thermogravimetric analysis
UV	Ultraviolet -radiation
UV–Vis	Ultraviolet visible spectrophotometer
XPS	X-ray photoelectron spectroscopic
ZnO	Zinc oxide

LIST OF APPENDICES

CHAPTER 1 INTRODUCTION

During the last fifty years, many studies have established various branches of gas sensing technology. However, most of the research focused on three main areas in sensing technology; the investigation of different kinds of sensors, research about sensing principles, and fabrication techniques [1-5]. Nevertheless, available gas sensor technologies have limitations such as difficulties in fabrication, operation only at high temperatures, poor performance in humid environments, degradation under ultraviolet irradiation, low selectivity, limited sensitivity, and high costs [1-5].

Air pollution is a worldwide concern, and it is acknowledged that carbon dioxide (CO_2) in the atmosphere contributes to the process of global warming, so, it is of vital interest to monitor CO_2 levels in the atmosphere [6]. CO_2 is a colorless, odorless, non-flammable gas that is a product of cellular respiration and the combustion of fossil fuels as it is considered one of the main greenhouse gases[6, 7]. CO_2 sensors are widely required for use in many environmental and industrial fields. The average CO_2 content outdoors is 400 ppm, but in some cities such as Los Angeles, the average increases up to 600 ppm. In order to reduce CO_2 emissions, it is necessary to reduce the energy consumption in buildings. Another application is the detection and monitoring of CO_2 concentrations in the food industry [6, 7]. Consequently, numerous CO_2 sensors have been proposed for detecting and monitoring the concentration of CO_2. In general, CO_2 detection shows a high sensitivity and a wide measurement range (see Table 1-1) [8-10], but the high operational temperatures of some of these sensors make the lifetime of the sensor shorter. Other problems are their poor performance regarding the stability and selectivity [11].

Since the most common gas sensing principle is the adsorption and desorption of gas molecules on sensing materials, it is evident that the sensitivity can be significantly enhanced by increasing the contact interfaces between the analytes and sensing materials [12, 13]. Therefore, the extremely high surface-to-volume ratio and hollow structure of nano-materials is ideal for the adsorption and storage of gas molecules. Gas sensors based on graphene show a high sensitivity to gas detection which has sparked considerable interest in the use of graphene [14-16]. However, many studies have reported that functionalization is the best way to achieve the best sensor performance from graphene. Functionalization gives two main features to graphene: (1) it increases its sensitivity to

the adsorption process and, (2) it decreases nonspecific binding and enhances selectivity for the desired analyte [17, 18].

Table 1-1 Carbon dioxide gas sensor based on different principles

Principle	**CO_2 Concentration range ppm**	**Temperature °C**	**Limitation**
$BaTiO_3$–CuO thin films [6].	500-5000	300	Operating at high temperature
Graphene/Sb_2O_3 QDs composite film [10].	1-50	194	Operating at high temperature and no selectivity
rGO [14].	350-1500	RT	Poor selectivity
PEI blended with polyelectrolytes [19].	400- 2000	RT	Long response and recovery times
LaOCl-functionalized SnO_2 nanowires [20].	450-4000	300	Operating at high temperature and poor selectivity at RT
Graphene/Al_2O_3 QDs composite [21].	1-200	124.85	Poor repeatability in the results

Barium titanate ($BaTiO_3$), Copper oxide (CuO), Quantum dots (QDs), Antimony oxide (Sb_2O_3), Polyethylenimine (PEI), Polyaniline (PANI), reduced graphene oxide (rGO), Tin dioxide (stannic oxide) (SnO_2), Titanium oxide (TIO_2), Aluminum oxide (Al_2O_3).

The present research aims at developing a novel room temperature gas sensing system with functionalized graphene/polyaniline nanofiber sensor for a rapid, sensitive, selective, reproducible, stable and cost-effective detection of CO_2 gas at low concentrations. The choice in using functionalized graphene for sensing applications is due to its variable conductivity, which makes it available for electron transport phenomena with very high electrical mobility in the presence of oxidizing and reducing gases [13]. In this research we combined functionalized graphene with polyaniline as the conducting materials are good candidates for sensor matrices, with the advantages of low cost, easy preparation and ready modulation of sensing properties by varying

their chemical structure. It is possible to increase the sensitivity and recovery of the sensor by *in situ* polymerization of the functionalized graphene/PANI onto the surface of flexible nanofibers substrates of poly(methyl methacrylate) (PMMA) and bacterial cellulose (BC). Moreover, these nanofiber mats also possess distinct advantages such as an extremely high surface area to volume ratio and porosity, which are extremely desirable properties in sensor applications [22].

This thesis consists of the following chapters: Chapter 2 provides a literature review on the related topics investigated in this research, Chapter 3, discusses the originality and main objectives of this thesis, the summary and organization of the articles are described in Chapter 4, the main contributions of this work are established in three scientific articles in Chapters 5, 6 and 7. The work in Chapter 5 characterizes and describes the primary materials and process factors needed to produce amino functionalized graphene (AmG). The morphology and microstructure of AmG are studied, in addition to investigating the morphology and properties of the AmG/PANI/PMMA nanofiber composites. The subsequent Chapters 6 and 7 consists of two articles concerning the development of a new type of a room-temperature (RT) CO_2 gas sensor based on an AmG/PANI nanofiber composite. Additionally, Chapter 6 contains the results of the second article which investigates AmG/PANI/PMMA electrospun nanofiber composites by in situ polymerization. The sensing characteristics of the nanofiber composites for various concentrations of CO_2 gas at RT were evaluated. In Chapter 7 the results of the third article explore the properties of a CO_2 gas sensor developed from CLBC-AmG/PANI nanofiber composites by in situ polymerization. The sensing performance of the CLBC-AmG/PANI and BC/PANI was examined at RT. Moreover, the efficiency of AmG/PANI/PMMA electrospun nanofibers was compared with that of CLBC-AmG/PANI nanofibers as credible sensing materials for detecting CO_2 gas.

The general discussion of the aforementioned articles is described in Chapter 8, followed by Chapter 9 which, discusses the conclusions and recommendations for future work based on this thesis. Finally, a book chapter of functionalized graphene/polymer nanofiber composites and their functional applications is included as an appendix (Appendix A) in this thesis.

CHAPTER 2 LITERATURE REVIEW

2.1 Nanotechnology in Sensing application

Sensor science and technology can be divided into three categories according to the type of technology applied, namely electrochemical, optical and others (ex. piezoelectric, pyroelectric and Field-Effect Transistors (FET)-based sensors) [23]. Optical and electrochemical are two types of technologies frequently used in Gas/chemical and bio sensors. Optical sensors are essentially based on the principle of a spectral transmission analysis, which examines the optical absorption properties of the target [5, 24]. However, optical sensors are easily vulnerable to physical damage and interference from environmental effects. They can be costly, often suffering from poor sensitivity when coupled with radioimmunoassay, have difficulty in adapting factors such as the short half-life of radioactive agents, present with concerns of health hazards and disposal problems [24, 25]. Conversely, electrochemical sensors enable rapid responses, are highly sensitive, simple, economic and free of the aforementioned problems [24, 25]. The electrochemical sensors utilize the fluctuations either in current, potential, conductivity, or capacitance in the testing sample triggered due to the interaction between the sensing element and analyte [24]. The sensors could either be amperometric from measurement of current, potentiometric from measurement of potential, or chemoresistive from measurement of resistance. It has been widely researched that sensors that are chemoresistive or electrochemical, function based on the change in electrical resistance of the sensing material in the presence of a target because of their important characteristics for example; sensitivity, cost effectiveness, simple sensing mechanism and easy integration [26, 27]. Chemoresistive sensor design is based on five key elements [28]: sensitivity, selectivity, response time, recovery time, and stability. The sensitivity refers to the minimum value of target or volume concentration needed for detection; the response of the sensor can be related to its sensitivity S shown in Equation (1), where ΔR is the change in electrical resistance [29].

$$S = \Delta R / R_0$$

where ΔR is the change in electrical resistance of the sensor denoted by $R_g - R_0$, R_g is the resistance of the sensor during exposure to the analyte and R_0 is the resistance of the sensor in air [29]. In this equation the response time is the time taken for the resistance in the sensor to change from the

baseline value to 90% of the saturated response during exposure to the analyte. Additionally, the recovery time is defined as the time it takes for the electrical resistance of the sensor to return to 90% of its baseline value after removing the analyte from the environment. Selectivity is the ability of sensors to identify a specific analyte; and stability is the consistency and steadiness of the sensor response after extended and repetitive exposure to the analyte [29].

Advancements in sensor nanotechnology are constant because of their wide use in many areas such as; (1) industrial production (e.g., methane detection in mines) [30]; (2) for medical applications (e.g., electronic noses simulating the human olfactory system) [31, 32]; (3) environmental studies (e.g., greenhouse gas monitoring) [33, 34]; (4) indoor air quality supervision (e.g., detection of carbon monoxide) [35, 36]; (5) the automotive industry (e.g., detection of polluting gases from vehicles) [37, 38]. Accordingly, improving gas sensors with faster response times, higher accuracies, increased sensitivities and other properties is an ongoing field of research [39]. A range of materials for example; semiconducting metal oxides [40-42], conducting polymers [43, 44], and carbon materials [39, 45, 46], have been utilized for developing sensing based on the variation of electrical properties (see Figure 2.1).

Conventional sensing materials for instance metal oxide semiconductors are problematic due to poor sensitivity at room temperature, whereas conducting polymers, in spite of their operations at room temperature, the ease of processing, and their easy incorporation into sensing devices, are limited by the effects of humidity and degradation [42, 44]. There are some carbon-based nanomaterials, namely carbon nanotubes (CNTs), graphene and its derivatives that are more popularly studied due to their unique electronic structures, mechanical, optical, thermal and magnetic properties [45, 47]. Nonetheless, the random network of one dimensional CNTs, the inevitable metallic impurities and the compositional heterogeneity of CNTs have resulted in low reproducibility of electrochemical sensing. The metallic impurities can dominate the electrochemistry of CNT owing to their electrochemical activity. Also, their application is still limited owing to a long recovery time and a complex fabrication process [46].

Graphene is a form of carbon which is one-atom thick, where carbon atoms are arranged regularly in a hexagonal lattice [48]. In view of a unique combination of excellent electrical, optical, chemical and mechanical properties, which remain desirable in developing resistive-type gas sensors, graphene is treated as a promising sensing material by the scientific community [15, 16].

Studies have reported that gas sensors based on graphene, show a high sensitivity to gas detection, which has sparked considerable interest in its use. Consequently, studies have discussed the experimental and theoretical assessment of graphene's performance in gas sensing and the ways adsorbing molecules alter its conductivity.

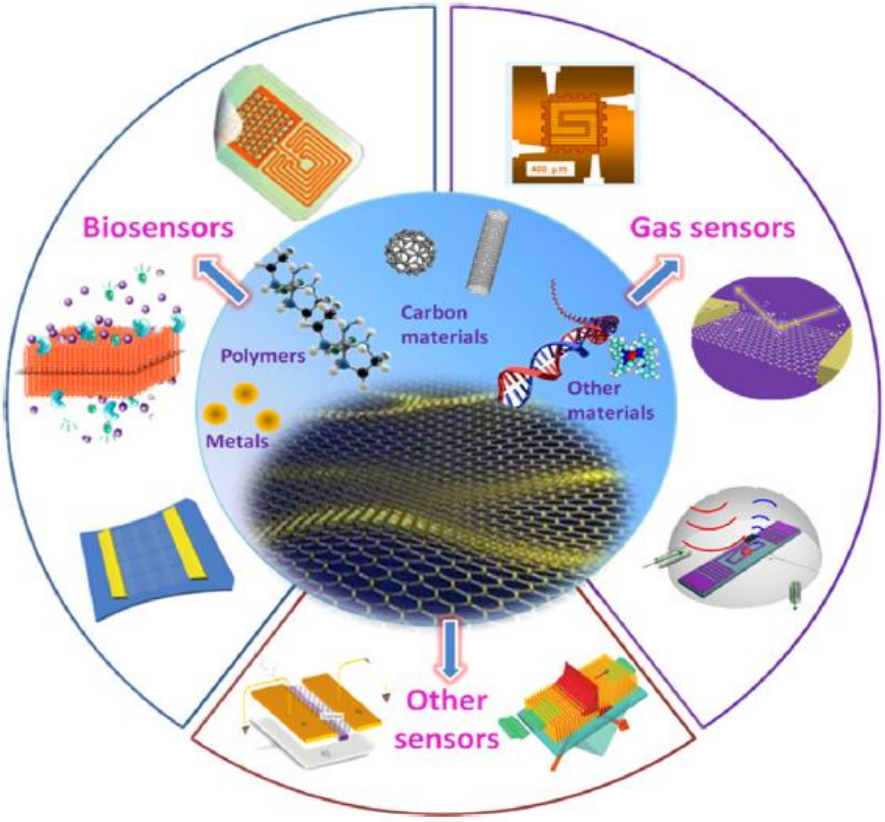

Figure 2-1 Different kinds of materials used for fabricating electrochemical sensors, [Reproduced from ref.28, © 2016 Elsevier B.V. All rights reserved].

2.2 History of Graphene

Graphene, first discovered by Geim and Novoselov [49] in 2004, is a planar monolayer of carbon atoms arranged into a two-dimensional (2D) honeycomb lattice structure with a carbon–carbon bond length of 0.142 nm [49]. Graphene forms the basic structure of carbon-based materials, for example; carbon nanotubes (several graphene sheets rolled up along a vertical axis), graphite (stacked graphene), and fullerene (wrapped up graphene) as shown in Figure 2.2 [48-51]. The discovery of graphene with its combination of extraordinary physical properties (high values of its

Young's modulus ~ 1,100 GPa) [16], fracture strength (130 GPa) [16], thermal conductivity (5,000 W m-1K^{-1}) [52], mobility of charge carriers (200,000 cm^2 V^{-1} s^{-1}) [53], and specific surface area (calculated value ~ 2,630 m^2 g^{-1}) [54]. Moreover, its ability to be dispersed in various polymer matrices has created a new class of polymer nanocomposites that has added a new dimension of research in the fields of physics, chemistry, biotechnology, and material science [55]. As such, graphene and graphene-based nanocomposites play a key role in the future of nanoscience [56]. The promising mechanical, electrical, optical, thermal and magnetic properties of graphene have led to the creation of a new area in nanoscience that studies graphene-based polymer nanocomposites [55, 56].

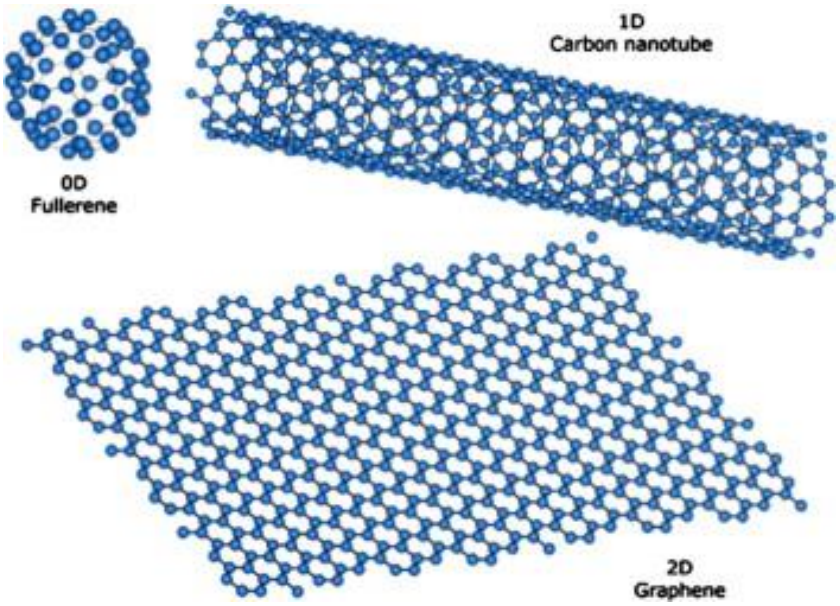

Figure 2-2 a Low-dimensional carbon allotropes: fullerene (0D), carbon nanotube (1D) and graphene (2D). [Reproduced from ref.51, Copyright © 2010 Elsevier Ltd. All rights reserved].

2.2.1 Chemical Functionalization of Graphene

The interest in the scientific community in investigating different aspects particularly in the surface modification (covalent and noncovalent) of graphene for its sensing abilities has been recently revived. The functionalization and dispersion of graphene sheets are critical for their use in

applications. The chemical functionalization of graphene helps in maintaining the inherent characteristics of graphene and prevents the agglomeration of single layer graphene during reduction in the solvent phase [17]. In addition, in order to enhance the sensing capabilities of graphene, it is often necessary to functionalize it with recognition elements that bring the detection targets onto the graphene surface through specific interactions, which also assist in signal transduction increasing sensitivity and selectivity [17]. Graphene may also be functionalized in order to enhance its specificity, loading capacity, biocompatibility, etc.

Graphene oxide (GO) has been utilized broadly as a starting material for producing graphene (material). The surfaces of GO sheets are highly oxygenated, and carboxyl, diol, ketone, epoxide and hydroxyl functional groups can alter the van der Waals interactions significantly and enable greater solubility in water and organic solvents [18, 55, 57]. The presence of additional carbonyl and carboxyl groups located at the edge of the sheets enables GO sheets to be strongly hydrophilic, allowing them to swell readily and disperse in water [57, 58]. Yet, GO is both thermally unstable and electronically insulating as it undergoes pyrolysis at increased temperatures due to the presence of the oxygen functional groups in its structure [18, 59, 60]. Therefore, reducing GO removes almost all of the hydroxyl, carboxylic acid and epoxy functional groups [59, 60]. It has been shown that by reducing GO to graphene it is possible to restore its electrical conductivity and perhaps even its thermal stability [61]. Owing to the defective structure of reduced GO, the electrical properties are not as outstanding as those of pristine graphene though they are still suitable for sensitive gas detection [61, 62]. Moreover, it has also been reported that graphene with a more defective structure shows an improved adsorption of gas molecules [61, 62] .

Reducing agents such as; hydrazine [61, 63], sodium borohydride followed by hydrazine [64], hydroquinone [65], dimethylhydrazine [56] and ascorbic acid [66] etc. can be used to chemically reduce GO to provide an efficient method for fabricating graphene, although, the cost and hazardous nature of these chemicals utilized during reduction could limit its application [67]. Conversely, reducing GO thermally by heating dry GO under inert gas and high temperature [67-70], for example, at 1000 °C for 30 s in an inert environment, results in the reduction and exfoliation of GO generating reduced GO layers. Consequently, the thermal reduction is a lucrative method for producing graphene at a large scale as it chemically modifies graphene layers without the need for dispersion in a solvent compared with other chemical reduction methods [67]. Accordingly, in

this study the thermal reduction of GO followed by chemical modification of reduced GO was used to obtain functionalized graphene.

2.2.1.1 Covalent Functionalization

Covalent techniques are usually used to obtain strong interactions between graphene and the modifier [71]. The covalent modification of graphene is mainly based on the reaction between the functional groups of the molecules and the oxygenated groups on the surfaces of graphene oxide (GO) or reduced GO [72, 73] such as carboxyls on the edges with epoxides and hydroxyls on their basal planes [71]. Therefore, the structural alteration can take place at the end of the sheets and/or on the surface. GO or reduced GO can be grafted onto polymeric chains, that have reactive groups like hydroxyls and amines, for example; poly(ethylene glycol), polylysine, polyallylamine and poly(vinyl alcohol). These materials can be incorporated to attain desired properties from their individual parts. For instance; the polymeric part offers dispersibility in certain solvents, mechanical strengthening, and many morphological properties, while the graphene sheets demonstrate characteristics such as chemical reactivity, electrical conductivity and reinforcement of mechanical properties. Through amide bond formation the amine-terminated PEG can be grafted onto GO [73]. Conversely, PEGylated GO is highly dispersible in water when compared with GO, in various biological solutions such as serum or cell medium. This important characteristic makes PEGylated GO a vital contender for delivering of hydrophobic drugs in biological systems [73]. Recently, chitosan modified with graphene was successfully achieved with microwave irradiation in a N,N-dimethylformamid (DMF) medium [74]. The functionalization occurred through reaction between the carboxyl groups of GO and the amine groups of chitosan, followed by reduction using hydrazine monohydrate. It was suggested that the dispersibility of the GO in aqueous acidic media could be improved by the amidation of GO with chitosan [75, 76]. In subsequent work, Vadukumpully *et al*. [77] reported a basic yet, flexible approach for the covalent modification of graphene with alkylazides, where the alkyl chains combined with various functional groups for instance, hydroxylundecanyl, dodecyl, hexyl and carboxy-undecanyl resulting in improved dispersibility that aided in generating composite fabrication. This technique provided a suitable platform for synthesising functional graphene nanocomposites using gold nanoparticles (the carboxyl groups trapped and immobilized the gold nanoparticles selectively). Moreover, it was discussed that GO could be used as a support for enzyme immobilization for producing biosensing

devices. The immobilization of glucose oxidase (GOx) onto GO was achieved through amide bonding [78].

2.2.1.2 Non-Covalent Functionalization

Non-covalent interactions mainly engage in hydrophobic, van der Waals, electrostatic forces, π-π stacking, and require the physical adsorption of suitable molecules on the graphene surface [17]. This is easier to carry out without altering the chemical structure of the graphene sheets and provides effective means to tailor the electronic/optical property and solubility of the nano-sheets [17]. GO can be modified noncovalently through interaction with polymers, such as; PANI, poly(3-hexylthiophene), poly(sodium 4-styrenesulfonate), porphyrin, pyrene, cellulose derivatives, and porphyrins or even biomolecules such as peptides and deoxyribonucleic acid (DNA), including adsorption of small aromatic molecules or surfactants. Moreover, non-covalent functionalization is a frequently used for the surface modification of carbon-based nanomaterials.

The first example of non-covalent functionalization of reduced GO by the in situ reduction of GO with hydrazine in the presence of poly(sodium 4-styrenesulfonate) was published by Stankovich *et al.* [79] in which the hydrophobic base of poly(sodium 4-styrenesulfonate) stabilized the reduced GO, and the hydrophilic sulfonate side groups control good dispersion of the hybrid sheets in water. Su and lu [80] have successfully functionalized the GO surfaces with ethylenediamine and 1,6-hexanediamine using N-(3-dimethylaminopropyl)-N′-ethylcarbodiimide hydrochloride and N-hydroxysuccinimide as the coupling reagents. In a subsequent study, Su *et al.* [81] reported a novel method to functionalize graphene sheets with pyrene and perylenediimide. A solar cell based on these functionalized graphene sheets revealed elevated conductivity. Moayeri and Ajji [82] have successfully functionalized the graphene via noncovalent π-π interactions with 1-pyrenebutanoic acid succinimidyl ester (G-PBASE). The functionalized G-PBASE nanosheets produced are electrically conductive and have good dispersibility in 5:1 mixture of chloroform/DMF and no sedimentation was observed after 10 days whereas neat graphene sedimented in the same solution. In further research, Xu *et al.* [83] developed a unique and easy 3D self-assembly approach to produce GO/DNA composite hydrogels with excellent environmental stability, increased mechanical strength and a high dye adsorption capacity, coupled with a self-healing function. It was concluded that the multifunctionality of the self-assembled hydrogel could be attributed to the unique structures, properties, and natural self-assembly of the GO and DNA building blocks.

The non-covalent functionalization can be used to retain the natural structure of graphene, yet it is generally remarked that interactions between functionalities and graphene surfaces remain weak and consequently unsuitable for applications demanding strong interactions.

In this study, we discuss producing composite materials based on noncovalent functionalization of graphene with amines. From previous studies, it was then reasoned that functionalizing graphene with amine groups improves the interfacial effects between graphene and polymers including the development of polymer materials for specific applications owing to their improved thermal properties. Moreover, other studies have reported that the primary, secondary and tertiary amine groups are highly efficient in adsorbing the CO_2 gas.

2.3 Preparation of Functionalized Graphene based Polymer Nanofiber Composites

Graphene nanocomposites are becoming increasingly used as electrochemical sensing platforms [84, 85]. However, many factors are responsible for controlling the characteristics and uses of graphene/polymer nanofiber composites such as the type of graphene utilized, its inherent properties, its manner of dispersion in the polymeric matrix, its interfacial interaction and the structure of its network within the matrix [86, 87]. Consequently, functionalizing graphene by either by covalent or noncovalent methods can provide a solution to the aforementioned concerns. Therefore, functionalizing graphene promotes its dispersion in various organic solvents, and this dispersibility is useful for producing graphene sheets, films, fibers composites, etc. An efficient and facile method for grafting various functional groups or polymeric chains onto graphene utilizing nitrene cycloaddition was reported by He and Gao [88]. Functional groups (e.g., hydroxyl, carboxyl, amino, bromine, long alkyl chain, etc.) or polymers (e.g., poly(ethylene glycol), polystyrene) were covalently attached onto the graphene, in a one-step reaction to fabricate single-layered, functionalized graphene with a variety of functional groups [88]. The resulting functionalized graphene was electrically conductive and had good dispersibility and processability in organic solvents advocating their candidacy in various applications of polymer nanofiber composites [89].

The large surface-to-volume ratio, specific surface area, and high porosity of the one dimensional (1D) fibrous nanostructures augments the diffusion and mass transportation of the gaseous species, resulting in better sensing performance compared with flat film [90]. The nanofibers have been studied for employ in several sensor applications owing to their flexibility in materials section and ease of incorporation active agents. The composite nanofibers are prepared using the two main processes of mixing and spinning. The modified graphene sheets are dispersed and combined into the mixing process in three main strategies: melt blending, in situ polymerization, or solution mixing (see Figure 2.3). Generally, three types of spinning methods are used: melt-spinning, wet-spinning and electrospinning.

In the in situ polymerization technique, generally, modified graphene is mixed with prepolymers or monomers then, heat or radiation applied to initiate the polymerization process [91]. This technique provides strong interaction between the functionalized graphene and the polymeric matrix and equally promotes excellent homogeneous dispersion. In this process, for example, Hou *et al*. [92] reported the preparation of functionalized graphene grafted by polyamide 6 by in situ polycondensation of caprolactam (CPL), by applying the melt spinning and drawing technique to fabricate the nanocomposite fibers. It was reported that the mechanical properties of the fibers increased significantly due to the good distribution of functionalized graphene in the polyamide 6 matrix [92].

Solution processing is the most straightforward method in the preparation of polymer nanocomposites. In this technique, functionalized graphene is mixed with a polymer solution after first dispersing in a solvent by using methods such as magnetic agitation, mechanical mixing, or high-energy sonication [86, 93]. The graphene layers can be easily dispersed since they are stacked together by weak forces, if a suitable solvent, for instance acetone, chloroform, tetrahydrofuran (THF), dimethyl formamide (DMF) or toluene, is chosen. However, the specific surface area of the graphene could decrease considerably due to their affinity for re-stacking, aggregation and folding. As a result, surface functionalization of graphene before the solution mixing phase is undertaken to overcome this challenge.

In the melt method, although no solvent is required, the graphene or modified graphene is mixed with the polymer matrix in a molten state. A thermoplastic polymer is mixed mechanically with modified graphene at elevated temperatures using conventional methods, such as extrusion

and injection molding [93, 94]. Chatterjee *et al*. [85] have produced polyamide 12 and graphene composite fibers by melt processing. They investigated the influence of graphene on the structure and mechanical properties of polyamide 12 fibers. It was found that the composite fibers showed improved elasticity, yield and tensile strength, the melt spinning process also revealed that there is a high risk of agglomeration [85].

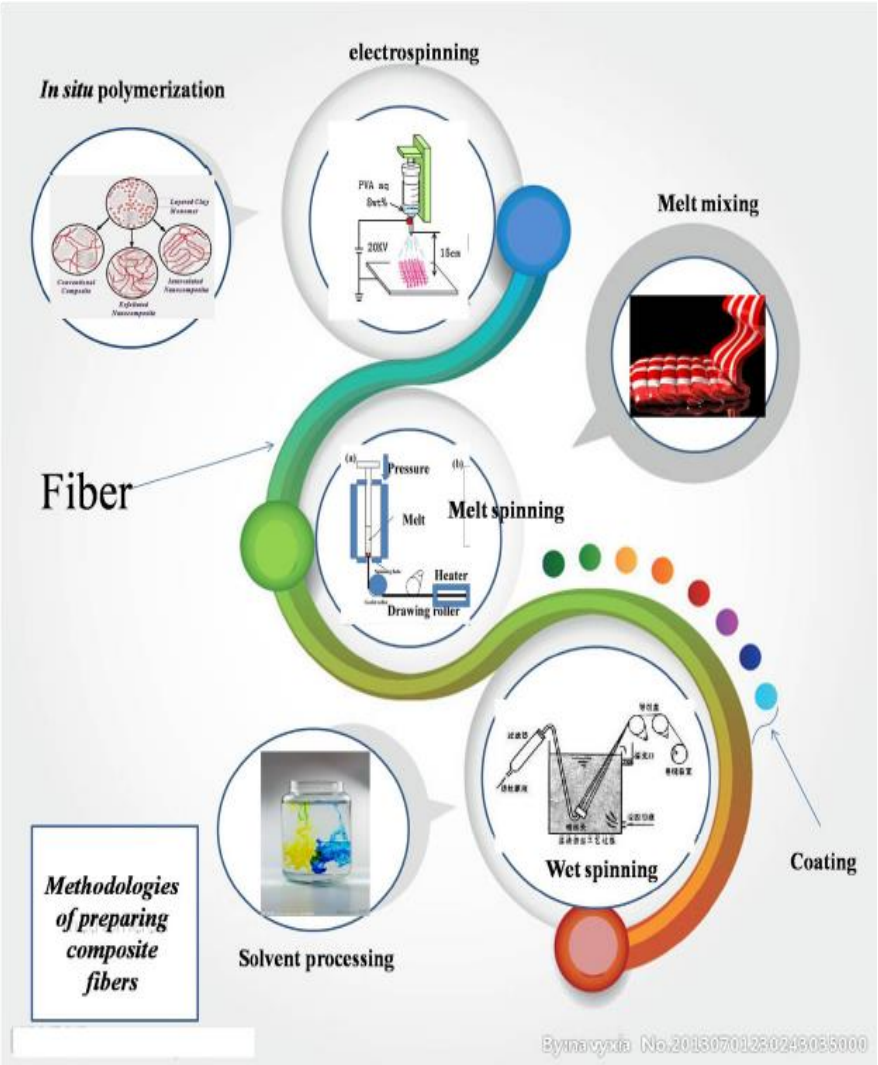

Figure 2-3 Schematic illustration of the methods used for preparation of functionalized graphene-based polymer fiber composite materials [Reproduced from ref.89, © 2016 Elsevier Ltd. All rights reserved].

2.4 Electrospinning

Increased interest in nano-scale technologies and their applications have heightened the use of electrospinning technologies in the last decade. Among methods such as; self-assembly [95], template synthesis [96], phase separation [97] that can be used to fabricated nanofibers, the electrospinning process is a relatively simple, efficient, and low-cost procedure which, can produce ultrafine fibers or fibrous structures of various polymers with diameters ranging from sub-microns to nanometers [22]. The electrospun nanofibers boast excellent properties for example; huge aspect ratios, specific surface areas approximately one to two orders of the magnitude larger than flat films, ability to spin into different shapes and sizes, along with the flexible porosity of the electrospun structure. Electrospinning can be used widely in many fields for sensors, energy storage, filtrations, tissue wound healing, engineering scaffolds, in catalyst and enzyme carriers applications [98]. Sensor performance of sensors designed from electrospun nanofibers is usually even more sensitive than cast film sensors made from the same material [99, 100] .

Technically, electrospinning is a process that applies a strong electric field to draw liquid polymer into fine filaments [101-103]. The electrospinning apparatus is made up of four main components (Figure. 2.4). The first is a high voltage supplier that gives the power used to get the charged polymer solution into a fiber form. The second is a syringe pump needed to control the flow rate of the polymer solution. The third is the needle to disperse the charge on polymer jet. The last one is the collector (usually a grounded conductor) that collects the electrospun fibers. There are several parameters that can affect the electrospinning of nanofibers, and those parameters can be broadly divided into three groups; 1) solution parameters such as viscosity, concentration, and molecular weight, 2) process parameters such as electric potential at the needle, the feed rate for the polymer solution, and the distance between the syringe and the collector screen [194]. 3) ambient parameters such as temperature and humidity , researchers usually keep the ambient conditions constant in their research [102]. Each of the above controlled parameters can influence electrospun fibers with the desired morphologies and diameters. Previous studies have demonstrated that studying the wide range of parameters which can affect the morphology of the final nanofibers that are obtained from the electrospinning process [98, 102]. The effect of these different parameters on fiber morphology and diameters can be summarized as below (Table 2.1).

PMMA is used in a wide range of applications in the field of nanotechnology. Several characteristics favor the selection of PMMA over other polymers available for this study, including high mechanical strength, thermal stability, non-toxicity, solubility in a variety of solvents and good dielectric properties improve the conductivity of the polymer solution obtained making it easy for electrospinning [104]. Many researchers have explored the influence of electrospinning parameters on PMMA nanofiber morphology and diameters [104, 105]. For example, Koysuren and Koysuren [106] studied the effects of polymer concentration and the processing parameters on the morphology and diameter of electrospun PMMA. It was discovered that by increasing the polymer concentration, the solution viscosity increased along with the average fiber diameter [106]. Moreover, by increasing the distance between the needle tip and the collector means that the jet will have a longer distance to travel (a longer flight time for the solution to be stretched) before it is deposited on the collector plate which results in a decrease in the average fiber diameter. Also they investigated the effect of the solvent type on the diameter and shape of the nanofibers. In this report, it was also found that with the same polymer concentration, polymer solutions with different viscosities were obtained [106]. The results showed that the PMMA electrospun mat from DMF solution resulted in thicker fibers when compared with those electrospun from acetone solution [106].

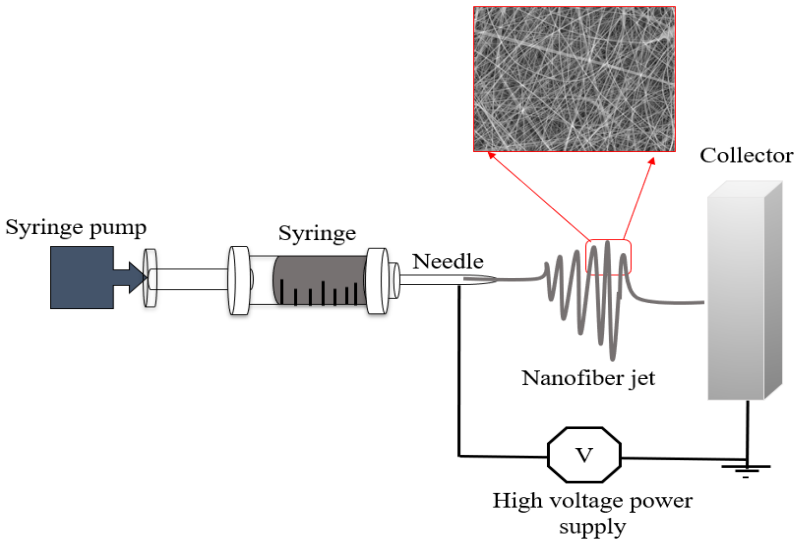

Figure 2-4 Basic electrospinning setup.

Table 2-1 The effect of the electrospinning parameters on fiber morphologies and diameters.

Conditions		Effect on fiber morphology	References
Solution Condition	Viscosity/ Polymer concentration	Very low concentrations or viscosities results in beads and increasing concentration or viscosity reduced the beads. Increase in fiber diameter with increasing concentration or viscosity.	[107-110]
	Surface tension	No conclusive link with fiber morphology, high surface tension results in instability of jets.	[110-112]
	Conductivity	Lower solution conductivity resulted in a larger fiber diameter.	[108, 113]
	Molecular weight of polymer	The amount of beads and droplets reduced with the increase in molecular weight	[114, 115]
Processing Conditions	Applied voltage	Decrease in fiber diameter with increase in voltage. Beaded fibers were generated with too high voltage.	[107, 108]
	Distance between tip and collector	Minimum distance required for uniform fibers. Beaded fibers were produced with very small and very large distance.	[109, 110]
	Flow rate	Decrease in fiber diameter with decrease in flow rate, generated beads with a too high flow rate.	[110, 116]
Ambient Condition	Humidity	High humidity extracted circular pores on the fibers.	[111, 117, 118]
	Temperature	Increase in temperature produced a decrease in solution viscosity, resulting in a smaller in fiber diameter.	[101, 111]

2.5 Bacterial Cellulose

In the field of nanotechnology, there has been a rise in interest to produce sensing materials using cellulose-based substrates [119]. Among the renewable polymers used, cellulose is regarded as the most abundant natural polymer and the initial component of a plant structure. The structure of cellulose is composed molecularly of a long chain of carbohydrates generated by repeating blocks of β-D-glucopyranose molecules that are covalently bound together by β(1→4)-glycosidic bonds [120, 121] (see Figure 2-5). Consequently, obtaining wood pulp has been one of the foremost methods used for extracting cellulose from plants due to the popularity for its final cellulosic products such as paper. Although paper has been used for over centuries due to its myriad advantages in flexibility, compatibility, biodegradability, capillary action, and porous structure, it has also made it an attractive option for the development of advanced diagnostic devices. Nery *et al*. [122] have reported the use of a paper platform for the fabrication of numerous sensing techniques. Interestingly, different types of paper have been developed exploring the sensitive and selective optical (colorimetric and fluorescent-based methods) and electrochemical (voltage, potential and conductivity-based methods) and these have made its mark as a substrate for the fabrication of solid-based diagnostic tools. Although the traditional fabrication of cellulosic material such as paper has its place in the field of science, it is unable to meet the demands in the generating modern cellulosic nanocomposites. Ongoing investigations for the extraction of cellulose in nanoscale structures have led to improvements in the deficiencies of the more traditional methods [123]. In these modern preparation and extraction methods, various forms of nanocellulose (NC) are created resulting in new substrates such as cellulose nanocrystals (CNCs), nanofibrillated cellulose (NFCs) and bacterial cellulose (BC) [124].

BC is an environmentally-friendly, polymeric material, increasingly explored by research in the last few decades. BC is a type of cellulose that can be synthesised by many microorganisms one of which is *Gluconacetobacter xylinum* under controlled culture conditions [124]. It is composed of a continuous ultrafine, three-dimensional (3D) network structure and its fibrils have diameters between 10 and 100 nm, this nanofibrous structure has a highly hydrophilic characteristic due to the many hydroxyl groups on its surface. Additionally, BC has good porosity, high purity, high mechanical properties in the dry state, renewability and excellent biocompatibility when modified,

which has led to its use in many applications such as biomedical applications [125-127], cosmetic applications, packaging materials and nanocomposites [128].

Accordingly, it has been found that BC is a useful supporting material that can be used to deposit nanofillers in order to create advanced BC-based functional nanomaterials for different technological applications. For instance, BC containing silver nanoparticle [129], titanium dioxide [130], platinum nanoparticle [131], zinc oxide [132], and graphene sheets [133], and other composites have been found to have high conductivity which can be used in various potential applications such as electrical instruments, sensors/ biosensors, batteries, proton exchange membranes and display devices. Moreover, BC has been also adopted to fabricate composites with conductive polymers such as PANI and polypyrrole [134, 135]. Yue *et al.* [136] successfully modified BC by carboxymethylation (CM) and then PANI was synthesized on the CM-BC by *in situ* oxidative polymerization to obtain the CM-BC/PANI nanocomposite. The CM-BC/PANI composite membranes showed certain flexibility with good electrical and mechanical properties. In a subsequent study, Carmona *et al.* [137] reported BC/ZnO composite nanofibers were suitable for the detection of nitrogen dioxide (NO_2), acetone and ethanol at room temperature. The sensor showed the best response was obtained for NO_2. Furthermore, the sensor showed a good stability at temperatures higher than room temperature.

In this study, BC was used to fabricate a new generation of CLBC-AmG/PANI gas sensors prepared using BC as a biomaterial substrate and AmG/PANI as a sensing layer with good sensitivity, selectivity, and stability.

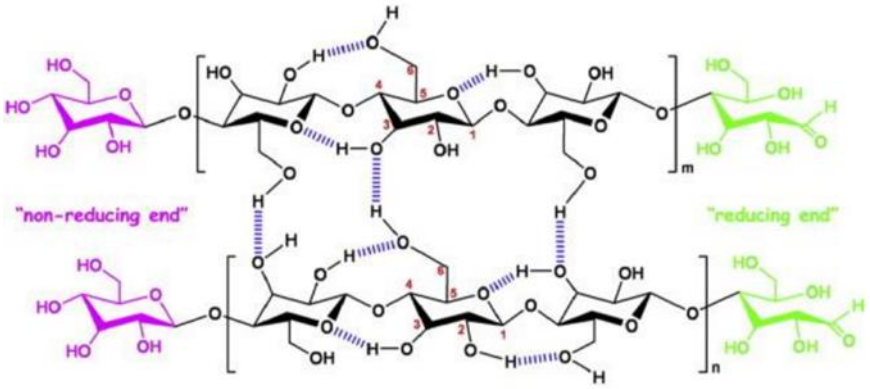

Figure 2-5 A schematic of the chemical structure of cellulose materials [Reproduced from ref.121, © 2014 Published by Elsevier Ltd.]

2.6 Polyaniline (PANI)

Conductive polymer nanofibers have created great interest in research for gas sensing nano technologies due to their structural diversity, flexibility, reversible doping/de-doping process, high surface areas, tunable electrical/electronic properties, easy processing and environmental stability [44, 138]. The electrical conductivity of such polymers is affected by exposure to various organic and inorganic gases. The main chains of these conducting polymers are derived from alternating single and double bonds leading to broad π-electron conjugation. However, it has been noted that they lack inherent selectivity and their conductivity is relatively low ($< 10^{-5}$ S cm^{-1}), where a doping process is necessary in order to achieve better conductivity [138]. Moreover, PANI has attracted great interest, in sensors, energy storage and electrochromic devices, because of its good optical and magnetic properties, low production cost, high environmental stability, and adjustable conductivity that can be controlled by oxidation and protonation states, as well as its ability to be synthesized easily [139].

PANI can be prepared by the oxidation of the monomer aniline through chemical or electrochemical methods [140, 141]. In electrochemical polymerization, the aniline monomer is oxidized by applying an electrical current resulting in a thin layer of the polymer which is deposited on the surface of a conductive electrode [141, 142]. The electrochemical polymerization is limited to conductive substrates such as metals, carbon and conductive oxides. Contrastingly, *in situ* chemical oxidative polymerization, the aniline monomer is oxidized by using ammonium persulfate as the redox initiator which has been effectively used to deposit the conductive PANI on both conductive and nonconductive substrates [141]. Polymerization occurs when the characteristic green color of PANI emeraldine salt becomes visible. Chemical oxidative polymerization offers a simple, quick and effective method for preparing PANI-coated substrates as it bypasses problems in the insolubility of PANI that would require toxic solvents to alter its solubility using methods like dip coating or spin coating.

PANI-based sensors can transform chemical interactions into electrical signals and are able to cover a broad spectrum of applications. Their efficiencies as sensors for monitoring organic and inorganic compounds, such as alcohols, ethers, ammonia (NH_3), or nitrogen, nitric oxide or dioxide (NO)x, hydrogen sulfide (H_2S), sulfur dioxide (SO_2), and CO_2 has been successfully demonstrated. In order to increase its interaction with gas molecules, research has been conducted to modify the

PANI nanostructure or increase inter-chain connections. The use of nano-structured polyaniline (such as nanowires, nanotubes, nanofibers, or nanorods) could greatly improve diffusion, favoring much greater penetration for gas molecules. However, PANI has some limitations such as the lack of specificity or selectivity toward the target species and long-time instability (which may degrade over time, even in dry, oxygen-free environments) which still remain a challenge. Consequently, the combination of PANI with semiconducting metal oxides, CNTs, or graphene has been utilized as highly efficient gas sensors due to their synergetic effects and enhanced capacity for gas detection as illustrated in Table 2.2 [44, 143, 144].

Table 2-2 Summarized research of different PANI-based gas sensors at room temperature

Materials	Gas	Limit detection (ppm)	Reference
PANI	Amines	100	[145]
PANI/HCSA	NH_3	10	[146]
	NO_2	1	
PANI/PMMA	$(C_2H_5)_3N$	20	[147]
PANI/PVP	NO_2	1	[148]
PANI/FeAl	CO	10	[149]
PANI/Fe_2O_3	NH_3	10.7	[150]
PANI/rGO	NH_3	50	[151]
PANI/Au	H_2S	1	[152]
	CH_3SH	1.5	
PANI/TiO_2	NH_3	25 ppt	[153]
PANI/ SWCNTs	NH_3	50	[154]
PANI/CNT	CO	100	[155]

2.7 Summary

As CO_2 is inert, the design of a solid state room temperature sensor with a suitable sensor interface material is still a challenge for the scientific community. Researchers have been working to develop stable, reliable, smaller, faster response, highly selective and cost-effective CO_2 sensors based on the demands of electrochemical technologies. Up to now, various CO_2 sensors have been proposed for detecting and monitoring the concentration of CO_2 where CO_2 detection displays high sensitivity and a wide measurement range. However, the high operational temperatures of these sensors affect their lifetimes and thus require more electricity for their operation. Other challenges include stability and selectivity. Yet, it is universally acknowledged, that performance features such as sensitivity, selectivity, response time, stability, durability, reproducibility and reversibility are greatly influenced by the properties of the sensing materials selected.

The literature presented above highlights the candidacy of functionalized graphene with intrinsic features such as extremely high surface-to-volume ratio and unique optical, electrical, thermal, and mechanical properties for various applications including sensor development. The choice in using functionalized graphene for sensing applications is due to its variable conductivity, which makes it available for electron transport phenomena with very high electrical mobility in the presence of oxidizing and reducing gases [9]. Furthermore, by combining amino functionalized graphene with PANI is a good candidate for CO_2 gas sensing due to its high sensitivity, fast response times and functionality at room temperature. Finally, it is notable that the sensitivity of gas sensors is strongly affected by the specific surface of the sensing materials used so that a higher specific surface of a sensing material leads to higher sensitivity and faster response times. Thereby, using PMMA and BC nanofibers as substrates due to their high surface area, allows for faster diffusion of gas molecules into the structures making them excellent candidates for applications in sensing platforms. This study suggests that combining functionalized graphene with PANI to design an ultrahigh sensor without the limitations present in conventional sensors, coupled with advantages such as low cost, easy preparation and ready modulation of the sensing properties by varying their chemical structure should result in a more efficient sensor.

Hence, the first part of this research identifies and details the primary materials and process factors necessary to produce AmG, then the morphology and the thermal stability of the PANI/PMMA/AmG nanofibers are investigated. The second part of this project focuses on

developing new sensing means for CO_2 gas detection, at room temperature using PMMA and CLBC-AmG nanofibers as substrates in order to grow AmG/PANI and PANI by *in situ* polymerization, respectively. Then, the efficiency of AmG/PANI/PMMA electrospun nanofibers against the CLBC-AmG/PANI nanofibers for detecting CO_2 gas is compared.

It must be mentioned that to the best of our literary knowledge in the field of nanofiber composites using CO_2-based sensors, there has been no work reported on nanofiber composites of AmG/PANI/PMMA and CLBC-AmG/PANI nanofiber-based CO_2 gas sensors.

CHAPTER 3 OBJECTIVES

The main objective of this research is:

To develop novel functionalized graphene/polyaniline nanofiber composites for highly selective and sensitive CO_2 gas detection.

The specific objectives of the current research are:

1) To investigate the fabrication of amino-functionalized graphene and determine the optimized processing parameters which leads to successful electrospinning of graphene filled PANI/PMMA.

2) To develop and characterize amino functionalized graphene/polyaniline/poly(methyl methacrylate) nanofibers for detecting carbon dioxide.

3) To develop a crosslinked bacterial cellulose-amino functionalized graphene/polyaniline nanostructure for fabricating a carbon dioxide sensor.

4) To examine and compare the efficiency of nanofiber composite amino functionalized graphene/polyaniline/poly(methyl methacrylate) with crosslinked bacterial cellulose-amino functionalized graphene/polyaniline nanostructure as a new material for sensing CO_2 gas.

CHAPTER 4 ORGANIZATION OF THE ARTICLES

The following three chapters comprise of the articles containing the main scientific findings of this study and represent the core of the thesis, which is presented in the form of three peer-reviewed journal papers.

Chapter 5 presents the results of the first paper "*Preparation of Electrospun Nanocomposite Nanofibers of Polyaniline/Poly(methyl methacrylate) with Amino-Functionalized Graphene"* that was published in *Polymers* (VOL. 9, NO. 9, 453, 2017) (impact factor = 3.364). This journal was chosen because it is one of the leading journals that focuses on publishing innovative, significant advances in polymer nanocomposites, in chemistry, and technology. This paper was published on September 16th, 2017. The manuscript investigates the preparation and characterization of functionalizing graphene with amine ($–NH_2$) groups through non-covalent functionalization to obtain AmG that easily disperses in $CHCl_3$/DMF. The electrospinning and solution parameters on the processability of AmG/PANI/PMMA solution and morphology of AmG/PANI/PMMA nanofibers were also examined. This study was of great importance regarding the many possible applications, such as organic photovoltaics, and supercapacitors.

Chapter 6 presents the results of the second paper "*Stable and Sensitive Amino-Functionalized Graphene/Polyaniline Nanofibers Composite for Room Temperature Carbon Dioxide Sensing*" that has been accepted in *RSC Advances - Royal Society of Chemistry* (impact factor = 3.049). This journal was selected because it is one of the most important journals in publishing work related to gas sensors. The manuscript investigates the features of a CO_2 gas sensor fabricated from AmG/PANI/PMMA nanofiber composites by *in situ* polymerization. The sensing characteristics of the nanofiber composites for various concentrations of CO_2 gas at RT was evaluated. In addition, the fabrication of PMMA nanofibers obtained by electrospinning were reported.

Chapter 7 contains the results of the third article "*Cellulose Nanopaper Cross-Linked -Amino Graphene/Polyaniline Sensors to Detect CO_2 Gas at Room Temperature*" that was published on November 28th, 2019 in *Sensors* (VOL. 19, No. 23, 5215, 2019) (impact factor = 3.031). This journal was selected because it addresses research in the area of analytical electrochemistry, electrochemical materials science, electrochemical process engineering and technology. The manuscript explores the properties of a CO_2 gas sensor developed from CLBC-AmG/PANI nanofiber nanocomposites by *in situ* polymerization. The sensing performance of the CLBC-

AmG/PANI and BC/PANI was examined at RT. Moreover, the efficiency of AmG/PANI/PMMA electrospun nanofibers was compared to that of CLBC-AmG/PANI nanofibers as credible sensing materials for detecting CO_2 gas.

CHAPTER 5 ARTICLE 1: PREPARATION OF ELECTROSPUN NANOCOMPOSITE NANOFIBERS OF POLYANILINE/POLY(METHYL METHACRYLATE) WITH AMINO-FUNCTIONALIZED GRAPHENE

Hanan Abdali[1,2] and Abdellah Ajji[1,*]

[1] Research Center for High Performance Polymer and Composite Systems (CREPEC), Department of Chemical Engineering, Polytechnique Montréal, P.O. Box 6079, Station Centre-Ville, Montréal, QC H3C 3A7, Canada

[2] Ministry of Education, Riyadh, Kingdom of Saudi Arabia, P.O. Box 225085, Postal Code 11153.

(This work was published online in *Polymers* on September 16th, 2017)

5.1 Abstract

In this paper we report upon the preparation and characterization of electrospun nanofibers of doped polyaniline (PANI) /poly(methyl methacrylate) (PMMA) /amino-functionalized graphene (Am-rGO) by electrospinning technique. The successful functionalization of rGO with amino groups is examined by Fourier transforms infrared (FTIR), X-ray photoelectron spectroscopy (XPS) and Raman microspectrometer. The strong electric field enables the liquid jet to be ejected faster and also contributes to the improved thermal and morphological homogeneity of PANI/PMMA/Am-rGO. This results in a decrease in the average diameter of the produced fibers and show that these fibers can find promising uses in many applications such as sensors, flexible electronics, etc...

Keywords: electrospun nanofibers; electrospinning; polyaniline; nanocomposites; amino-functionalized graphene

5.2 Introduction

Electrospinning is an efficient, relatively simple and low-cost process used to produce continuous nanofibers on a large scale, where the fiber diameter can be adjusted from nanometers to microns by applying a high voltage to a polymer solution from a micro-syringe pump [1-5]. Polymer nanofibers produced via electrospinning have specific surface areas approximately one to two orders of the magnitude larger than flat films, making them the most promising candidates for applications in filtrations, engineering tissue scaffolds, wound healing, release control, energy storage and sensors [5-8].

Polyaniline (PANI) is one of the most conductive polymers, that has been used in many electronic, optical and electrochemical applications, due to its low cost, good environmental stability, redox reversibility, and electrical conductivity [9-10]. However, processing PANI into nanofibers by using the electrospinning, is a challenge, mainly due to its rigid backbone that is related to its high degree of aromaticity making the elastic properties of the solution insufficient for electrospinning [11-12]. In this regard, non-conductive hosting polymers such as poly(methyl methacrylate) (PMMA), is blended to assist polyaniline to form composite fibers [13-14]. Consequently, the nanofibers of PANI have garnered much interest because of their properties as candidates for chemical sensors [15], light-emitting and electronic devices [16]. Yet, some disadvantages such poor mechanical properties do exist, though upon combining PANI with carbon materials reinforces its stability and enhances some of its properties such as capacitance [17-18].

Graphene is a potential nanofiller that can efficiently enhance the mechanical, thermal and electrical properties of polymer-based nanocomposites at a very low loading, useful for various novel applications due to its high thermal conductivity, superior mechanical strength, high specific surface area, excellent mobility of charge carriers and high chemical stability [19-21]. However, the homogenous dispersion of graphene in a polymer matrix is a necessary feature when it is used as a nanofiller. Graphene is predisposed to agglomerate because of its hydrophobic nature, high surface energy, and intrinsic van der Waals forces preventing its uniform distribution in the polymer matrix [21-23]. This reduces its beneficial effects and therefore dispersing the graphene in an electrospinning solution is an important step in forming the nanofibers [21]. The problems can be overcome by functionalizing the graphene. This procedure provides multiple bonding sites to the resin matrix where the remarkable properties of graphene can be successfully transferred to

a polymer composite [23-25]. Amine groups are attributed with high reactivity enabling them to react with other chemical groups easily and providing a favorable approach in the preparation and applications of graphene/polymer nanocomposites [23]. As the Nitrogen atom in amine is more nucleophilic than the oxygen atom, it can be expected that substituting graphene or graphene oxide with amine will increase the nucleophilic properties of graphene. Consequently, interfacial binding can result between graphene and the materials of interest. These interactions will improve the performance and functionality of the intended applications of graphene [23-24]. Former studies about the functionalization of graphene with amine groups have indicated it could be a promising strategy to improve the electrical conductivity of graphene, due to the electron donating effect of amine groups [23].

Herein, the ethylenediamine (NH_2–$(CH_2)_2$–NH_2) was utilized to functionalize graphene surfaces, which produced stitched graphene owing to the presence of two amine (–NH_2) functionalities on both sides of the ethylene moiety [24]. Therefore, due to the intriguing properties of graphene and the advantages of PANI, composites of graphene and PANI fibers are eminently suitable for many applications such as organic photovoltaics, supercapacitors and resistance-based sensors. In this article, the preparation of electrospun fiber mats of doped polyaniline/poly(methyl methacrylate)/ amine-functionalized graphene using the electrospinning process is studied. Literature has reported on graphene/polyaniline composites [26,27,28] but, in this study, for the first time, amino-functionalized graphene/polyaniline nanofibers are investigated using the electrospinning process.

More specifically, the objectives of this study were to identify and detail the primary materials and process factors necessary to produce amino-graphene/polyaniline nanofibers using the electrospinning process. The details of the amine functionalization of graphene is presented and the morphology and the thermal stability of the PANI/PMMA/Am-rGO nanofibers are investigated.

5.3 Materials and Methods

5.3.1 Materials

Graphene oxide (GO), poly(methyl methacrylate) (PMMA) Mw ~ 996,000 g mol^{-1}, polyaniline (PANI, emeraldine base) Mw ~ 100,000 g mol^{-1}, camphor-10-sulfonic acid (HCSA,98%), N,N dimethylformamide (DMF,99.8%), chloroform ($CHCl_3$,≥99%), ethylenediamine (EDA,≥99%),

were all purchased from Sigma-Aldrich (Oakville, ON, Canada). Deionized (DI) water was used for all the experiments.

5.3.2 Reduction of Graphene Oxide to Graphene

Commercial graphene oxide (GO) was reduced by thermal annealing treatment [29]. First, the GO powder was heated in a tubular quartz furnace (High Temperature Tube Furnace (HTF), GSL-1300-40X, MTI Corporation, California, USA) from room temperature to 400 $^{\circ}$C at the rate of 5 $^{\circ}$C min^{-1}, and kept at 400 $^{\circ}$C for 30 min under an argon (Ar) gas flow of 80 mL min^{-1}; secondly, the temperature was increased from 400 to 650 $^{\circ}$C at a rate of 5 $^{\circ}$C min^{-1}, and kept at 650 $^{\circ}$C for 30 min under an Ar gas flow of 80 mL min^{-1}. Finally, the reduced GO samples were naturally cooled to room temperature without argon.

5.3.3 Surface Modification of Graphene with Amines

The rGO made in the previous step, where 150 mg of rGO was mixed with 10 ml of EDA, in a vessel under vigorous stirring. The reaction was continued for 24 h under reflux at 80 $^{\circ}$C. Afterwards, the aminated-rGO (Am-rGO) was centrifuged at 10,000 rpm for 1 h and was thoroughly washed with deionized water, filtered, and dried in a vacuum oven at 80 $^{\circ}$C for 24 h [23].

5.3.4 Preparation of the PANI/PMMA/Am-rGO Solution

10 mg of the Am-rGO was dispersed in 2.96 g of DMF by sonication for 1 h. 100 mg of PANI was mixed with 130 mg of HCSA to dope it and dissolving it in 14.78 g of chloroform. The solution was stirred constantly for 6 h and subsequently filtered using Whatman Puradisc PTFE syringe filter (pore size - 0.45 µm, GE Healthcare, Buckinghamshire, UK) to remove the particulate matter. Then, the Am-rGO solution was mixed with PANI solution and subsequently 85 mg of PMMA (as a carrier polymer) was added to the solution and stirred for 24 h to form the solution for electrospinning (see Table 5-1). The PANI/PMMA solution was similarly prepared without the addition of functionalized graphene for comparative analysis.

Table 5-1 Composition of electrospun PANI/PMMA/Am-rGO and PANI/PMMA solutions.

PANI (mg)	**HCSA (mg)**	**Am-rGO (mg)**	**$CHCl_3$ (g)**	**DMF (g)**	**PANI:PMMA (wt.%)**	**Am-rGO:PANI (wt.%)**
100	130	10	14.78	2.96	54.05	9.09
100	130	-	14.78	2.96	54.05	-

5.3.5 Electrospinning Setup

Figure. 5-1 shows the schematic diagram of the fabrication of graphene-polymer nanofiber composite by electrospinning. The homogeneous dispersed solutions were electrospun using a homemade horizontal set up containing a programmable micro-syringe pump (Harvard Apparatus, PHD 2000, Holliston, MA, USA) and a variable high DC voltage power supply (ES60P-5W Gamma High Voltage Research Inc, Omaha Beach, FL, USA). Parameters such as the flow rate, voltage and distance were harnessed at peak efficiency to obtain the desired nanofibers with the least beading to perform the subsequent experiments. The PANI/PMMA/Am-rGO solution was loaded into a 3 mL syringe with Luer–Lock connection to an 18-gauge blunt tip needle (Cadence Science, Cranston, RI, USA). The syringe was mounted on the pump with a grip and grounded by use of an alligator clip. The applied voltage was in the range of 18-20 kV between the needle tip and the collector. A syringe pump was utilized to control the flow rate of the solution which was 0.3 ml/h and the distance between the needle and the collector was 15 cm. The spun nanofiber mats were collected on an aluminum foil attached to a stationary collector plate. All experiments were conducted in a chamber at a relative humidity of 19–25 %.

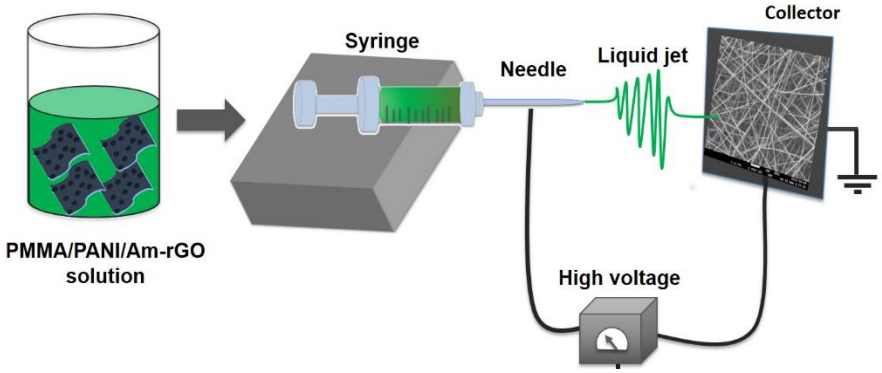

Figure 5-1 Schematic illustration of the electrospinning setup.

5.3.6 Characterization of Amino Functionalized Graphene

In order to ensure the presence of functional groups that should be present from the successful reduction of GO to rGO and functionalization of rGO with amino group, the Fourier transform infrared (FTIR) spectroscopy analysis was undertaken using Perkin Elmer 65 FTIR-ATR instrument (PerkinElmer, Woodbridge, ON, Canada). A total of 128 scans were accumulated for signal averaging of each IR spectral measurement with a 4 cm^{-1} resolution. The spectra of the samples were recorded over a wavenumber range of 4000–650 cm^{-1}. Raman microspectrometer and the electron diffraction (SAED) patterns were utilized to investigate the structural changes of GO, rGO, and Am-rGO. Characterization of graphene specimens were performed by Raman microspectrometer with a Renishaw InVia Raman microscope (Renishaw, Mississauga, ON, Canada) at an excitation laser wavelength of 514 nm. Raman spectroscopy is a powerful non-destructive tool for studying disorder and defects in crystal structure, it is often used to characterize microstructure of carbon materials. All specimens were deposited on glass slides in powder form without any solvent. For SAED patterns characterization, the graphene specimens were scooped onto a transmission electron microscopy (TEM) copper grid with supporting carbon film (CF400-Cu, Electron Microscopy Sciences) directly. The dispersion characteristics of rGO and Am-rGO were measured by ultraviolet visible (UV–Vis) spectrophotometer at ambient temperature utilizing Infinite 200 PRO (Tecan, Männedorf, Switzerland) cuvette reader. The chemical composition of the samples were determined by X-ray photoelectron spectroscopic (XPS) analysis using a VG Scientific ESCALAB 3 MK II X-ray photoelectron spectrometer (VG Escalab 3 Mk, East Grinstead, England) using an Mg Kα source (15 kV, 20 mA).

5.3.7 Characterization of the PMMA/PANI/Am-rGO Nanofibers

The scanning electron microscope (SEM, JSM-7600TFE, FEG-SEM, Calgary, AB, Canada) at an operational voltage of 2 kV was used to study the morphology of electrospun fibers. Fiber diameters were calculated using Image-Pro Plus®software by taking an average of about 300 fibers. To confirm the presence of graphene sheets in the nanofibers of PANI/PMMA/Am-rGO, transmission electron microscopy (TEM, JEOL, JEM 2100F, JEOL, Pleasanton, CA, USA) was used. For TEM observation, fibers were directly deposited onto a TEM copper grid with supporting carbon film (CF400-Cu, Electron Microscopy Sciences). Thermogravimetric analysis (TGA) was conducted under nitrogen atmosphere using Q5000 TGA (TA Instruments, New Castle, DE, USA) in the temperature range of 20–900 ˚C, with a heating ramp of 10 ˚C·min^{-1}.

5.4 Results and Discussion

5.4.1 Morphology and Structure Analysis of Am-rGO

The UV–Vis spectrum of rGO suspension showed an absorption peak at around 265 nm. This observation confirms the formation of C=C conjugated graphene structure after the thermal reduction process (see Figure 5-2b) [24]. The UV–Vis spectroscopy was used also for monitoring the stability of the rGO and Am-rGO in mixture of $CHCl_3$/DMF (5:1). As shown in Figure 5-2b-c, there is a very slight decrease in the absorbance spectra of Am-rGO over five days in comparison with rGO, indicating a good stability of the Am-rGO dispersion. Visually, dispersion of Am-rGO is more stable, whereas in comparison with dispersions of rGO in the same solution, which means that the dispersion of Am-rGO is greatly improved within $CHCl_3$/DMF in the presence of amino groups (in the inset of Figure 5-2c).

FTIR spectroscopy was performed on GO, rGO and Am-rGO in order to ensure the presence of functional groups that should be present from the successful reduction of GO to rGO and functionalization of rGO with amino groups (see Figure 5-3a). Different oxygen containing functional groups were observed on the GO spectrum bands as shown in Figure 5-3a. The C=O stretching vibrations in the carboxyl groups at 1700 cm^{-1}; the C–OH deformation from the hydroxyl groups attached to the aromatic graphene network at 1409 cm^{-1}; the C–O (hydroxyl) stretching at 1601 cm^{-1}; the C–O (epoxy) stretching at 1040 cm^{-1} and the C–O (phenolic) stretching at 1213 cm^{-1} [18,30]. The band at 1620 cm^{-1} is ascribed to the skeletal vibration of unoxidized sp^2

graphitic domains. After the thermal reduction of GO, the skeletal vibration of sp^2 graphitic domain still remains shifts to 1573 cm^{-1}. Besides, some residual presence of bands at 1710, 1150, and 1280 cm^{-1} were detected providing evidence of the different types of oxygen functionalities in the rGO and their decreases in intensity and others vanished due to thermal reduction [18,30]. In the spectrum of Am-rGO, the N–H deformation peaks at 1565 cm^{-1}; the C–N stretching vibrations at 1180 and 1120 cm^{-1}; and the C=O stretching vibrations of carboxyl group at 1725 cm^{-1}. Furthermore, the Am-rGO has peaks of the C–H stretch of alkyl chain at 2918 and 2854 cm^{-1}; and the C–O stretching in hydroxyl groups at 1015 cm^{-1}. The FTIR spectroscopy results indicate that the chemically functionalized graphene (Am-rGO) was successfully synthesized. Similar results for functionalization of graphene with amino groups have been previously reported in literature [23,30].

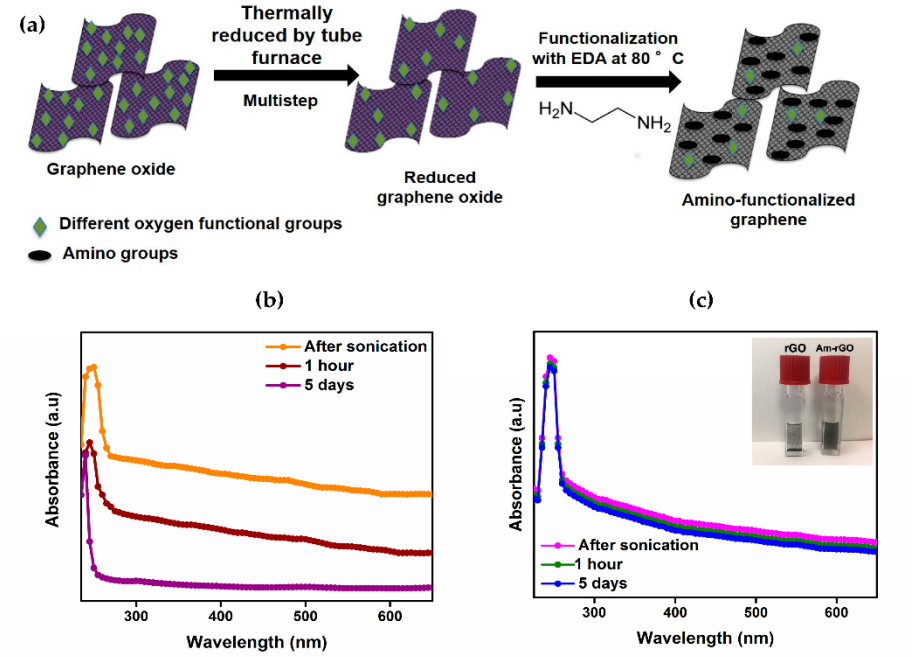

Figure 5-2 (**a**) Schematic illustration of the non-covalent functionalization of graphene surfaces with amino groups. Time evolution of UV-Vis absorption spectra of (**b**) rGO and (**c**) Am-rGO dispersed in $CHCl_3$/DMF (inset shows photograph of GO, rGO and Am-rGO).

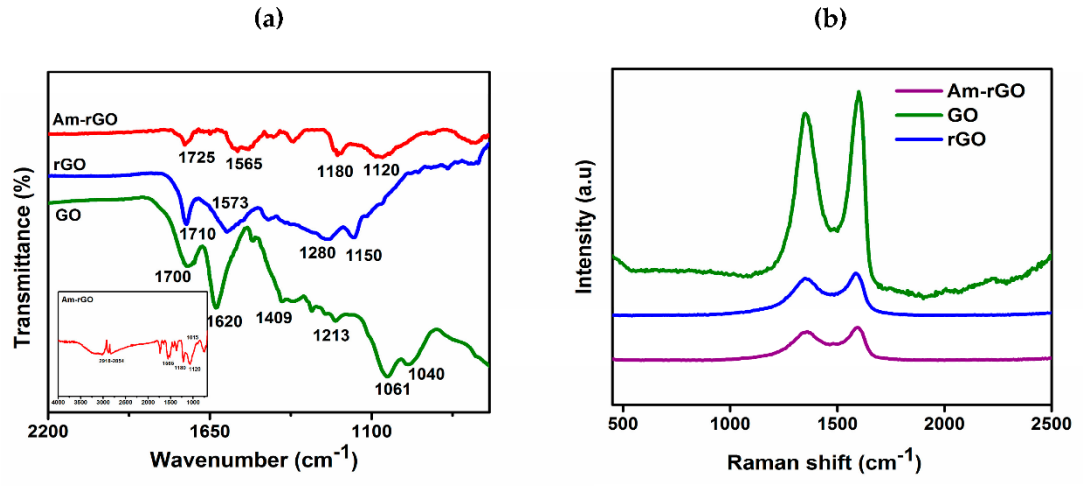

Figure 5-3 (**a)** FTIR and (**b**) Raman spectra of GO, rGO and Am-rGO.

Raman spectra was employed to analysis the graphitic structures of of GO, rGO, Am-rGO, as shown in Figure 5-3b. The G band is derived from stretching the C–C bond, and is usual for all sp^2 carbon forms system, and it is obtained from the first order Raman scattering [31,32], and the D band is due to disordered carbon atoms [31,32]. As expected, the GO revealed an intensive G band at 1600 cm^{-1} owing to the oxygenation of graphite, which results in the formation of sp^3 while, the D band is presented at 1350 cm^{-1} because of the reduction in size of the sp^2 domains by the creation of defects, and distortions during oxidation [32,33]. Moreover, in rGO and Am-rGO, the G band were shifted to lower wavenumber exhibited at 1587 and 1595 cm^{-1} and the D band positions remained unchanged at 1350 cm^{-1}, respectively. The G band appears in lower frequency due to the increased number of sp^2 carbon atoms following reduction of GO. The intensity ratio of D and G band I_D/I_G is slightly increased from (0.89) in GO to (0.93) in rGO, demonstrating a decrease in the size of the in-plane sp^2 domains after reduction, and can be explained that the thermal redaction creates many new graphitic domains, that are more numerous in number and smaller in size [32–34]. Whereas, the Am-rGO showed a higher I_D/I_G intensity ratio (0.97) than the rGO, which is attributed to the formation of the chemical bond between amino groups and basal planes of the rGO. This corresponds to other results reported for functional graphene [34–36].

The XPS was also applied as an effective tool to characterize the presence of different elements such as carbon, oxygen and nitrogen in GO, rGO and Am-rGO samples. Table 5-2 shows that the elemental analysis of GO, rGO and Am-rGO. The results confirm the successful functionalization of rGO with amino groups. The increase in C/O atomic ratio in Am-rGO indicates that EDA can

successfully functionalized graphene sheets. The presence of N containing groups in Am-rGO can also be demonstrated from its XPS spectrum, where three peaks corresponding to N, C and O elements can be clearly visualized. As shown in Figure 5-4a, only the carbon (C1s at 284.8 eV) and oxygen (O1s at 531.2 eV) appeared in the wide-scan spectrum in the GO, rGO and Am-rGO. After the functionalization of rGO with amino groups, as expected, the nitrogen (N1s at 400.1 eV) was clearly evident in the wide-scan spectrum in the Am-rGO [30,37]. The appearance of the N1s peak and the greatly decreased intensity of the O1s peak in the XPS spectrum of Am-rGO indicate the efficient displacement of oxygen moieties by amino groups during the chemical amination of rGO [30,37]. Peak fitting of C1s and N1s high resolution C1s and N1s XPS spectrum reveals the diverse carbon and nitrogen components in the Am-rGO framework. As shown in Figure 5-4b, carbon atoms exists in different functional groups: at 284.6 (C–C/C=C), 285.5 (C–N/C=N), 286.5 (C–O), 287.9 (O=C–N) and 289.3 eV (O–C=O). The amination process led to the formation of (N=C) at 398.5 eV, (C–NH_2) at 399.7 eV, (C–N–C) at 400.4 eV, and (C–N+–C) at 401.6 eV (see Figure 5-4c) [29,30]. As it can be seen in Figure 5-4c, the most intense peak is assigned to the C–NH_2, indicating that amino functionalized-rGO was successfully prepared. These XPS results were consistent with other studies presented in the literature [30,37].

The morphology and microstructure of the GO, rGO and Am-rGO and the electron diffraction (SAED) patterns in the selected area were analyzed by TEM (see Figure 5-5a–f). The TEM images of the GO, rGO and Am-rGO in Figure 5-5a–c, respectively, clearly show the presence of wrinkles, ripples and scrolls in the GO, rGO and Am-rGO indicating the occurrence of few-layered graphene sheets [38,39]. The SAED patterns of GO, rGO and Am-rGO (Figure 5-5d–f) were compared in order to understand the successful reduction and fictionalization with amino groups. Only diffraction rings are found in the SAED pattern of the GO, demonstrating the disordered structure of GO, while the diffraction spots in the rGO confirm the crystalline structure obtained after the thermal reduction of GO [38–40], as shown in Figure 5-5d–e. Moreover, owing to the addition of amino functional groups, the bright spots were not fully restored into the hexagonal graphene framework [40] (see Figure 5-5f). These results show that functionalization caused less damage to the graphene structure.

Table 5-2 Elemental composition of GO, rGO and Am-rGO samples extracted based on the XPS results.

Elements	Relative atomic percent (%)			C/O ratio
	C	O	N	
GO	66.4	32.5	0.3	2.0
rGO	86.1	12.7	0.3	6.7
Am-rGO	83.2	10.2	6.6	8.2

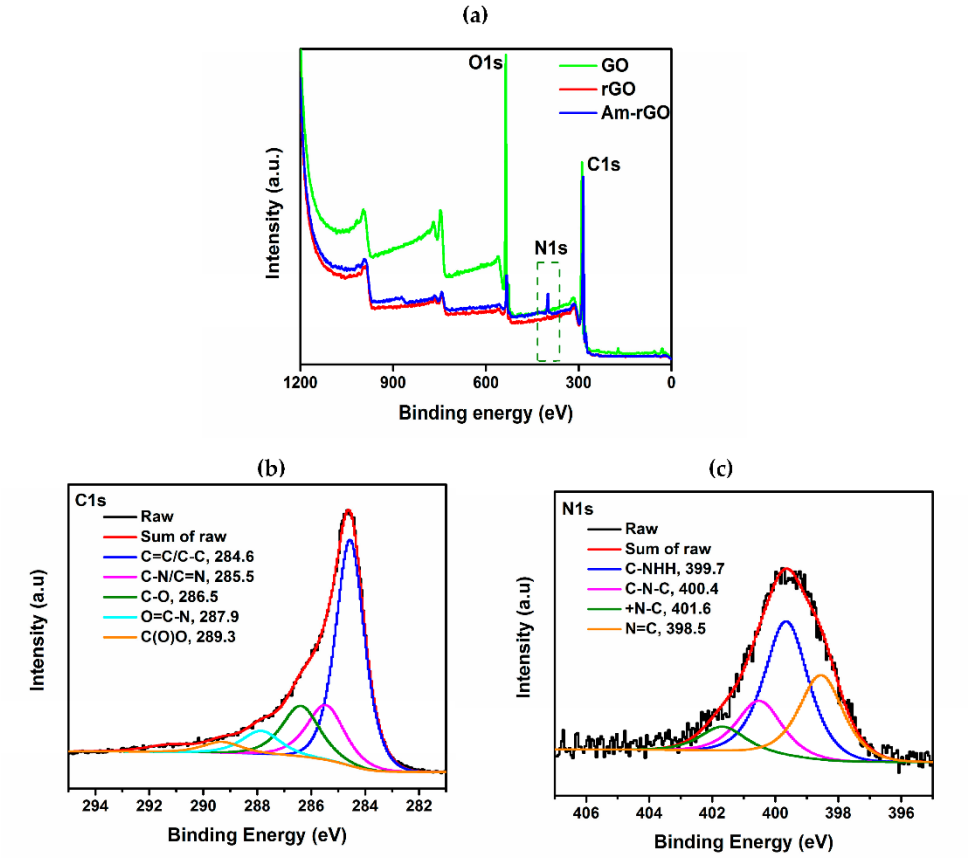

Figure 5-4 (**a**) XPS survey of GO, rGO and Am-rGO. High resolution XPS spectra of (**b**) C1s and (**c**) N1s of Am-rGO.

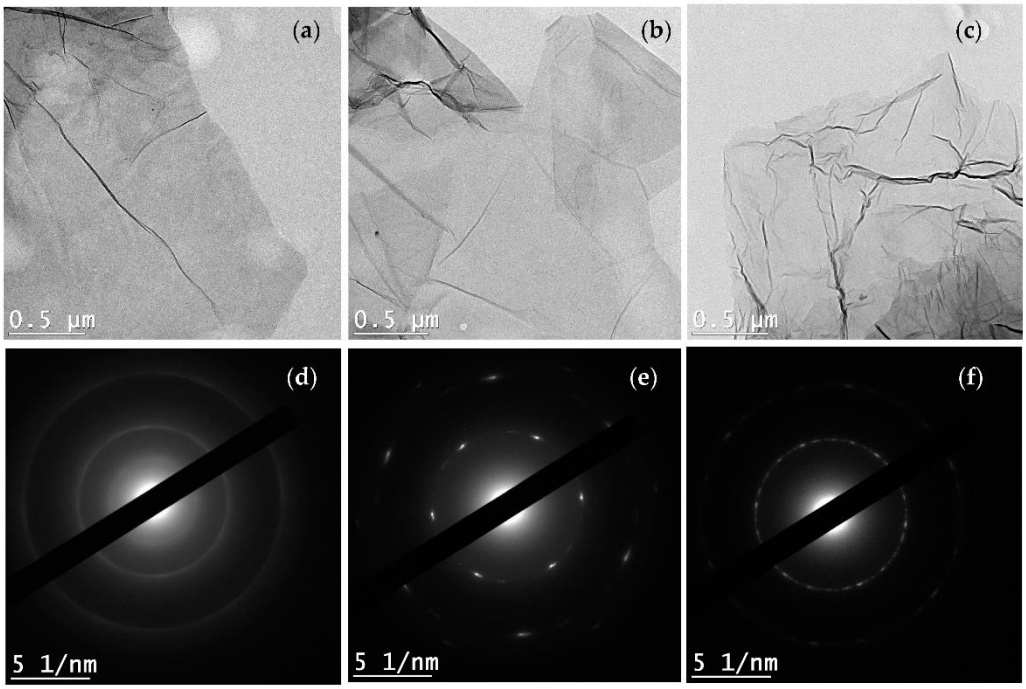

Figure 5-5 TEM images of (**a**) GO; (**b**) rGO and (**c**) Am-rGO with (**d**–**f**), respective SAED pattern.

5.4.2 Nanofibers Morphology

SEM was used to characterize the fabricated PANI/PMMA and PANI/PMMA/Am-rGO nanofibers (see Figure 5-6a–d). It is observed that the surface of nanofibers are relatively smooth and randomly oriented forming an web-like pattern [18,41]. Yet, owing to the instability of the liquid jet, beads can be observed in the image of PANI/PMMA/Am-rGO. Additionally, the average diameter before adding Am-rGO were in the range 267 ± 55 nm and after adding Am-rGO, the average diameter decreased to the range 133 ± 35 nm. This decrease in the average fiber diameter of PANI/PMMA/Am-rGO in comparison to PANI/PMMA is due to the presence of graphene sheets in the fibers. This could be attributed to the electrical conductivity in the starting solution enhanced by the presence of the graphene where the more conductive the solution, the better the chance of getting thinner fibers [18,41]. Therefore, incorporating graphene into PANI/PMMA solution enhances the conductivity of the solution to be electrospun and as a result of this improved conductivity, the produced fibers become thinner compared with fibers produced from PANI/PMMA solution [18,41].

TEM was conducted to confirm the presence of the graphene filler in the nanofibers. Figure 5-7a shows that some of the incorporated Am-rGO are randomly embedded in the sidewall of PANI/PMMA nanofibers. Moreover, Figure 5-7b–c illustrate that along the nanofibers some dark scattering spots could be observed; these aligned dark dots corresponded to graphene flakes in the PANI/PMMA nanofibers. These figures clearly show the individual graphene sheets dispersed in the PANI/PMMA matrix without aggregation, because the lateral size of graphene (a few 100 nm to a few μm) is comparable to the fiber diameter [37–41].

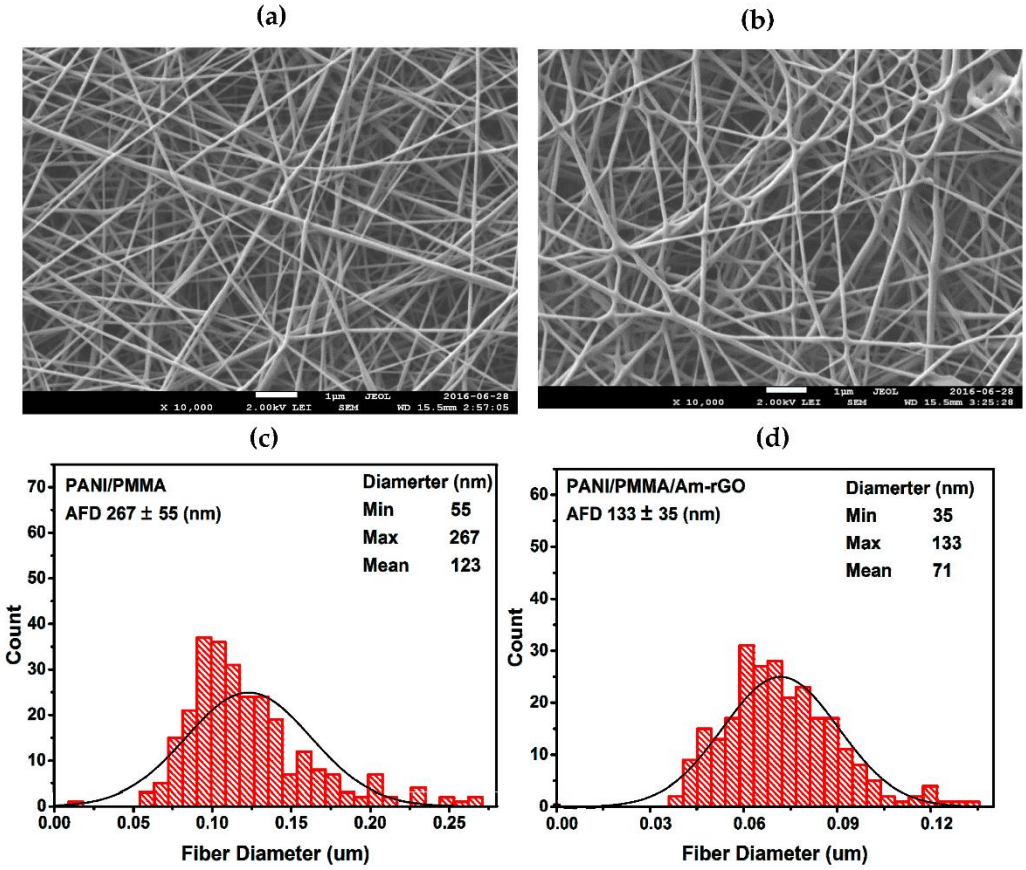

Figure 5-6 (**a**,**b**) SEM micrograph of the PANI/PMMA and PANI/PMMA/Am-rGO nanofibers, respectively; (**c**,**d**) the distribution of dimeters of the PANI/PMMA and PANI/PMMA/Am-rGO nanofibers, respectively.

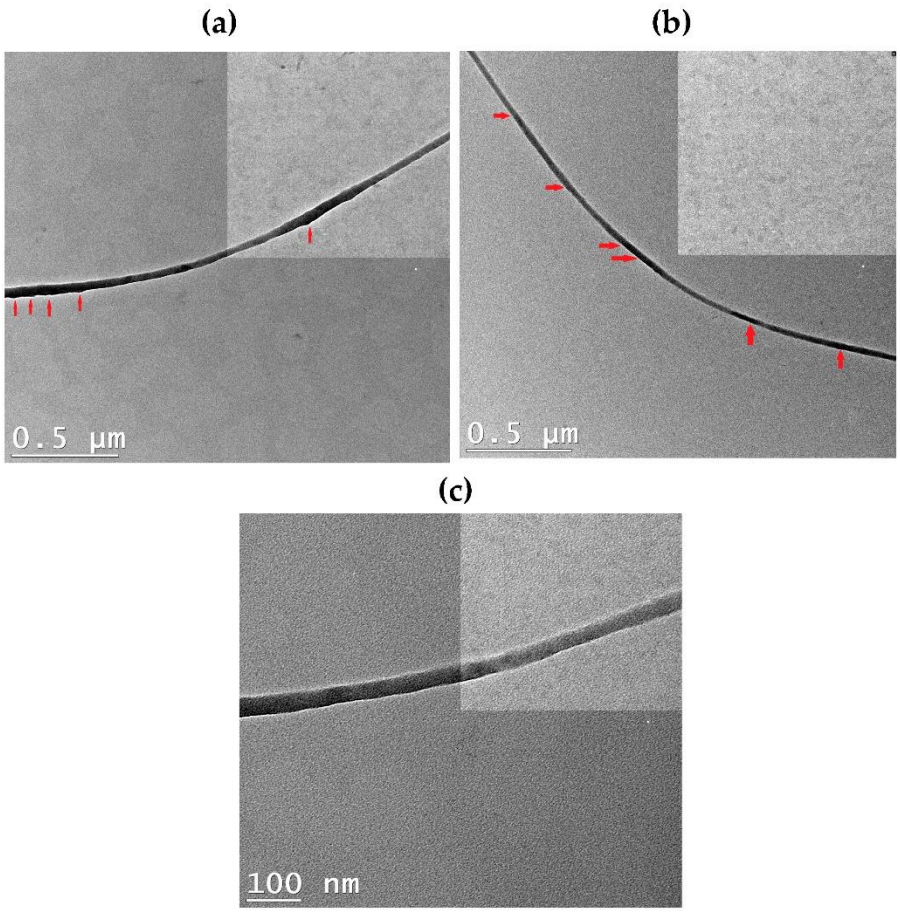

Figure 5-7 (**a**–**c**) High-resolution TEM images of PANI/PMMA/Am-rGO nanofibers at different magnification.

5.4.3 Thermal Stability

TGA was performed to observe the thermal stability of the rGO, Am-rGO and electrospun PANI/PMMA and PANI/PMMA/Am-rGO nanofiber mat (see Figure 5-8a–b), respectively, under N_2 atmosphere in temperature range between 20 and 900 $^{\circ}$C, with a heating ramp of 10 $^{\circ}$C·min^{-1}. GO is thermally unstable resulting in three stages of weight loss. In the first stage, a rapid weight loss occurs at about 173 $^{\circ}$C, mostly attributed to the removal of the trapped water molecules and epoxy oxygen functional groups. The second stage occurs at 515 $^{\circ}$C which can be attributed to the removal of phenolic groups and decomposition of sp^3 hybridized carbon atoms located at the defect site of GO. These results were congruent with other studies presented in literature [30,37]. On the other hand, the rGO was the most thermally stable, there is almost no weight loss below 600 $^{\circ}$C,

demonstrating the effective reduction and removal of oxygen functional groups. Comparing with GO, the Am-rGO exhibits good thermal stability. The thermal stability increases and major weight loss starts at temperatures of about 449 °C. This can be ascribed to the decomposition of amino-carbons, which is similar to the previously reported results for functionalization of graphene with amino groups [30,37]. Therefore, the larger thermal stability compared with GO and the greater mass lost compared with rGO indicates the efficient displacement of oxygen moieties by amino groups during the chemical amination of rGO [37].

Incorporating a small amount of Am-rGO in PANI nanofibers improves its thermal stability. As shown in Figure 5-8b, the thermal degradation temperature of PMMA/PANI/Am-rGO nanofibers increased to ~441 °C, a magnitude higher than that of the PMMA/PANI samples at ~348 °C, accredited to the presence of interfacial bonding [18,41]. In comparison to PMMA/PANI/Am-rGO, the thermal degradation temperature of the PMMA/PANI/rGO was presented around 420 °C, and corroborating the strong interaction exists between the PANI and the Am-rGO. This thermal reinforcement of the electrospun PANI nanofibers by Am-rGO (nano-carbon) fillers is very important in many different technological applications such as those mentioned in the introduction.

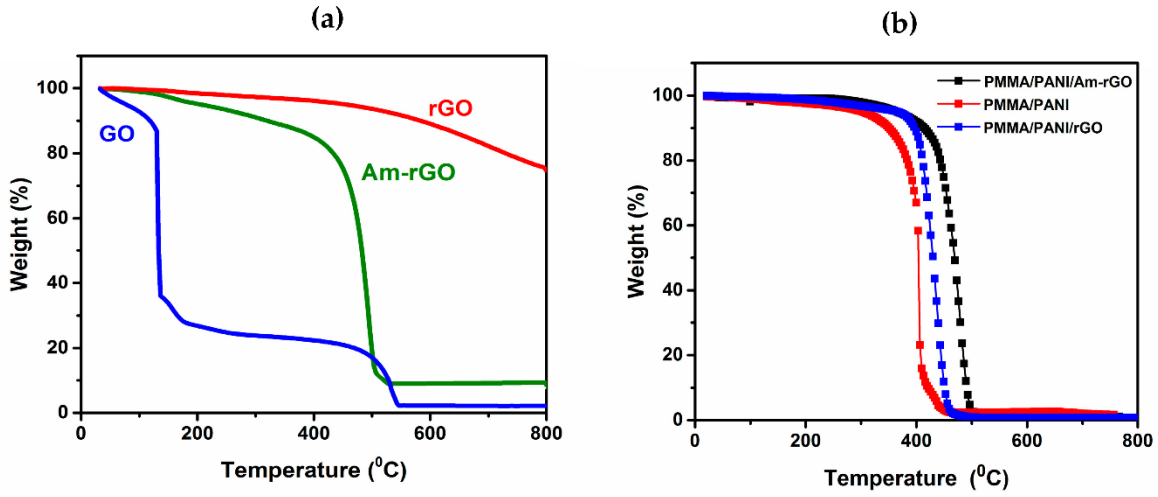

Figure 5-8 TGA curves (**a**) of GO, rGO and Am-rGO; and (**b**) for electrospun PMMA/PANI/Am-rGO, PMMA/PANI/rGO and PMMA/PANI nanofibers.

5.5 Conclusions

In this study, Am-rGO was successfully prepared and electrospun nanofibers of PANI/PMMA with amino-functionalized graphene were prepared by a simple electrospinning technique. The FTIR, XPS and Raman spectroscopy analysis confirmed the successful functionalization of the graphene with amino groups, while the TEM observation demonstrated that the addition of amino-functional groups to graphene generated less damage to the graphitic structure of the graphene. SEM micrographs indicated the formation of PANI/PMMA/Am-rGO nanofibers with a diameter ranging between 35 and 133 nm, with a general uniform thickness along the nanofibers. TGA measurements show an improvement of the thermal stability of the PANI in the presence of graphene. In conclusion, the resulting non-woven porous mats with amino-functionalized graphene result in electrospun nanofibers that can be used in future technological applications in various fields.

5.6 Acknowledgements

This research was supported by NSERC (National Science and Engineering Research Council of Canada). We are sincerely grateful to the Saudi Ministry of Higher Education for their financial support to Hanan Abdali. Also, we are grateful to Josianne Lefebvre for her indispensable help with the XPS analysis and Gwenaël Chamoulaud at UQAM University for his invaluable help with thermal annealing treatment. We would also like to thank Jean Philippe Masse for his invaluable help with TEM imaging and Samir Elouatik at University of Montreal for his help with the Raman microspectrometer.

Author Contributions

Hanan Abdali designed the experiments, performed the experiments, analyzed the data and drafted the manuscript. Abdellah Ajji designed the experiments, analyzed the data and reviewed and edited the manuscript.

Conflicts of Interest

The authors declare no conflict of interest.

5.7 References

1. Huang, Z.; Zhang, Y.; Kotaki, M.; Ramakrishna, S. A review on polymer nanofibers by electrospinning and their applications in nanocomposites. Compos. Sci. Technol. 2003, 63, 2223–2253.

2. Gu, B.K.; Shin, M.K.; Sohn, K.W.; Kim, S.I.; Kim, S.J. Direct fabrication of twisted nanofibers by electrospinning. Appl. Phys. Lett. 2007, 90, 263902.

3. Doshi, J.; Reneker, D.H. Electrospinning process and application of electrospun fibers. J. Electrost. 1995, 35, 151–160.

4. Li, Z.; Wang, C. Effects of working parameters on electrospinning. Chapter 2. In One-Dimensional Nanostructures Electrospinning Technique and Unique Nanofibers; Springer Berlin Heidelberg: 2013; pp. 15–28.

5. Jabal, J.M.F.; McGarry, L.; Sobczyk, A.; Aston, D.E. Substrate effects on the wettability of electrospun Titania-Poly(vinylpyrrolidone) fiber mats. Langmuir 2010, 26, 13550–13555.

6. Jian, F.; HaiTao, N.; Tong, L.; XunGai, W. Applications of electrospun nanofibers. Chin. Sci. Bull. 2008, 53, 2265–2286.

7. Teo, W.E.; Ramakrishna, S. A review on electrospinning design and nanofiber assemblies. Nanotechnology 2006, 17, R89–R106.

8. Nain, A.S.; Wong, J.C.; Amon, C.; Sitti, M. Drawing suspended polymer micro-/nanofibers using glass micropipettes. Appl. Phys. Lett. 2006, 89, 183105.

9. Fong, H.; Chun, I.; Reneker, D.H. Beaded nanofibers formed during electrospinning. Polymer 1999, 40, 4585–4592.

10. Yang, Q.; Li, Z.; Hong, Y.; Zhao, Y.; Qiu, S.; Wang, C.; Wei, Y. Influence of solvents on the formation of ultrathin uniform poly(vinyl pyrrolidone) nanofibers with electrospinning. J. Polym. Sci. B 2004, 42, 3721–3726.

11. Ruiz, J.; Gonzalo, B.; Dios, J.R.; Laza, J.M.; Vilas, J.L.; León, L.M. Improving the process-ability of conductive polymers: The case of polyaniline. Adv. Polym. Technol. 2013, 32, E180–E188.

12. Zhang, Y.; Rutledge, G.C. Electrical conductivity of electrospun polyaniline and polyaniline-blend fibers and mats. Macromolecules 2012, 45, 4238–4246.

13. Bai, H.; Shi, G. Gas sensors based on conducting polymers. Sensors 2007, 7, 267–307.

14. Fratoddia, I.; Vendittia, I.; Camettib, C.; Russoa, M.V. Chemiresistive polyaniline based gas sensors: A mini review. Sens. Actuators B 2015, 220, 534–548.

15. Huang, J.; Virji, S.; Weiller, B.H.; Kaner, R.B. Polyaniline nanofibers: Facile synthesis and chemical sensors. J. Am. Chem. Soc. 2003, 125, 314–315.

16. Liang, L.; Liu, J.; Windisch, C.F.; Exarhos, G.J.; Lin, Y. Direct assembly of large arrays of oriented conducting polymer nanowires. Angew. Chem. Int. Ed. 2002, 41, 3665–3668.

17. Yang, W.; Ratinac, K.R.; Ringer, S.P.; Thordarson, P.; Gooding, J.J.; Braet, F. Carbon nanomaterials in biosensors: Should you use nanotubes or graphene? Angew. Chem. Int. Ed. 2010, 49, 2114–2138.

18. Moayeri, A.; Ajji, A. Fabrication of polyaniline/poly(ethylene oxide)/noncovalently functionalized graphene nanofibers via electrospinning. Synth. Metals 2015, 200, 7–15.

19. Geim, A.K.; Novoselov, A.K. The rise of graphene. Nat. Mater. 2007, 6, 183–191.

20. Potts, J.R.; Dreyer, D.R.; Bielawski, C.W.; Ruoff, R.S. Graphene-based polymer nanocomposites. Polymer 2011, 52, 5–25.

21. Du, J.; Cheng, H.M. The fabrication, properties and uses of graphene/polymer composites. Macromol. Chem. Phys. 2012, 213, 1060–1077.

22. Klimchitskaya, G.; Mostepanenko, V. Van der Waals and Casimir interactions between two graphene sheets. Phys. Rev. B 2013, 87, 1–18.

23. Arbuzov, A.A.; Muradyan, V.E.; Tarasov, B.P.; Sokolov, E.A. Preparation of amino-functionalized graphene sheets and their conductive properties. In Proceedings of the International Conference Nanomaterials: Applications and Properties, the Crimea, Ukraine, 16–21 September 2013; Volume 2.

24. Kim, N.H.; Kuilab, T.; Lee, J.H. Simultaneous reduction, functionalization and stitching of graphene oxide with ethylenediamine for composites application. J. Mater. Chem. A 2013, 1, 1349–1358.

25. Zheng, W.; Shen, B.; Zhai, W. Surface Functionalization of Graphene with Polymers for Enhanced Properties. In New Progress on Graphene Research; InTech: Janeza Trdine Rijeka, Croatia, 2013.

26. Liu, S.; Liu, X.H.; Li, Z.P.; Yang, S.R.; Wang, J.Q. Fabrication of Free-Standing Graphene/Polyaniline Nanofibers Composite Paper via Electrostatic Adsorption for Electrochemical Supercapacitors. New J. Chem. 2011, 35, 369–374.

27. Rodthongkuma, N.; Ruechab, N.; Rangkupana, R.; Vachetd, R.W.; Chailapakule, O. Graphene-loaded nanofiber-modified electrodes for the ultrasensitive determination of dopamine. Anal. Chim. Acta 2013, 804, 84–91.

28. Wang, L.; Lu, X.; Leib, S.; Song, Y. Graphene-based polyaniline nanocomposites: Preparation, properties and applications. J. Mater. Chem. A 2014, 2, 4491–4509.

29. Song, N.J.; Chen, C.M.; Lu, C.; Liu, Z.; Kongb, Q.Q.; Caib, R. Thermally reduced graphene oxide films as flexible lateral heat spreaders. J. Mater. Chem. A 2014, 2, 16563–16568.

30. Tu, Q.; Pang, L.; Chen, Y.; Zhang, Y.; Zhang, R.; Lu, B.; Wang, J. Effects of surface charges of graphene oxide on neuronal outgrowth and branching. Analyst 2014, 139, 105–115.

31. Yang, D.; Velamakanni, A.; Bozoklu, G.; Park, S.; Stoller, M.; Piner, R.D.; Stankovich, S.; Jung, I.; Field, D.A.; Ventrice, C.A.; et al. Chemical analysis of graphene oxide films after heat and chemical treatments by X-ray photoelectron and micro-Raman spectroscopy. Carbon 2009, 47, 145–152.

32. Ganguly, A.; Sharma, S.; Papakonstantinou, P.; Hamilton, J. Probing the thermal deoxygenation of graphene oxide using high-resolution in situ X-ray-based spectroscopies. J. Phys. Chem. C 2011, 115, 17009–17019.

33. Botas, C.; Álvarez, P.; Blanco, C.; Santamaría, R.; Granda, M.; Gutiérrez, M.D.; Reinoso, F.R.; Menéndez, R. Critical temperatures in the synthesis of graphene-like materials by thermal exfoliation–reduction of graphite oxide. Carbon 2013, 52, 476–485.

34. Perumbilavil, S.; Sankar, P.; Rose, T.P.; Philip, R. White light Z-scan measurements of ultrafast optical nonlinearity in reduced graphene oxide nanosheets in the 400–700 nm region. Appl. Phys. Lett. 2015, 107, 051104.

35. Wang, Y.; Zhou, L.; Wang, S.; Li, J.; Tang, J.; Wang, S.; Wang, Y. Sensitive and selective detection of Hg2+ based on an electrochemical platform of PDDA functionalized rGO and glutaraldehyde cross-linked chitosan composite film. R. Soc. Chem. 2016, 6, 69815–69821.

36. Wu, N.; She, X.; Yang, D.; Wu, X.; Su, F.; Chen, Y. Synthesis of network reduced graphene oxide in polystyrene matrix by a two-step reduction method for superior conductivity of the composite. J. Mater. Chem. 2012, 22, 17254–17261.

37. Navaee, A.; Salimi, A. Efficient amine functionalization of graphene oxide through the Bucherer reaction: An extraordinary metal-free electrocatalyst for the oxygen reduction reaction. R. Soc. Chem. Adv. 2015, 5, 59874–59880.

38. Cui, T.; Lv, R.; Huang, Z.H.; Zhu, H.; Jia, Y.; Chen, S.; Wang, K.; Wu, D.; Kang, F. Low-temperature synthesis of multilayer graphene/amorphous carbon hybrid films and their potential application in solar cells. Nanoscale Res. Lett. 2012, 7, 453.

39. Song, P.; Zhang, X.; Sun, M.; Cui, X.; Lin, Y. Synthesis of graphene nanosheets via oxalic acid-induced chemical reduction of exfoliated graphite oxide. R. Soc. Chem. 2012, 2, 1168–1173.

40. Lavanya, J.; Gomathi, N.; Neogi, S. Electrochemical performance of nitrogen and oxygen radio-frequency plasma induced functional groups on tri-layered reduced graphene oxide. Mater. Res. Express 2014, 1, 1–18.

41. Barzegar, F.; Bello, A.; Fabiane, M.; Khamlich, S.; Momodu, D.; Taghizadeh, F.; Dangbegnon, J.; Manyala, N. Preparation and characterization of poly(vinyl alcohol)/graphene nanofibers synthesized by electrospinning. J. Phys. Chem. Solids 2015, 77, 139–145.

.

CHAPTER 6 ARTICLE 2: STABLE AND SENSITIVE AMINO-FUNCTIONALIZED GRAPHENE/POLYANILINE NANOFIBER COMPOSITES FOR ROOM TEMPERATURE CARBON DIOXIDE SENSING

Hanan Abdali[1,2], Bentolhoda Heli[1] and Abdellah Ajji[1*]

[1] Research Center for High Performance Polymer and Composite Systems (CREPEC), Department of Chemical Engineering, Polytechnique Montréal, P.O. Box 6079, Station Centre-Ville, Montréal, QC H3C 3A7, Canada

[2] Ministry of Education, Riyadh, Kingdom of Saudi Arabia, P.O. Box 225085, Postal Code 11153

(This work was accepted in The *Royal Society of Chemistry* on October 10th, 2019)

6.1 Abstract

This article describes the preparation and characterization of amino-functionalized graphene (AmG) /polyaniline (PANI)/ poly(methyl methacrylate) (PMMA) nanofiber mats and the efficiency of these nanofiber composites as new material for sensing carbon dioxide (CO_2) gas. The surfaces of the PMMA nanofibers were treated at room temperature by ultraviolet (UV) radiation and then the AmG/PANI was synthesized by a chemical oxidative polymerization on the surface of the PMMA nanofibers. It was concluded that UV radiation reduced the hydrophobicity of PMMA surface by introducing oxidized groups onto the nanofiber surface. The electrical responses of the gas sensor, based on the composite nanofibers towards various concentrations of CO_2 gas, were investigated at room temperature. The AmG/PANI nanofiber composites displayed a good electrical-resistance response to CO_2 at room temperature compared with the PANI/PMMA nanofiber composites. The AmG/PANI nanofiber composites exhibited enhanced CO_2-sensing properties such as high sensitivity and a faster response time (10s) under the same conditions.

Keywords: Polyaniline; Nanocomposites; Functionalized graphene; Gas sensing; Nanofibers; UV radiation.

6.2 Introduction

Carbon dioxide (CO_2) is used in a various areas such as; analytical chemistry, environmental processes, medical diagnoses, and industrial processing. Air pollution is a worldwide concern, and the continuous increase of CO_2 in the atmosphere contributes to global warming, resulting in melting glaciers and the corresponding rise of sea levels [1]. Moreover, human exposure to higher concentrations of CO_2 in ambient environment causes suffocation and creates unconsciousness, thus, there is a significant interest by researchers to monitor CO_2 levels in both ambient (outdoor) and household (indoor) environments [2-4]. Gas sensors used for CO_2 detection typically use the change of electrical responses upon exposure to various CO_2 concentrations [5]. As such, research in developing sensing materials has been concentrated on manufacturing high performance and increasing efficiencies in gas sensing elements using appropriate materials capable of detecting abnormal concentrations of CO_2 in the atmosphere [5]. Therefore, a variety of materials have been considered for gas sensor applications, including inorganic semiconductors, metal oxides, dyes, conducting polymers, and carbon nanomaterials [6-9].

Amongst these sensing materials, graphene, a two-dimensional monolayer of carbon atoms has been identified as a promising sensing material owing to its exceptional chemical and excellent electronic properties, optimal mechanical stiffness, and electrical conductivity [10-12], which are desirable properties in fabricating resistive-type CO_2 gas sensors. Research on graphene has focused on understanding the extensive range of electronic, optical, thermal and mechanical properties of these materials [10-13]. Nevertheless, numerous features of these characteristics can only be exploited once the graphene is integrated into more complex assemblies [14, 15]. The chemical functionalization of graphene is the more common technique used for these assemblies as it enables chemical bonding between the graphene and the material of interest (small molecules or polymer chains) [16-20]. Moreover, the chemical functionalization of graphene is a particularly attractive target because it can improve the solubility and processability of the graphene [21, 22].

Functionalizing the graphene with organic, monomeric amines, consisting of primary, secondary, or tertiary amine groups which are known to be sensitive to CO_2 gas [23]. The binding of CO_2 to

amino groups uses the Hard Soft Acid Base rule [24-26]. CO_2 is a hard acid and can efficiently interact with hard base amino groups to form carbamates or bicarbonates which results in an increase in resistance [24, 25]. In this work, we used ethylenediamine (NH_2–$(CH_2)_2$–NH_2) to functionalize the graphene surfaces, similar in our previous work [27]. Many studies have demonstrated that primary amine groups are highly efficient in adsorbing the CO_2 gas [23-25]. Therefore, the fundamental mechanism in this study for CO_2 sensing is the efficient binding of amino-functionalized graphene with CO_2 at room temperature (RT) to form carbamates by a reversible reaction.

Polyaniline (PANI) on the other hand has been widely researched for detecting gases based on its high sensitivity, fast response times, and functionality at room temperature [7, 28]. However, the poor cycling stability of PANI-based sensors remains a significant obstacle for practical applications. However, the incorporation of conductive carbon material is currently used for improving the cycle lifespan of PANI-based sensors. It is expected that the amine-functionalized graphene AmG/PANI composite can enhance the stability, sensitivity and selectivity of the sensor, through the combination of these excellent sensing materials. The poly(methyl methacrylate) PMMA is used in a wide range of applications in the field of nanotechnology. Several characteristics favor the selection of PMMA over other polymers available for this study, including high mechanical strength, thermal stability, non-toxicity, solubility in a variety of solvents and good dielectric properties, which improve the conductivity of the polymer solution obtained, making it easy for electrospinning. Therefore, further improvement in the sensitivity and recovery of the sensor is possible by in situ, polymerization of the AmG/PANI onto the surface of the electrospun, flexible substrates PMMA. These nanofiber mats have distinct advantages such as an extremely high surface area to volume ratio and porosity, both of which, are desirable properties in sensor applications.

To the best of our literature survey in the field of nanofiber, composite-based, CO_2 sensors, there has been no work reported on nanofiber composites of AmG/PANI based CO_2 gas sensors. Therefore, in this present article, the PMMA nanofiber mats were produced by using electrospinning. Then, these mats were treated with UV-radiation at wavelength 365 nm. After that, the AmG/PANI were in situ, polymerized at the surface of electrospun PMMA nanofibers to obtain flexible, composite nanofibers for CO_2 gas detection. It was revealed that the

AmG/PANI/PMMA sensor showed a high sensitivity towards CO_2 gas of 20 ppm. In addition, the responses were reproducible towards CO_2 gas ranging from 20 to 2000 ppm.

6.3 Results and Discussion

6.3.1 Effect of the UV-Radiation Treatment on the Substrate Morphology

Figure 6-1a SEM image shows the morphology of the neat PMMA nanofibers obtained from electrospinning. The nanofibers with smooth surfaces are randomly distributed in the membrane and are relatively uniform in size range 685 ± 220 nm. After the deposition of AmG/PANI by in situ polymerization, as illustrated in Figure 6-1b, the polymerization occurred only on the PMMA nanofiber surfaces and did not infiltrate the PMMA nanofiber, due to the hydrophobicity of the PMMA nanofiber surfaces [28, 29]. Therefore, the PMMA nanofibers were treated by the UV-radiation for 5 min (each side) at wavelength 365 nm. UV-radiation modified the surface by oxidizing, resulting in carboxylic acid groups, and increased the radical oxygen content to the exposed surfaces, resulting in the nanofiber surface becoming more hydrophilic [30-32]. The UV-treatment resulted in a modification of the PMMA nanofiber surfaces, however, no remarkable changes in nanofiber morphology (668 ± 209 nm), can be observed as seen in Figure 6-1c. In Figure 6-1d, the AmG/PANI were uniformly dispersed into the PMMA nanofibers, which indicated that the UV-treatment reduced the hydrophobicity of the PMMA surface by introducing oxidized groups onto the nanofiber surfaces. Similar results for surface oxidation of the PMMA material have been previously reported in literature [33-35].

The contact angle measurements were performed on the PMMA nanofibers before and after UV-radiation, in order to study the surface wettability of PMMA nanofibers. As it can be seen in Figure 6-2, the contact angle of PMMA nanofibers before the UV-radiation was 133.1° and after the UV-radiation, the contact angle was significantly decreased to 85.3°, which corresponds to better wettability. By introducing active sites onto the nanofiber surfaces suggests that UV-radiation enhances the wettability of PMMA nanofibers. [29]. These results corresponded to the SEM results reported above.

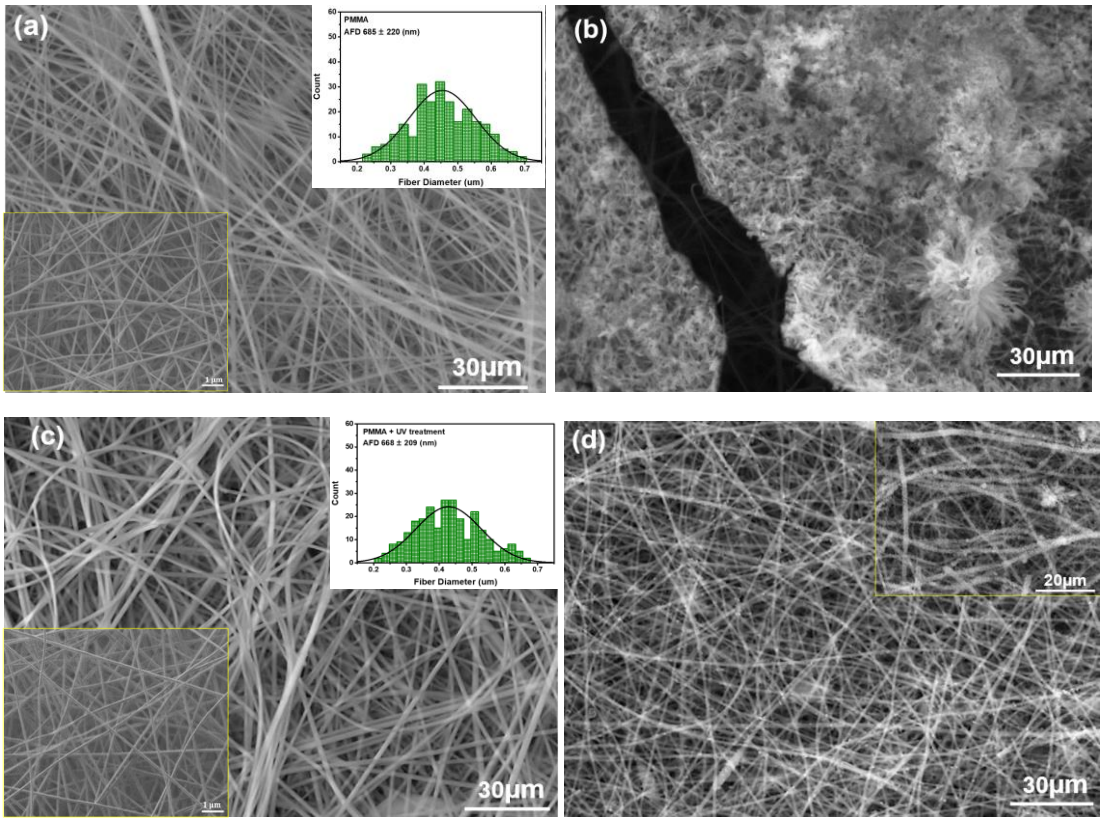

Figure 6-1 (**a**) SEM micrograph of the PMMA nanofibers and the distribution of diameters of the PMMA (inset shows SEM image with higher magnification); (**b**) the PMMA after the depiction of the AmG/PANI; (**c**) the PMMA after the UV treatment and the distribution of diameters of the PMMA (inset shows SEM image with higher magnification; (**d**) the PMMA nanofibers after the UV treatment and the depiction of the AmG/PANI.

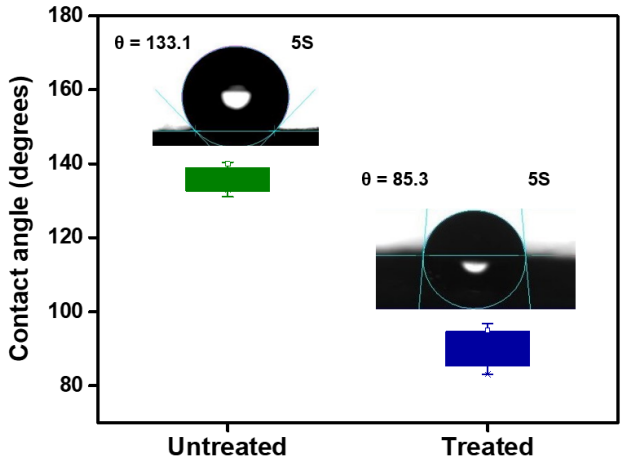

Figure 6-2 Water contact angle of untreated PMMA and treat PMMA nanofiber surfaces.

6.3.2 The Gas Sensing Properties of AmG/PANI Nanofiber Composites

A flexible nanofiber composite sensor was placed in the sensing chamber to observe its sensing behavior toward CO_2 gas at room temperature. Figure 6-3 exhibits the response of the AmG/PANI nanofiber composites which increases dramatically when exposed to various concentrations of CO_2 ranging from 20 ppm to 2000 ppm and recovers to the original values when the CO_2 is replaced by N_2.

This corresponds to other results reported for resistance-increasing responses observed in the case of π-conjugated amine (NBA) and zinc oxide (ZnO) nanohybrid based CO_2 sensor by Mandal et al. [25], polyethylenimine (PEI) for CO_2 sensors by Doan et al. [37], graphene (G) and aluminum oxide (Al_2O_3) quantum dot composites-based CO_2 sensor by Nemade and Waghuley [38], and in another study they reported G/ antimony oxide (Sb_2O_3) quantum dot composites as a CO_2 sensing material [39], as well as gas sensors based on G/PANI/polystyrene (PS) nanocomposite film for CO_2 detection by Bhadra et al.[40]. The high sensitivity towards CO_2 of the AmG/PANI nanofiber composite is due to the formation of a carbamate moiety which is the basis of the reversible CO_2 response that occurs more efficiently at lower temperatures.

The sensing properties of the AmG/PANI nanofiber composites, and PANI nanofiber composites for 20 ppm of CO_2 gas were also investigated. Figure 6-4a reveals the responses of AmG/PANI and PANI nanofiber gas sensors toward 20 ppm of CO_2 at room temperature. It was established that the sensor-based PANI nanofiber composites exhibited no sensitivity to CO_2 gas at 20 ppm, compared with the sensor-based AmG/PANI nanofibers. Figure 6-4b represents the response and recovery characteristics of a single cycle, of the AmG/PANI nanofiber gas sensor to 20 ppm of CO_2 gas. The time required for resistance to increase to 90 % of the highest value is known as the response time of gas sensor. The time required for decrease from 90 % of highest value to the initial resistance value is known as the recovery time. It was observed that the response time and recovery time of the AmG/PANI nanofiber gas sensor were ~ 10 s, and ~20 s, respectively. The values of the response and recovery time of the AmG/PANI nanofiber sensor show much improved results when compared with those reported in the published literature on CO_2 sensors (Table 6-1).

From the Table 6-1. we demonstrated that our sensors showed higher sensitivity toward CO_2 at RT compared with those reported in other published literature on CO_2 sensors except for the case of

G/PANI/PS nanocomposites. However, our response and recovery times were much better as discussed above.

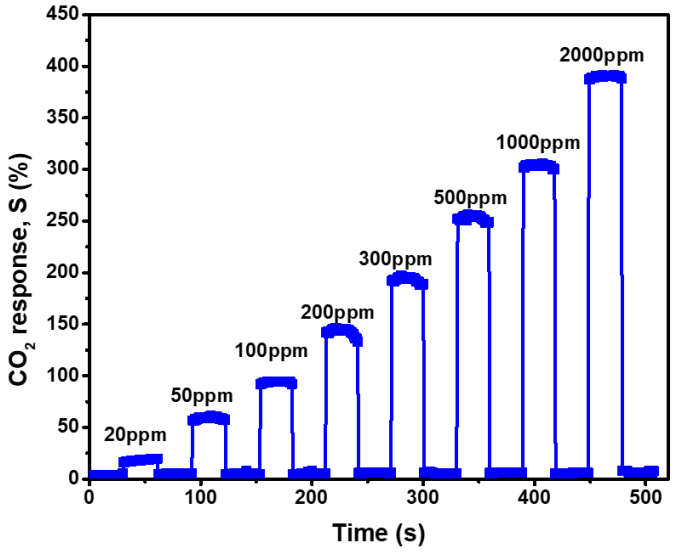

Figure 6-3 Response of AmG/PANI nanofiber gas sensor to different CO_2 concentrations.

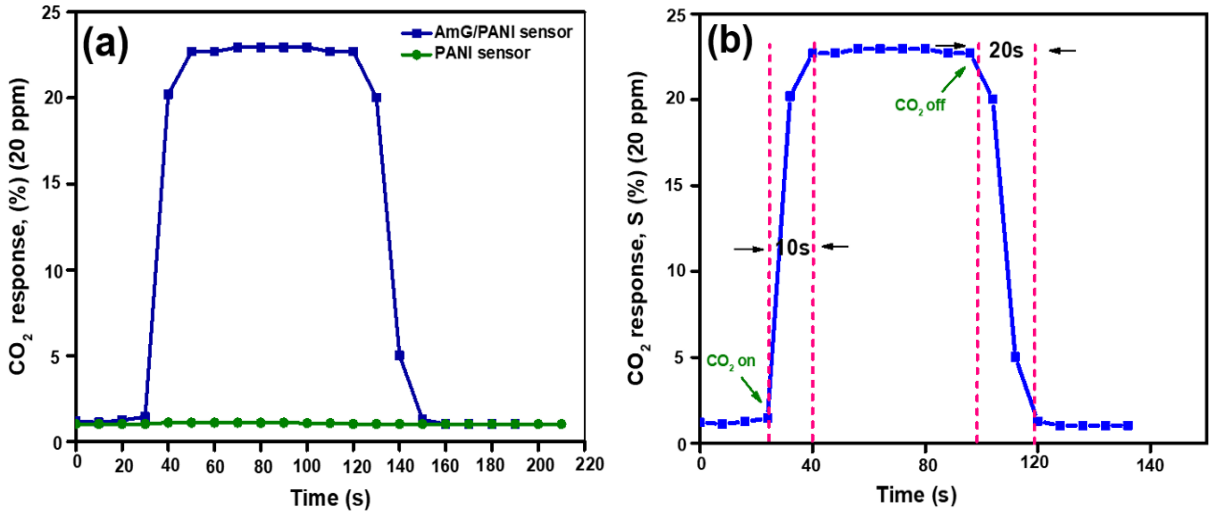

Figure 6-4 (a) Dynamic response of the two types of sensors to 20 ppm of CO_2 gas; (b) the response and recovery characteristics of a single-cycle of the AmG/PANI nanofiber gas sensor to 20 ppm of CO_2 gas.

Table 6-1 AmG/PANI sensor performance of this work compared with literature.

Materials	CO_2 concentration (ppm)	Response time (s)	Recovery time (s)	Temp. (°C)	Ref.
AmG/PANI nanofiber composite	20	10	20	RT	This work
NBA/ZnO nanohybrids	500	206	354	RT	[25]
G/Sb_2O_3 composite	50	16	22	RT	[42]
G/PANI/PS nanocomposite	20	65	65	RT	[43]
Carbon nanotube (CNT) thin film	800	>20	>75	RT	[44]

As shown in Figure 6-5, a bar graph illustrates the selectivity of the sensor's detection of CO_2 over carbon monoxide (CO), ammonia (NH_3) and hydrogen (H_2) at the concentration of 100 ppm. The selectivity results indicated that the sensor shows extreme selectivity to CO_2 when compared with any other gas used for testing at the same concentrations. Mandal et al. [25] showed that a high selectivity at 5000 ppm was observed using NH_3, CO, and H_2S gases. It can be said that this study obtained a similar result at a considerably lower ppm.

The stability of the AmG/PANI nanofiber gas sensor was examined for 30 days at an approximate constant stability which is also essential for evaluating the sensor for the purpose of practical applications. Figure 6-6 presents the stability of the AmG/PANI sensors exposed to 300 ppm of CO_2 for 30 days where the test was taken every day for ten days and after observing no change in the sensitivity, the tests were then taken every three days. The results indicated clearly the sensor exhibited nearly constant sensing signals for one month.

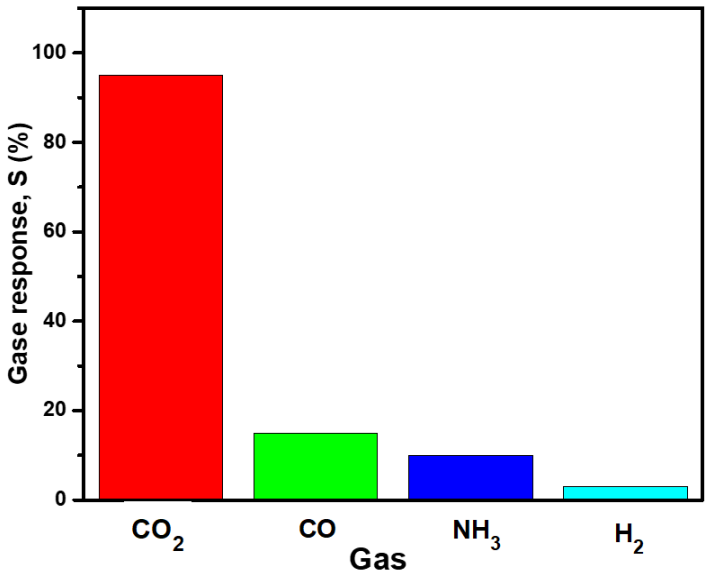

Figure 6-5 The selectivity of the AmG/ PANI nanofiber composite gas sensor to various gases of 100 ppm concentration.

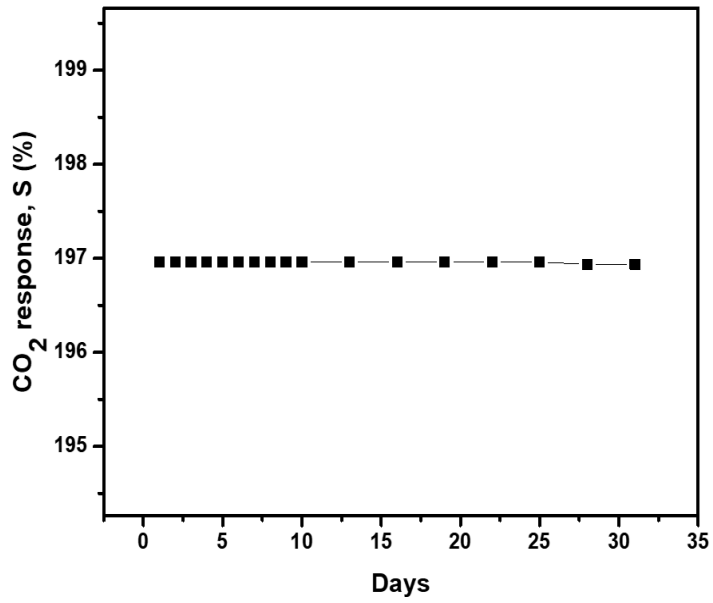

Figure 6-6 Long-term stability of AmG/PANI nanofiber composite gas sensor to 300 ppm CO_2.

The excellent sensing properties of AmG/PANI nanofiber composites toward CO_2 gas can be described by the following two mechanisms. It is usually primary amine that has been observed to

react with CO_2 to produce carbamates between the three types of amine**.** The reaction mechanism of CO_2 with primary amine for the formation of carbamates is shown in equation (1).

$$CO_2 + 2RNH_2 \leftrightarrow RNHCOO^- + RNH_3^+ \qquad (1)$$

Theoretically, two primary amines are needed to trap CO_2 [24]. At first, a lone pair of amine attaches to the carbon from the CO_2 to form zwitterionic then another free amine deprotonates zwitterionic to form the carbamate. Caplow *et al.* [36] were the first to describe the zwitterionic mechanism in the formation of carbamate from the interaction between the primary amine and CO_2. During this reaction, the number of free amines are reduced and subsequently the proton mobility is reduced which in turn increases the resistance [37, 38]. In addition, for the second mechanism, the p-type PANI and n-type AmG in AmG/PANI nanofiber composites may form a p-n junction at the interface inbetween them, [39, 40] consequently, a depletion layer occurs at the interface [40, 41]. As presented in Figure 6-7, the schematic illustration of the formation of the p-n junction between p-type PANI and n-type AmG. When CO_2 gas is injected into the chamber the gas molecules are adsorbed by the surface of the AmG/PANI nanofiber composites when, the electrons are released at the junction, into the PANI, the majority carriers (holes) in the PANI could be compensated, which might increase the thickness of the depletion layer. As a result, this increases the resistance of the AmG/PANI sensor further, in the presence of CO_2 [25, 41]. Consequently, the elevated CO_2 sensing properties of AmG/PANI nanofiber sensors can be attributed to the presence of primary amine functional group, p-n junction between p-type PANI and n-type AmG.

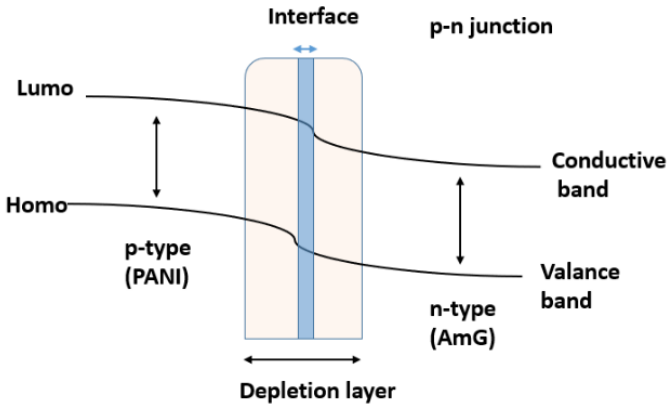

Figure 6-7 Schematic illustration of the formation of the p-n junction between p-type PANI and n-type AmG.

6.4 Conclusions

In summary, we designed and synthesized a CO_2 gas sensor using PMMA nanofibers as the flexible substrate and AmG/PANI as the active material using a chemical polymerization. The sensors fabricated, revealed good CO_2 sensing properties at room temperature, fast response (10 s) and recovery time (20 s) along with good stability. It can be reasoned that the easy preparation and excellent properties of the AmG/PANI have significantly propelled the viability of electrospun nanofibers as gas sensing materials into the limelight. The sensing mechanisms of the AmG/PANI nanofiber sensor toward CO_2 were discussed. The results demonstrated that AmG/PANI/PMMA nanofiber composites could serve as a candidate to fabricate CO_2 sensors in practice.

6.5 Experimental

6.5.1 Materials

Amino functionalized graphene (AmG) synthesized in our lab, Graphene oxide (GO), aniline (ACS reagent, ≥99.5%), N,N dimethylformamide (DMF, 99.8%), poly(methyl methacrylate) (PMMA) Mw ~ 996,000 g mol^{-1}, ethylenediamine (EDA, ≥99%), ammonium persulfate (APS, ≥98.0%), 5-Sulfosalicylic acid dihydrate (SSA , ≥99%) were all appropriated from Sigma-Aldrich, (Oakville, ON, Canada). Deionized (DI) water was used for all the experiments.

6.5.2 Synthesis of amino-functionalized graphene

GO was reduced by thermal annealing treatment as reported before [27]. Briefly, reduced GO (200 mg) was dispersed in 15 ml of EDA in a vessel under vigorous stirring for 24 h under reflux at 80 °C. Then, the AmG was isolated by centrifugation and was thoroughly washed with DI water, filtered, and dried in a vacuum oven at 80 °C for 24 h.

6.5.3 Preparation of PMMA nanofibers by electrospinning

The homogeneous dispersed solutions of 1.06 g PMMA in 20 g DMF were electrospun using a homemade horizontal setup (see Figure 6-8a) The setup consisted of a 5-ml glass syringe and metallic needle (ID = 0.84 mm) (Cadence Science, Cranston, RI, USA), a syringe pump (Harvard Apparatus, PHD 2000, Holliston, MA, USA), and a high voltage power supply (ES60P-5W

Gamma High Voltage Research Inc, Omaha Beach, FL, USA). The PMMA solutions were electrospun at room temperature for 24 h using a positive voltage of 27 kV, a working distance of 20 cm (distance between the needle tip and the collecting plate), and a solution feed rate of 0.6 ml/h. The nanofibers were collected continuously until mats of nanofibers with a thickness of ~ 0.75 mm were formed.

6.5.4 Ultraviolet (UV) radiation treatment

The PMMA nanofiber mats were cut into square pieces (40X40 mm) and exposed to UV-radiation in a homemade setup and the distance between the UV-radiation and the mats was 15.25 inches as seen in Figure 6-8b. The PMMA electrospun nanofibers were subjected to UV-radiation at a wavelength 365 nm for different exposure times of 10 min and 20 min with ensuing periods of 10 min was chosen for subsequent studies.

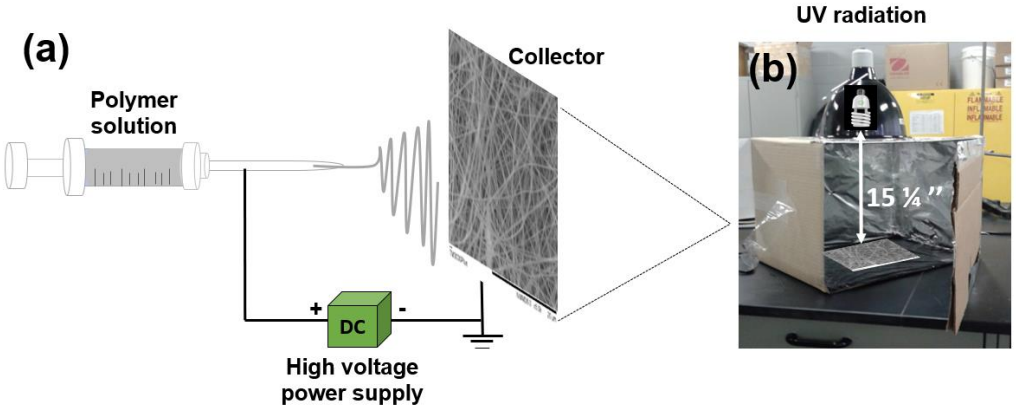

Figure 6-8 (**a**) Schematic illustration of the electrospinning setup consisting of a power supply, syringe, and conducting collector, (**b**) the homemade UV radiation.

6.5.5 Fabrication of Sensors

Treated and untreated PMMA nanofiber mats were fixed to Teflon film (25X25 mm) as a substrate by adhesive tape. Then, AmG/PANI were grown on the surface of electrospun PMMA nanofibers by in situ polymerization. As displayed in Figure 6-9, the schematic illustrates the fabrication process of AmG/PANI/PMMA nanofiber composite sensors. First, 10 mg AmG was dispersed in

50 ml DI water by sonication for 1 h and then 2.45 g SSA and 1.86 g aniline were dissolved and mechanically stirred for 30 min to form a solution A. Secondly, 4.45 g APS was dissolved in 50 ml DI water and stirred constantly for 30 min to make solution B. Then, solutions A and B were kept for 1h in the refrigerator at 5 °C. Subsequently, the PMMA nanofiber mats were immersed in solution A and next solution B was added dropwise into solution A which was stirred in an ice-water bath for different polymerization times of 1, 2 and 4 h and consequently a period of 1 h was chosen for further studies. Afterward, the nanofiber mats were taken out, washed with a large amount of DI water and several times by ethanol to remove the residual oxidant. At the end, all nanofiber composites were dried at room temperature. The A and B solutions were similarly prepared without the addition of AmG for comparative analysis. Copper tape was used as an electrode on the two opposite ends of Teflon film for the electrical connection. The sensors were stored at room temperature under vacuum until the sensing properties were tested.

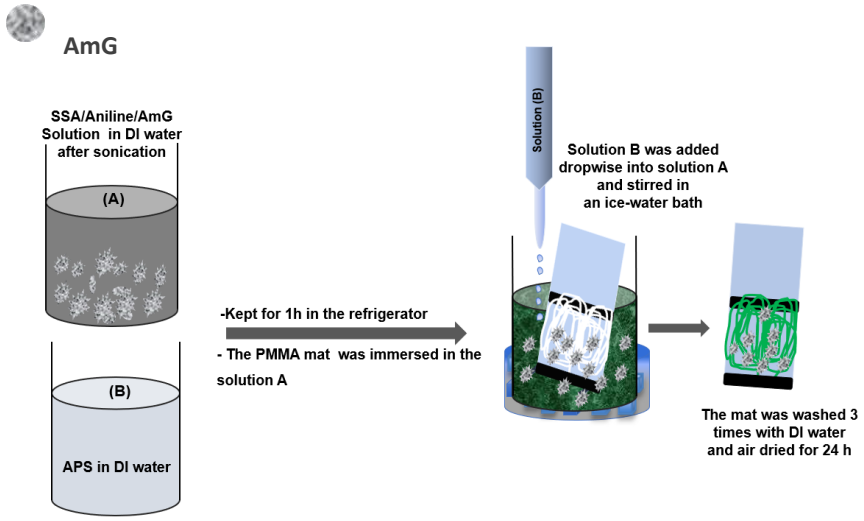

Figure 6-9 Illustrates the schematic depiction of the fabrication process of AmG/PANI/PMMA nanofiber sensor.

6.5.6 Measurements

In order to study the morphology of the PMMA nanofibers before and after the UV-radiation treatments, PANI/PMMA and AmG/PANI/PMMA nanofiber composites were examined using a table-top scanning electron microscope (TM3030 plus, Toshiba, Rexdale, ON, Canada) without any metallic coating. Fiber diameters were determined using Image-Pro Plus® software.

Approximately, 900 nanofibers were randomly selected from three independent specimens with a scale bar of 1 μm (300 from each specimen) were utilized for analysis. The contact angle measurements were carried out by utilizing the sessile drop method at room temperature in atmospheric conditions with a Contact Angle System OCA (DataPhysics Instruments GmbH, Filderstadt, Germany) in combination with SCA 20 software (Dataphysics Instruments) for image analysis and contact angle calculation. A droplet of small volume (2 μL) was pipetted onto the nanofiber surfaces (treated and untreated) and the images were automatically taken as function of time. The reported contact angles are the average of five measurements taken at different positions on each sample.

To characterize the performance of the fabricated AmG/PANI/PMMA nanofiber composites as a CO_2 sensor, the sensor resistance values were recorded by using PalmSens3 (PalmSens EmStat+Potentiostat w/Bluetooth, Compact Electrochemical interfaces, BASi®, West Lafayette, IN, USA) upon exposure to CO_2 gas at different concentrations (see Figure 6-10). The flow rates of CO_2 and nitrogen were controlled by mass flow controllers (MFCs) (MKS instruments Inc., 1179C mass-flow®, Kanata, ON, Canada). The concentration of CO_2 gas was varied from 20 to 2000 ppm by adjusting the flow rates of CO_2 and nitrogen. The sensitivity of the sensors was investigated in a square, sealed, glass test chamber with inlet and outlet for gas along with electrical connections. When the sensor resistance was stable, CO_2 gas was injected into the test chamber via a micro-injector through a rubber plug. After the resistance reached a new value, nitrogen gas was injected into the test chamber for gas sensor recovery. The sensitivity (response) of the sensor was defined as the ratio of change in the resistance S. where R_{N_2} (R_{air}) is the initial resistance was taken according to the N_2 (air) that acts as a base gas during the measurement and R_{gas} is the resistance of the sensors in CO_2, as shown in equation (2).

$$S = (R_{gas} - R_{N_2 \text{ or air}})/R_{N_2 \text{ or air}} \times 100 \qquad (2)$$

The response time is the time taken for the sensor to achieve a minimum of 90% of the total resistance change in the case of adsorption and the recovery time in the case of desorption. All experiments were conducted at room temperature (RT) and the relative humidity within the

chamber was the same as ambient relative humidity, which was between 30% and 35% upon measuring.

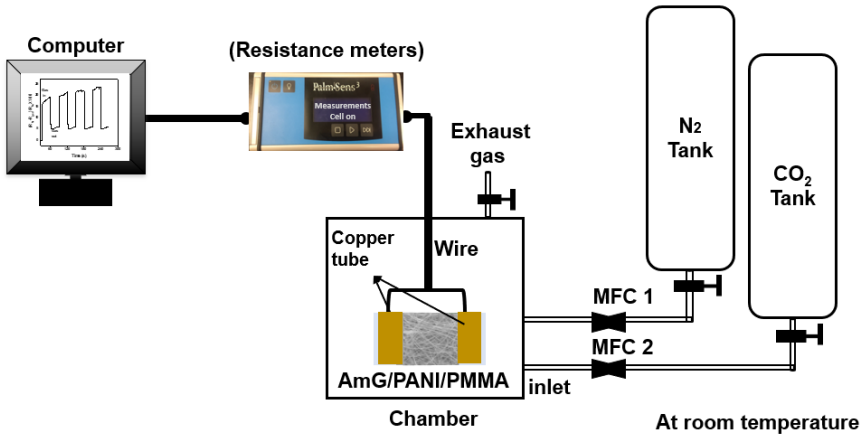

Figure 6-10 Schematic diagram for gas sensing measurements.

Conflicts of interest

There are no conflicts to declare.

6.6 Acknowledgments

This research was supported by NSERC (National Science and Engineering Research Council of Canada). The authors thank the Ministry of Education for their financial support to Hanan Abdali. The authors also thank Mr. Sébastien Chenard for his in-valuable help in building up the gas detection setup. The authors are grateful to Mrs. Claire Cerclé and Mr. Matthieu Gauthier for their kind help during this study. Finally, the authors acknowledge the reviewers of RSC Advances for their invaluable comments in improving this manuscript.

Notes

Author Contributions

Hanan Abdali designed the study, performed the experiments, collected test data, interpreted results and drafted the manuscript. Bentolhoda Heli helped in performing the experiments and interpreted the results. Abdellah Ajji designed. the study, interpreted results, reviewed and edited the manuscript.

6.7 References

1. Booth, C.E., D.G. McDONALD, and P.J. Walsh, *Acid-base balance in the sea mussel, Mytilus edulis. I. Effects of hypoxia and air-exposure on hemolymph acid-base status.* Mar. Biol. Lett, 1984. **5**: p. 347-358.
2. Desai, R., et al., *Indium sesquitelluride (In2Te3) thin film gas sensor for detection of carbon dioxide.* Sensors and Actuators B: Chemical, 2005. **107**(2): p. 523-527.
3. Mandayo, G.G., et al., *Performance of a CO2 impedimetric sensor prototype for air quality monitoring.* Sensors, 2011. **11**(5): p. 5047-5057.
4. Herrán, J., G.G. Mandayo, and E. Castano, *Solid state gas sensor for fast carbon dioxide detection.* Sensors and Actuators B: Chemical, 2008. **129**(2): p. 705-709.
5. Chiang, C.-J., et al., *In situ fabrication of conducting polymer composite film as a chemical resistive CO_2 gas sensor*. Microelectronic Engineering, 2013. **111**: p. 409-415.
6. Wang, C., et al., *Metal oxide gas sensors: sensitivity and influencing factors.* Sensors, 2010. **10**(3): p. 2088-2106.
7. Park, S., C. Park, and H. Yoon, *Chemo-electrical gas sensors based on conducting polymer hybrids.* Polymers, 2017. **9**(5): p. 155.
8. Llobet, E., *Gas sensors using carbon nanomaterials: A review.* Sensors and Actuators B: Chemical, 2013. **179**: p. 32-45.
9. Tung, T.T., et al., *Recent advances in sensing applications of graphene assemblies and their composites.* Advanced Functional Materials, 2017. **27**(46).
10. Novoselov, K.S., et al., *Two-dimensional gas of massless Dirac fermions in graphene.* nature, 2005. **438**(7065): p. 197.
11. Novoselov, K.S., et al., *Electric field effect in atomically thin carbon films.* science, 2004. **306**(5696): p. 666-669.
12. Lee, C., et al., *Measurement of the elastic properties and intrinsic strength of monolayer graphene.* science, 2008. **321**(5887): p. 385-388.
13. Balandin, A.A., et al., *Superior thermal conductivity of single-layer graphene.* Nano letters, 2008. **8**(3): p. 902-907.
14. Du, J. and H.M. Cheng, *The fabrication, properties, and uses of graphene/polymer composites.* Macromolecular Chemistry and Physics, 2012. **213**(10-11): p. 1060-1077.
15. Kuila, T., et al., *Chemical functionalization of graphene and its applications.* Progress in Materials Science, 2012. **57**(7): p. 1061-1105.
16. Cai, D. and M. Song, *Recent advance in functionalized graphene/polymer nanocomposites.* Journal of Materials Chemistry, 2010. **20**(37): p. 7906-7915.

17. Bao, C., et al., *In situ preparation of functionalized graphene oxide/epoxy nanocomposites with effective reinforcements.* Journal of Materials Chemistry, 2011. **21**(35): p. 13290-13298.

18. Ioniţă, M., et al., *Graphene and functionalized graphene: extraordinary prospects for nanobiocomposite materials.* Composites Part B: Engineering, 2017. **121**: p. 34-57.

19. Xu, J., Y. Wang, and S. Hu, *Nanocomposites of graphene and graphene oxides: synthesis, molecular functionalization and application in electrochemical sensors and biosensors. A review.* Microchimica Acta, 2017. **184**(1): p. 1-44.

20. Hu, K., et al., *Graphene-polymer nanocomposites for structural and functional applications.* Progress in Polymer Science, 2014. **39**(11): p. 1934-1972.

21. Salavagione, H.J., *Promising alternative routes for graphene production and functionalization.* Journal of Materials Chemistry A, 2014. **2**(20): p. 7138-7146.

22. Georgakilas, V., et al., *Functionalization of graphene: covalent and non-covalent approaches, derivatives and applications.* Chemical reviews, 2012. **112**(11): p. 6156-6214.

23. Ko, Y.G., S.S. Shin, and U.S. Choi, *Primary, secondary, and tertiary amines for CO_2 capture: Designing for mesoporous CO_2 adsorbents.* Journal of colloid and interface science, 2011. **361**(2): p. 594-602.

24. Stegmeier, S., et al., *Mechanism of the interaction of CO2 and humidity with primary amino group systems for room temperature CO_2 sensors.* Procedia Chemistry, 2009. **1**(1): p. 236-239.

25. Mandal, B., et al., *π-Conjugated Amine–ZnO Nanohybrids for the Selective Detection of CO_2 Gas at Room Temperature.* ACS Applied Nano Materials, 2018. **1**(12): p. 6912-6921.

26. Chen, S.-A. and G.-W. Hwang, *Structures and properties of the water-soluble self-acid-doped conducting polymer blends: sulfonic acid ring-substituted polyaniline/poly (vinyl alcohol) and poly (aniline-co-N-propanesulfonic acid aniline)/poly (vinyl alcohol).* Polymer, 1997. **38**(13): p. 3333-3346.

27. Abdali, H. and A. Ajji, *Preparation of Electrospun Nanocomposite Nanofibers of Polyaniline/Poly(methyl methacrylate) with Amino-Functionalized Graphene.* Polymers, 2017. **9**(9): p. 453.

28. Polini, A., et al., *Collagen-functionalised electrospun polymer fibers for bioengineering applications.* Soft Matter, 2010. **6**(8): p. 1668-1674.

29. Rabiatul, A., et al., *Surface modification of electrospun poly (methyl methacrylate)(PMMA) nanofibers for the development of in vitro respiratory epithelium model.* Journal of Biomaterials Science, Polymer Edition, 2015. **26**(17): p. 1297-1311.

30. Pashkuleva, I., et al., *Surface modification of starch based biomaterials by oxygen plasma or UV-irradiation.* Journal of Materials Science: Materials in Medicine, 2010. **21**(1): p. 21-32.

31. Yusilawati, A., et al., *Surface modification of polystyrene beads by ultraviolet/ozone treatment and its effect on gelatin coating.* American Journal of Applied Sciences, 2010. **7**(6): p. 724.

32. Goddard, J.M. and J. Hotchkiss, *Polymer surface modification for the attachment of bioactive compounds.* Progress in polymer science, 2007. **32**(7): p. 698-725.

33. Dekhtyar, Y., et al. *Surface properties of ocular prostheses material change under UV influence*. in *5th European Conference of the International Federation for Medical and Biological Engineering*. 2011. Springer.

34. Nematollahzadeh, A., et al., *Increasing the interfacial adhesion in poly (methyl methacrylate)/carbon fibre composites by laser surface treatment.* Polymers and Polymer Composites, 2006. **14**(6): p. 585-589.

35. Rymuszka, D., et al., *Changes in surface properties of polymethylmethacrylate (PMMA) treated with air plasma.* Annales UMCS, Chemia, 2015. **70**(1): p. 65-78.

36. Caplow, M., *Kinetics of carbamate formation and breakdown.* Journal of the American Chemical Society, 1968. **90**(24): p. 6795-6803.

37. Choi, S., J.H. Drese, and C.W. Jones, *Adsorbent materials for carbon dioxide capture from large anthropogenic point sources.* ChemSusChem: Chemistry & Sustainability Energy & Materials, 2009. **2**(9): p. 796-854.

38. Doan, T.C., et al., *Carbon dioxide detection with polyethylenimine blended with polyelectrolytes.* Sensors and Actuators B: Chemical, 2014. **201**: p. 452-459.

39. Majumdar, D., *Highly responsive carbon dioxide sensing by graphene/Al2O3 quantum dots composites at low operable temperature.* Journal of Physics, 2014. **88**(6): p. 577-583.

40. Tai, H., et al., *Fabrication and gas sensitivity of polyaniline–titanium dioxide nanocomposite thin film.* Sensors and Actuators B: Chemical, 2007. **125**(2): p. 644-650.

41. Sun, J., et al., *Preparation of polypyrrole@ WO_3 hybrids with pn heterojunction and sensing performance to triethylamine at room temperature.* Sensors and Actuators B: Chemical, 2017. **238**: p. 510-517.

42. Nemade, K. and S. Waghuley, *Role of defects concentration on optical and carbon dioxide gas sensing properties of Sb2O3/graphene composites.* Optical Materials, 2014. **36**(3): p. 712-716.

43. Bhadra, J., et al., *Fabrication of polyaniline–graphene/polystyrene nanocomposites for flexible gas sensors.* RSC advances, 2019. **9**(22): p. 12496-12506.

44. Lin, Z.-D., S.-J. Young, and S.-J. Chang, *CO_2 gas sensors based on carbon nanotube thin films using a simple transfer method on flexible substrate.* IEEE Sensors Journal, 2015. **15**(12): p. 7017-7020.

CHAPTER 7 ARTICLE 3: CELLULOSE NANOPAPER CROSS-LINKED AMINO GRAPHENE/POLYANILINE SENSORS TO DETECT CO_2 GAS AT ROOM TEMPERATURE

Hanan Abdali[1,2], Bentolhoda Heli[1] and Abdellah Ajji[1*]

[1] Research Center for High Performance Polymer and Composite Systems (CREPEC), Department of Chemical Engineering, Polytechnique Montréal, P.O. Box 6079, Station Centre-Ville, Montréal, QC H3C 3A7, Canada

[2] Ministry of Education, Riyadh, Kingdom of Saudi Arabia, P.O. Box 225085, Postal Code 11153

(This work was published online in *Sensors* on November 28th, 2019)

7.1 Abstract

A nanocomposites of cross-linked bacterial cellulose-amino graphene/polyaniline CLBC-AmG/PANI was synthesized by covalent interaction of AmG and BC via one step esterification and then the aniline monomer was grown on the surface of CLBC-AmG through in situ chemical polymerization. The morphological structure and properties of the samples were characterized by using scanning electron microscopy (SEM), and thermal gravimetric analyzer (TGA). The CLBC-AmG/PANI showed good electrical-resistance response toward carbon dioxide (CO_2) at room temperature, compared to the BC/PANI nanopaper composites. The CLBC-AmG/PANI sensor possesses high sensitivity and fast response characteristics over CO_2 concentrations ranging from 50 to 2000 ppm. This process presents an extremely suitable candidate for developing novel nanomaterials sensors owing to easy fabrication and efficient sensing performance.

Keywords: Cellulous nanopaper; Polyaniline; Nanocomposites; Functionalized graphene; CO_2 sensing.

7.2 Introduction

It is commonly regarded that high sensitivity, fast response and recovery times, as well as excellent selectivity and functionality at room temperature are important parameters for the evaluation of gas sensors [1, 2]. Correspondingly, in the field of material sciences and chemical engineering, the quest to discover advanced materials with excellent performance is perpetual and immediate [3-5]. In the last few decades, research into functional material with special nanoscale architecture has attracted great interest and presented with enhanced properties in numerous applications. These include energy storage application [6-8], catalysis application [9], medical applications [10], and the gas sensing [3, 11]. For gas sensing applications in particular, functionalized graphene-based, gas sensing materials have been prominent and as a result, the subject of much research, because of its large surface area, unique mechanical, optical, thermal, magnetic, and electrochemical properties, and its variable conductivity, which makes it available for electron transport phenomena with very high electrical mobility, in the presence of oxidizing and reducing gases [5, 11, 12].

Polyaniline is commonly used in gas sensor materials due to its unique electrical conductivity, redox properties, low production cost, easy preparation in solution and good stability at room temperature [13, 14]. These properties are crucial in gas sensors as they lower the detection limit, decrease the response time, and improve sensitivity. PANI can be synthesized by the oxidation of the monomer aniline through the chemical oxidative polymerization method [15, 16]. In situ chemical oxidative polymerization, the aniline monomer is oxidized by the utilizing ammonium persulfate as the redox initiator which has been effectively used to deposit the conductive PANI on both conductive and nonconductive substrates [15]. Moreover, it is known that combined PANI with functionalized graphene is an effective way in improving the sensing performance not only due to the unique properties of graphene but also the combined effect of both materials [17-19].

It is well accepted that the sensitivities of gas sensors are strongly affected by the specific surface of the sensing materials used, so that a higher specific surface area is directly proportional to the sensitivity and response times of the sensing material [20, 21]. Bacterial cellulose (BC) as a special type of cellulose, could be a promising flexible substrate due to its good chemical stability, excellent mechanical strength, and biocompatibility [22-25]. Research indicates that BC is an excellent supporting material that can be used as deposit nanofillers needed to create advanced BC-

based, functional nanomaterials for various technological applications including gas sensors [25-27].

This is the first report on the nanopaper composites of cross-linked bacterial cellulose-amino graphene/polyaniline (CLBC-AmG/PANI) based carbon dioxide (CO_2) gas sensors. As reported in our previous work, the graphene surfaces were functionalized by using ethylenediamine (NH_2–$(CH_2)_2$–NH_2) because it is well known that the amine groups are very sensitive and highly efficient in adsorbing the CO_2 gas [28]. In this work, we designed and fabricated a flexible, freestanding sensor using BC as the flexible substrate and AmG and PANI as active sensing materials. An easy procedure for synthesizing CLBC/AmG nanopaper by the esterification between the carboxyl groups of AmG and hydroxyl groups of BC was reported, in addition to the surface morphology and thermal stability of the CLBC/AmG nanopaper were tested. Then, the PANI was polymerized *in situ* at the surface of CLBC/AmG nanopaper and the CO_2 sensing properties of the CLBC-AmG/PANI sensors were investigated and the mechanism of the sensor was discussed.

7.3 Materials and Methods

7.3.1 Materials

Bacterial cellulose (BC) nanopaper was appropriated from Nanonovin Polymer Co. (Mazandaran, Iran)**,** amino functionalized graphene (AmG) synthesized in our lab, Graphene oxide (GO), aniline (ACS reagent, ⩾99.5%),, N,N dimethylformamide (DMF,99.8%), ethylenediamine (EDA, ⩾ 99%), N,N′-Dicyclohexylcarbodiimide (DCC, 99%) ammonium persulfate (APS, ⩾98.0%), 5-Sulfosalicylic acid dihydrate (SSA , ⩾99%) were all received from Sigma-Aldrich, (Oakville, ON, Canada). Deionized (DI) water was used for all the experiments.

7.3.2 Synthesis of CLBC-AmG Nanopaper

As showing in Figure. 7-1, the synthesis AmG (10 mg) as reported previously in [28], and BC (50 mg) in DMF (50 ml) were stirred for 1 h. Under vigorous stirring, DDC (100 mg) was added as a dehydration reagent. The esterification between the carboxyl group (COOH) of AmG and hydroxyl group (OH) of BC was conducted under N_2 atmosphere at 80 °C for 48 h to create the crosslinked

bacterial cellulose-amino-functionalized graphene (CLBC-AmG). Then the CLBC-AmG fibers were washed several times with ethanol and DI water and then dried under vacuum at room temperature (RT) for 24 h.

7.3.3 Fabrication of CLBC-AmG/PANI Nanopaper Electrodes

To grow the PANI on the surface of CLBC/AmG nanopaper by *in situ* polymerization. The two solutions were kept for 1h in the refrigerator at 5 °C before immersing the CLBC/AmG and mixing. The CLBC-AmG nanopaper were immersed in 50 ml DI water of (2.45 g) SSA and (1.86 g) aniline (solution 1). Then the 50 ml DI water of (4.45 g) APS (solution 2) was added dropwise into solution 1, which was stirred in an ice-water bath for different polymerization times 30 min, 1h , and 2 h. Finally, the period of 30 min was chosen for further studies because it reported more flexibility and good electrical conductivity for sensing purposes. It must be mentioned that the two solutions were kept for 1h in the refrigerator at 5 °C before immersing the CLBC/AmG and mixing the two solutions. Next, the flexible electrodes of CLBC-AmG/PANI were rinsed three times by DI water and ethanol until the residual oxidant was removed (see Figure. 7-2). For comparison, the BC/PANI electrodes were prepared without AmG by a similar procedure. Finally, the samples were left to dry in air at RT. All samples were cut into square pieces (20x20 mm) and fixed onto glass slides by applying copper tape to provide the appropriate electrical connection between the sensing substrate and measuring device. At the end, the electrodes were stored at RT under vacuum for two months until the sensing properties were investigated.

7.3.4 Characterization Methods

A Raman microspectrometer was recorded on Renishaw InVia Raman microscope (Renishaw, Mississauga, ON, Canada) at an excitation laser wavelength of 514 nm. Thermogravimetric analysis (TGA) was performed using Q5000 TGA (TA instruments, USA) under a nitrogen atmosphere in the temperature range of 20–800 °C, with a heating ramp of 10 °C min^{-1}. Image using a scanning electron microscope (SEM JSM-7600TFE, FEG-SEM, Calgary, AB, Canada) images were collected to study the morphology of the nanocomposites with a very thin layer of (1 nm) gold coating.

7.3.5 Measurement of Gas Sensors

The performance measurements of the fabricated CLBC-AmG/PANI electrodes as a CO_2 sensor is similar to that which was described in our previous paper [29]. The measurements of the gas sensing properties were tested under laboratory conditions (35-40% relative humidity, RT) using a PalmSens3 (PalmSens EmStat+Potentiostat w/Bluetooth, Compact Electrochemical interfaces, BASi®, West Lafayette, IN, USA) and the mass flow controllers (MFCs) (MKS instruments Inc., 1179C mass-flow®, Kanata, ON, Canada) were used to control the flow rates of the injected gases.

The measurements were obtained using a static process: initially, the sensor was put into a glass chamber with an inlet and an outlet for gas along with electrical connections. The chamber is first injected with N_2 via a micro-injector through a rubber plug to measure the initial resistance of the sensor. Then a CO_2 gas (50-2000 ppm) is injected into the chamber. When the response reaches a constant value, the sensor is exposed to N_2 to remove CO_2 and the recovery behavior of the sensor is investigated.

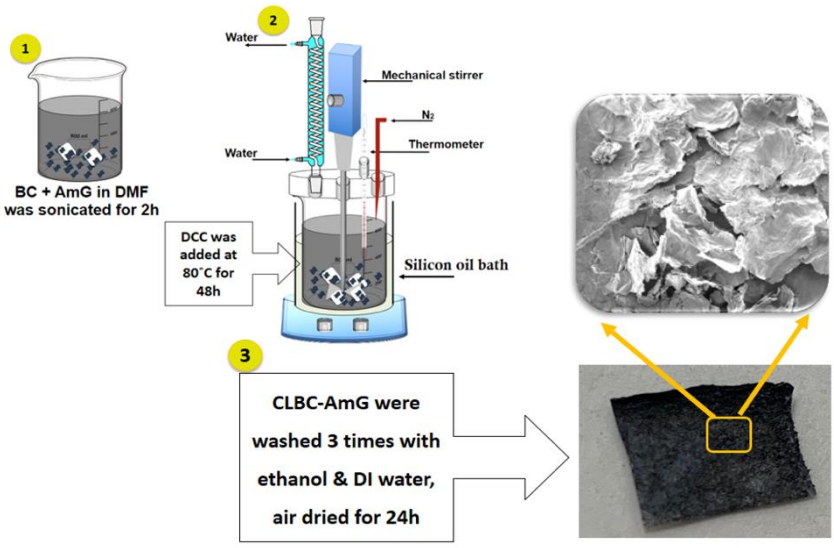

Figure 7-1 Illustrates the schematic of fabrication process of CLBC-AmG.

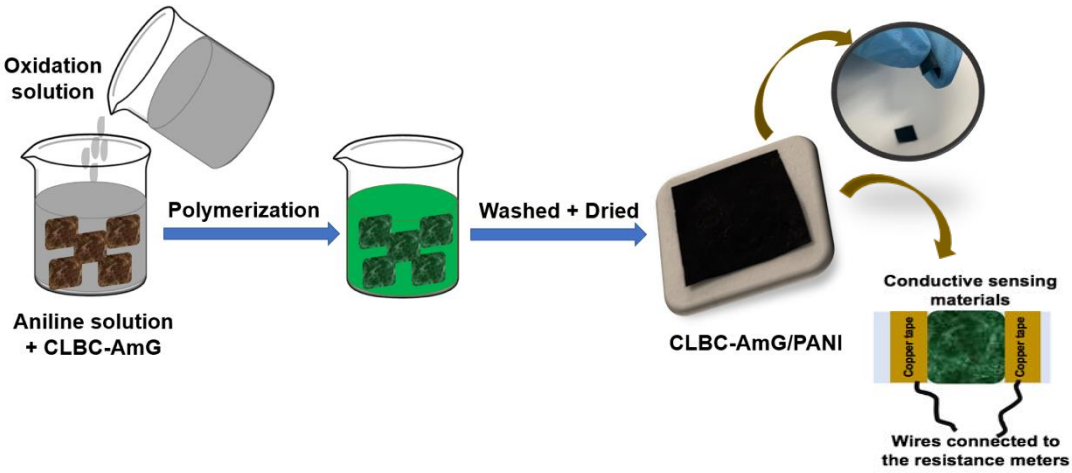

Figure 7-2 The schematic diagram of the process preparation of CLBC-AmG/PANI flexible electrodes.

7.4 Results and Discussion

7.4.1 Characterization of CLBC-AmG and CLBC-AmG/PANI Nanopaper

The structure of AmG and CLBC-AmG were studied by using Raman spectra, both the AmG and CLBC-AmG nanopaper have two characteristic peaks at 1595 and 1349 cm-1 corresponding to the G and D bands, respectively (see Figure 7-3a) [29, 30]. The G band indicates the graphitic structure or whiskers like carbon, whereas the D band refers to the disorder in chemically functionalized graphene sheets. The intensity ratio of D and G bands (I_D/I_G) is used to infer the degree of chemical functionalization in the carbon materials. The CLBC-AmG showed a higher I_D/I_G intensity ratio (1.1) than the AmG (0.97), which is ascribed to BC nanopaper intercalating between the AmG sheets which resulted in increased disorder in the graphene sheets.

A TGA was conducted to observe the thermal stability of the AmG, BC, and CLBC-AmG. As shown in Figure 7-3b, the AmG exhibited good thermal stability and large weight loss starts at temperatures of about 449 °C as the result of the decomposition of amino-carbons, corresponding to previously reported results for the functionalization of graphene with amino groups [28]. The three stages of weight loss can be observed for BC at an initial stage of 35-310 °C, which could be mostly attributed to the moisture evaporation. The major weight loss occurred at the second stage 310-410 °C, and a final weight loss 410-800 °C as the result of degradation and decomposition of

the cellulose backbone [29]. In the CLBC-AmG samples, the AmG can considerably improve the thermal stability of BC nanopaper as shown in Figure 7-3b.

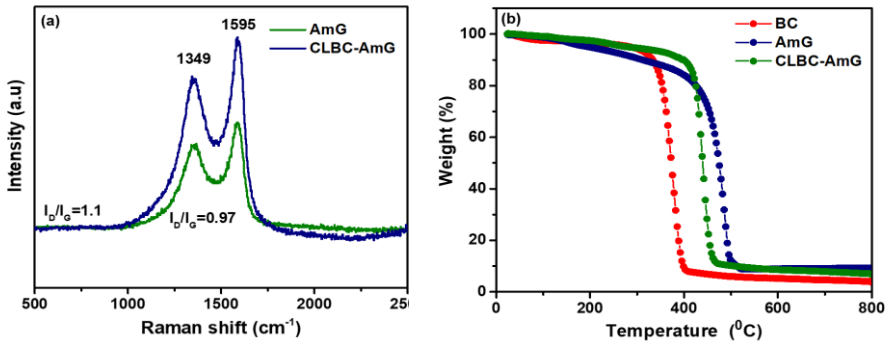

Figure 7-3 (a) Raman spectra of AmG and CLBC-AmG nanopaper. (b) TGA curves of BC, AmG and CLBC-AmG nanopaper.

The morphology and structure of BC, CLBC-AmG, and CLBC-AmG/PANI nanopaper are presented in Figure 7-4a-e. In Figure 7-4a, the SEM image of BC shows an interconnected, three-dimensional (3D), nanoporous network structure. After the crosslinked BC/AmG via one step esterification, the AmG sheets are clearly interlocked within the 3D web-like arrangement of the BC nanopapers by covalent bonds, as covalent bonding occurs between the reactive groups of both BC and AmG (see Figure 7-4b). After in situ polymerization, the surfaces of CLBC-AmG are fully covered by hierarchical PANI, which indicates that the PANI are uniformly grown on the surfaces of CLBC-AmG (Figure 7-4c) [31]. Moreover, the PANI and AmG can be distributed into the BC and forms many channels to provide effective electrolyte transport and active site accessibility as shown in the cross-section of CLBC-AmG/PANI compared with BC/PANI (see Figure 7-4d-e) [31]. It should be noted that the freestanding electrode of CLBC-AmG/PANI has good flexibility and can be easily bent as shown in Figure 7-4f.

7.4.2 Evaluation and Discussion of Sensor Behavior

We investigated the sensing performance of the CLBC-AmG/PANI for CO_2 in terms of percentage response, which is defined by the percentile resistance change when the sensors exposed to CO_2 as follows: Percentage response = $(R_g- R_0)/R_g \times 100$, where R_0 and R_g are the resistances of the sensor before and after exposure to CO_2, respectively. The response and recovery times of the sensor was defined as the time required to reach 90% of the final resistance.

The performance of the CLBC-AmG/PANI and BC/PANI were studied to verify whether the fabricated CLBC-AmG/PANI have any enhanced CO_2 sensing properties compared with BC/PANI. Figure. 7-5a shows the response of the sensors to 50 ppm, 150 ppm and 250 ppm of CO_2. It was indicated that the sensors based on CLBC-AmG/PANI nanopaper exhibit resistance increasing, fast and stable response to CO_2 at RT. It was reported that, upon CO_2 molecule adsorption, the electrons are released at the p-n junction, which might increase the thickness of the depletion layer [32, 33].

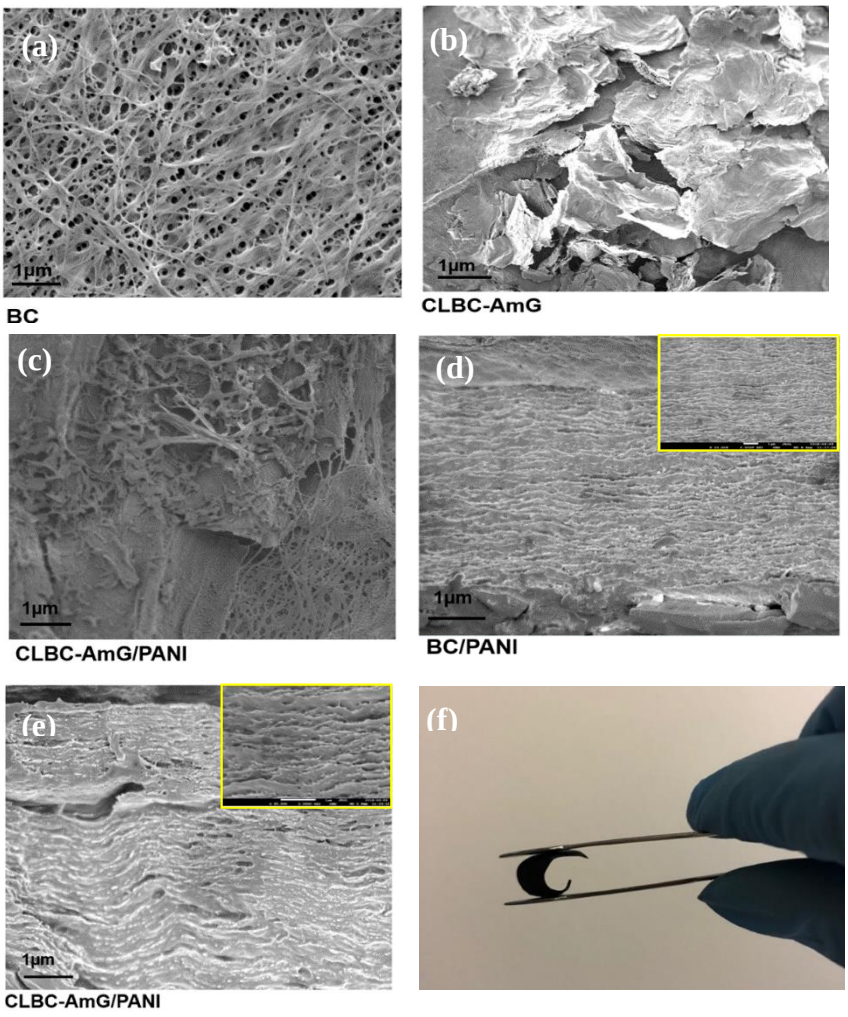

Figure 7-4 (a, b and c) SEM micrograph of BC, CLBC-AmG and CLBC-AmG/PANI. (d and e) Cross-sectional SEM images of BC/PANI and CLBC-AmG/PANI, (f) Photograph of CLBC-AmG/PANI nanopaper.

Thus, when the thickness of the depletion layer at the interface, between the p-type PANI and n-type AmG in AmG/PANI sensors increased, the resistance also increased [33, 34] Besides, the resistance can be increased due to the reaction between the CO_2 and primary amine functional groups to form carbamate where, the number of free amines are reduced and subsequently the proton mobility is reduced which in turn increases the resistance [34]. Furthermore, the CLBC-AmG/PANI sensors were then exposed to various concentrations of CO_2 gas (50, 150, 250, 550, 1500, and 2000 ppm) and the corresponding response of the sensors were recorded. The sensitivity of the CLBC-AmG/PANI based CO_2 sensor was the maximum at 2000 ppm with good response times (~20 s) as shown in Figure 7-5b. Figure 7-5c exhibits the sensitivity of sensor as a function of CO_2 concentration from 50 to 2000 ppm. The sensor has a wide detection range towards CO_2 gas: the response greatly increases with the CO_2 concentration, and is nearly linear with the correlation coefficient close to 0.9867. The limit of quantification (LOQ) of the sensor is defined as the lowest concentration of CO_2 that can be detected, LOQ = 10*Standard deviation (SD)/slope [35, 36]. The detection limit was repeated three times with SD= 2.62. The calculation of LOQ for CLBC-AmG/PANI sensor is ~ 26.55 ppm. It was noted that the sensing properties of the CLBC-AmG/PANI sensor toward 550 ppm CO_2 gas at RT and under humidity levels of 0%, 40% and 80% RH were tested (see Figure 7-a6). No remarkable change in the sensitivity of CLBC-AmG/PANI sensor with the increase in the relative humidity was observed, yet, the response time slightly increased as the relative humidity increased. Moreover, the selectivity is another key factor for the evaluation of a gas sensor, and the results are shown in Figure 7-6b. The CLBC-AmG/PANI sensors were exposed to various gases of ammonia (NH_3), hydrogen (H_2), and carbon monoxide (CO) at 550 ppm. We observed that the response to CO_2 gas displayed more than thrice the magnitude in comparison with the other analytes. It clearly demonstrates that the sensor CLBC-AmG/PANI nanopaper show an excellent selectivity and can be used as a viable candidate for the detection of CO_2 gas.

In our previous publication, we introduced AmG/PANI electrospun nanofiber composites for detecting CO_2 gas. The device features a chemoresistive sensor that can detect the concentration of CO_2 accurately. In this sensor, the functionalized graphene with polyaniline as the active material was deposited onto the surface of the electrospun nanofiber substrate of poly(methyl methacrylate) (PMMA) . Despite the success, the sensor exhibited less flexibility. In this work, we present a freestanding CO_2 sensor with excellent flexibility and manageability, a high response and

high selectivity to CO_2 at RT. In addition, it should be noted that the sensing performance of the CLBC-AmG/PANI nanopaper exhibited better sensitivity and fast response time at RT compared with the previously reported CO_2 sensors as showing in Table 7-1. However, the sensor is irreversible and non-reusable at RT. In conclusion, the CO_2 sensor based on the CLBC-AmG/PANI shows superior flexibility, high selectivity, and accurate detection of CO_2 concentrations ranging from 50 to 2000 ppm, and this concentration range sufficiently covers the need for CO_2 detection for many environmental and industrial applications.

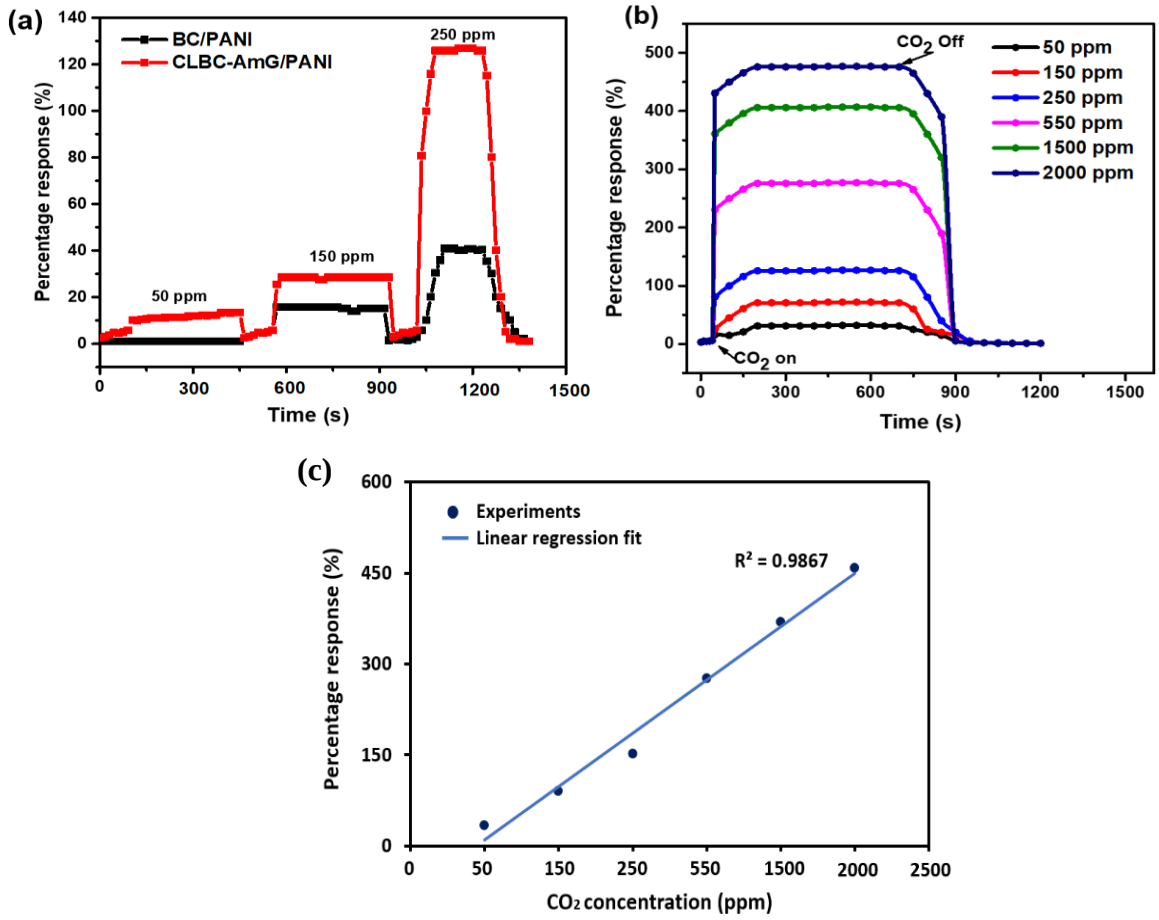

Figure 7-5 (a) displays the comparison of the dynamic response of the resultant sensors based on BC/PANI and CLBC-AmG/PANI toward CO_2 at 50, 150, and 250 ppm concentrations. (b) Percentage response of CLBC-AmG/PANI under various concentrations of CO_2 gas. (**c**) Percentage responses of CLBC-AmG/PANI as a function of CO_2 concentrations.

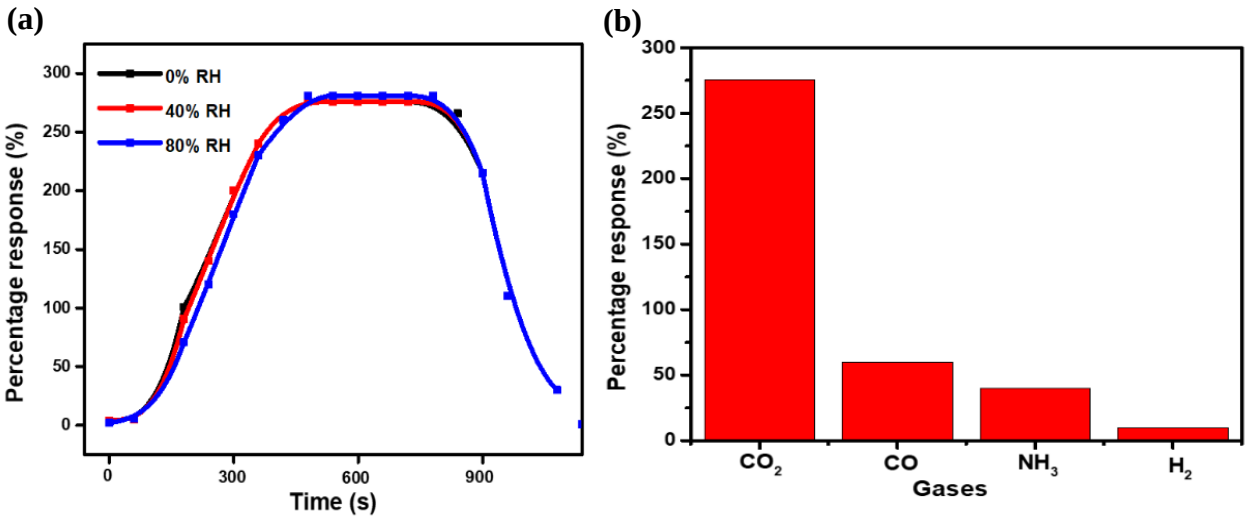

Figure 7-6 (**a**) Percentage response of CLBC-AmG/PANI exposure to CO_2 (550 ppm) under different RHs ranges at RT. (b) Selectivity study of CLBC-AmG/PANI at 550 ppm against other gases.

Table 7-1 Comparison of sensing performance of our proposed CO_2 sensor with other published CO_2 sensors.

Materials	**Range of CO_2 concentration (ppm)**	**Response time (s)**	**Temp. (°C)**	**Ref.**
$La_2O_2CO_3$ nanorods	100-3000	15	325	[37]
La-loaded ZnO	500-5000	90	400	[38]
LaOCL-doped SnO_2 nanofibers	100-20000	24	300	[39]
ZnO nanoflakes	200-1025	<20	250	[40]
CLBC-AmG/PANI nanopaper	50-2000	>20	RT	This work

Lanthanum dioxide carbonate ($La_2O_2CO_3$), Lanthanum (La), Stannic oxide (SnO_2), and Zinc oxide (ZnO).

7.5 Conclusions

We have developed a sensitive room-temperature CO_2 gas sensor based on the CLBC-AmG/PANI nanopaper which was formed by crosslinked BC and AmG via covalent interaction and the PANI was deposited onto the CLBC-AmG surfaces. The CLBC-AmG nanopaper was characterized using SEM, Raman and TGA techniques. The sensor exhibited a high sensitivity (50 ppm) and selectivity for CO_2 gas, including superior flexibility and manageability. The sensor responses showed a nearly linear relationship with CO_2 concentration. Since the preparation process for the CLBC-AmG/PANI sensors was easy and the sensing performance reliable, we believe it has great potential for the sensitive detection of CO_2 gas in different fields.

Author Contributions

Conceptualization, H.A.; methodology, H.A. and B.H.; software H.A and B.H.; validation, H.A., B.H. and A.A.; formal analysis, H.A.; investigation, H.A.; resources, A.A.; data curation, H.A.; writing—original draft preparation, H.A.; writing—review and editing, H.A; .B.H. and A.A.; visualization, H.A.; supervision, A.A.; project administration, A.A.; funding acquisition, A.A.

Funding

This research was supported by NSERC (National Science and Engineering Research Council of Canada).

7.6 Acknowledgments

The authors thank the Ministry of Education of Saudi Arabia for their financial support to Hanan Abdali. The authors also thank Mrs. Anic Desforges for her help in building the system for CLBC-AmG preparation and Mr. Sébastien Chenard for his invaluable help in designing the gas detection setup. The authors are grateful to Mrs. Claire Cerclé and Mr. Matthieu Gauthier for their kind help during this study.

Conflicts of Interest

The authors declare no conflict of interest.

7.7 References

1. Yuan, Z., et al., *Approaches to Enhancing Gas Sensing Properties: A Review.* Sensors, 2019. **19**(7): p. 1495.
2. Hafiz, S.M., et al., *A practical carbon dioxide gas sensor using room-temperature hydrogen plasma reduced graphene oxide.* Sensors and Actuators B: Chemical, 2014. **193**: p. 692-700.
3. Lee, J.-H., *Gas sensors using hierarchical and hollow oxide nanostructures: overview.* Sensors and Actuators B: Chemical, 2009. **140**(1): p. 319-336.
4. Li, Y. and J. Shi, *Hollow-structured mesoporous materials: chemical synthesis, functionalization and applications.* Advanced Materials, 2014. **26**(20): p. 3176-3205.
5. Latif, U. and F.L. Dickert, *Graphene hybrid materials in gas sensing applications.* Sensors, 2015. **15**(12): p. 30504-30524.
6. Bai, L., et al., *Graphene for Energy Storage and Conversion: Synthesis and Interdisciplinary Applications.* Electrochemical Energy Reviews, 2019: p. 1-36.
7. Sun, L., et al., *Super-aligned carbon nanotube/graphene hybrid materials as a framework for sulfur cathodes in high performance lithium sulfur batteries.* Journal of Materials Chemistry A, 2015. **3**(10): p. 5305-5312.
8. Chen, K., et al., *Graphene-based materials for flexible energy storage devices.* Journal of energy chemistry, 2018. **27**(1): p. 12-24.
9. Qiu, B., M. Xing, and J. Zhang, *Recent advances in three-dimensional graphene based materials for catalysis applications.* Chemical Society Reviews, 2018. **47**(6): p. 2165-2216.
10. Priyadarsini, S., et al., *Graphene and graphene oxide as nanomaterials for medicine and biology application.* Journal of Nanostructure in Chemistry, 2018. **8**(2): p. 123-137.
11. Llobet, E., *Gas sensors using carbon nanomaterials: A review.* Sensors and Actuators B: Chemical, 2013. **179**: p. 32-45.
12. Ioniţă, M., et al., *Graphene and functionalized graphene: extraordinary prospects for nanobiocomposite materials.* Composites Part B: Engineering, 2017. **121**: p. 34-57.
13. Fratoddi, I., et al., *Chemiresistive polyaniline-based gas sensors: A mini review.* Sensors and Actuators B: Chemical, 2015. **220**: p. 534-548.
14. Sengupta, P.P., S. Barik, and B. Adhikari, *Polyaniline as a gas-sensor material.* Materials and manufacturing processes, 2006. **21**(3): p. 263-270.
15. Abu-Thabit, N.Y., *Chemical oxidative polymerization of polyaniline: A practical approach for preparation of smart conductive textiles.* Journal of Chemical Education, 2016. **93**(9): p. 1606-1611.
16. Tran, H.D., et al., *The oxidation of aniline to produce "polyaniline": a process yielding many different nanoscale structures.* Journal of Materials Chemistry, 2011. **21**(11): p. 3534-3550.

17. Wu, Z., et al., *Enhanced sensitivity of ammonia sensor using graphene/polyaniline nanocomposite.* Sensors and Actuators B: Chemical, 2013. **178**: p. 485-493.

18. Konwer, S., A.K. Guha, and S.K. Dolui, *Graphene oxide-filled conducting polyaniline composites as methanol-sensing materials.* Journal of Materials Science, 2013. **48**(4): p. 1729-1739.

19. Zou, Y., et al., *Doping composite of polyaniline and reduced graphene oxide with palladium nanoparticles for room-temperature hydrogen-gas sensing.* international journal of hydrogen energy, 2016. **41**(11): p. 5396-5404.

20. Khan, M.A.H., M.V. Rao, and Q. Li, *Recent advances in electrochemical sensors for detecting toxic gases: NO2, SO2 and H2S.* Sensors, 2019. **19**(4): p. 905.

21. Heli, B., *Bacterial Cellulose Supported Sensor for Bacteria and Gas Detection Development*. 2017, Ph.D Thesis. École Polytechnique de Montréal. p. 1-147.

22. Eichhorn, S., et al., *Current international research into cellulosic fibres and composites.* Journal of materials Science, 2001. **36**(9): p. 2107-2131.

23. Wei, H., et al., *Environmental science and engineering applications of nanocellulose-based nanocomposites.* Environmental Science: Nano, 2014. **1**(4): p. 302-316.

24. Moon, R.J., et al., *Cellulose nanomaterials review: structure, properties and nanocomposites.* Chemical Society Reviews, 2011. **40**(7): p. 3941-3994.

25. Heli, B., et al., *Modulation of population density and size of silver nanoparticles embedded in bacterial cellulose via ammonia exposure: visual detection of volatile compounds in a piece of plasmonic nanopaper.* Nanoscale, 2016. **8**(15): p. 7984-7991.

26. Kiziltas, E.E., et al., *Electrically conductive nano graphite-filled bacterial cellulose composites.* Carbohydrate polymers, 2016. **136**: p. 1144-1151.

27. Nery, E.W. and L.T. Kubota, *Sensing approaches on paper-based devices: a review.* Analytical and bioanalytical chemistry, 2013. **405**(24): p. 7573-7595.

28. Abdali, H. and A. Ajji, *Preparation of Electrospun Nanocomposite Nanofibers of Polyaniline/Poly(methyl methacrylate) with Amino-Functionalized Graphene.* Polymers, 2017. **9**(9): p. 453.

29. Liu, Y., et al., *Facile synthesis of bacterial cellulose fibres covalently intercalated with graphene oxide by one-step cross-linking for robust supercapacitors.* Journal of Materials Chemistry C, 2015. **3**(5): p. 1011-1017.

30. Jorio, A., et al., *Measuring disorder in graphene with the G and D bands.* physica status solidi (b), 2010. **247**(11-12): p. 2980-2982.

31. Liu, R., et al., *A flexible polyaniline/graphene/bacterial cellulose supercapacitor electrode.* New Journal of Chemistry, 2017. **41**(2): p. 857-864.

32. Sun, J., et al., *Preparation of polypyrrole@ WO3 hybrids with pn heterojunction and sensing performance to triethylamine at room temperature.* Sensors and Actuators B: Chemical, 2017. **238**: p. 510-517.

33. Tai, H., et al., *Fabrication and gas sensitivity of polyaniline–titanium dioxide nanocomposite thin film.* Sensors and Actuators B: Chemical, 2007. **125**(2): p. 644-650.

34. Doan, T.C., et al., *Carbon dioxide detection with polyethylenimine blended with polyelectrolytes.* Sensors and Actuators B: Chemical, 2014. **201**: p. 452-459.
35. Shrivastava, A. and V.B. Gupta, *Methods for the determination of limit of detection and limit of quantitation of the analytical methods.* Chronicles of young scientists, 2011. **2**(1): p. 21.36.
36. Zaki, S.E., et al., *Role of oxygen vacancies in vanadium oxide and oxygen functional groups in graphene oxide for room temperature CO_2 gas sensors.* Sensors and Actuators A: Physical, 2019. **294**: p. 17-24.
37. Chen, G., et al., *Lanthanum dioxide carbonate La2O2CO3 nanorods as a sensing material for chemoresistive CO2 gas sensor.* Electrochimica Acta, 2014. **127**: p. 355-361.
38. Jeong, Y.-J., C. Balamurugan, and D.-W. Lee, *Enhanced CO2 gas-sensing performance of ZnO nanopowder by La loaded during simple hydrothermal method.* Sensors and Actuators B: Chemical, 2016. **229**: p. 288-296.
39. Xiong, Y., et al., *Effective CO2 detection based on LaOCl-doped SnO2 nanofibers: insight into the role of oxygen in carrier gas.* Sensors and Actuators B: Chemical, 2017. **241**: p. 725-734.
40. Kanaparthi, S. and S.G. Singh, *Chemiresistive Sensor Based on Zinc Oxide Nanoflakes for CO2 Detection.* ACS Applied Nano Materials, 2019. **2**(2): p. 700-706.

CHAPTER 8 GENERAL DISCUSSION

Environmental pollution has become a hot topic faced by the whole world where issues of prevention remain a challenge. As such, sensors are being designed to detect toxic levels of various gasses such as CO_2 in order to avoid cataclysmic disasters. Gas sensors are devices that convert the gas concentration into corresponding electrical signal. Sensors can play a crucial part in environmental monitoring, public safety, industrial chemical processing, agriculture and even medicine. The science and technology for developing gas sensors lean towards high sensitivity, high selectivity, fast response times, low cost, low power consumption, stability and portability has increased research into new and superior gas-sensing materials. For gas sensing applications in particular, graphene-based gas sensors have attracted tremendous attention, mainly due to their exceptional chemical and excellent electronic properties, optimal mechanical stiffness, and electrical conductivity, however, many of these characteristics can only be exploited once the graphene is attached to functional groups. Additionally, PANI with its unique electrical, electrochemical, and optical properties can also be utilized as efficient sensors for monitoring organic and inorganic compounds. Besides these properties, the sensor-based on nanofibers has a high specific surface area to volume ratio and porosity, which would provide high sensitivity, fast response, and high recovery.

Despite extensive studies in CO_2 sensing consisting of various complex structures and sensing conditions, better performing CO_2 sensors that can be easily designed and fabricated are needed. For this purpose, the first part of this work is aimed at modifying the graphene surfaces with amino groups which are known to be sensitive to CO_2 gas by using EDA (NH_2–$(CH_2)_2$–NH_2). Amine groups are attributed with high reactivity enabling them to react with other chemical groups easily and providing a favorable approach in applications of graphene/polymer nanocomposites. As the Nitrogen atom in amine is more nucleophilic than the oxygen atom, it can be expected that substituting graphene with amine will increase the nucleophilic properties of graphene. Consequently, interfacial binding between the materials of interest and graphene can result. These interactions will improve the performance and functionality for the intended applications of graphene. The successful functionalization of graphene with amino groups was confirmed when the C/O atomic ratio in AmG was increased to 8.2 compared with GO and rGO 2.0 and 6.2, respectively. Also, the amination process led to the formation of (N=C) at 398.5 eV, (C–NH_2) at

399.7 eV, (C–N–C) at 400.4 eV, and (C–N^+–C) at 401.6 eV in N1s spectra of AmG and the most intense peak is assigned to the C–NH_2, indicating that AmG was successfully prepared.

Then, the electrospinning of PANI nanofibers with highly dispersed AmG nanosheets in the nanofibers were successfully fabricated. The functionalized graphene with amino groups leads to stabilizing graphene dispersion in the electrospinning solution of $CHCl_3$/DMF, which prevents the aggregation of the AmG nanosheets. Subsequently, the non-conductive hosting polymer PMMA was added as copolymer to the electrospinning solution to improve PANI's processability. Consequently, electrospinning the solution of AmG/PANI/PMMA resulted in highly interconnected nanofibers with a diameter ranging between 35 and 133 nm. This decrease in the average nanofiber diameter of AmG/ PANI/PMMA in comparison to PANI/PMMA average nanofibers diameter 267 ± 55 nm occurs owing to the presence of AmG nanosheets in the nanofibers. This is attributed to the electrical conductivity in the starting solution reinforced by the presence of the AmG where the more conductive the solution, the more likelihood of obtaining thinner fibers. The presence of AmG nanosheets in the PANI/PMMA nanofibers were confirmed by TEM. The TEM images clearly display the individual AmG nanosheets dispersed in the PANI/PMMA matrix without aggregation, because the lateral size of AmG (a few 100 nm to a few μm) is comparable to the fiber diameter. Finally, to understand the effect of the addition of AmG on the thermal properties of PANI/PMMA nanofibers, the TGA was performed. The thermal degradation temperature of the AmG/PANI/PMMA was presented around 441 °C, and this substantiates the strong interaction that exists between the PANI and the AmG. However, the electrical conductivity of electrospun nanofibers of AmG/PANI/PMMA was not as expected, as one of the objectives was to have electrospun nanofibers of AmG/PANI/PMMA with good electrical conductivity.

Therefore, it was decided in the second part to fabricate polymerized nanofiber nanocomposites. The AmG/PANI as a sensing material for sensing CO_2 gas were deposited on the surface of the electrospun PMMA nanofibers. The PMMA nanofiber mats were produced by using electrospinning process. Then, these mats were treated with UV-radiation for 5 min (on each side) at wavelength 365 nm to modify the PMMA surfaces by oxidizing, resulting in carboxylic acid groups, and by increasing the radical oxygen content to the exposed surfaces, resulting in the

nanofiber surface becoming more hydrophilic. The contact angle of PMMA nanofibers after UV-radiation was significantly decreased to 85.3° from 133.1°, which corresponds to better wettability.

Afterwards, the AmG/PANI were *in situ* polymerized at the surface of electrospun PMMA nanofibers for different polymerization times of 1, 2 and 4 h and consequently a period of 1 h was chosen for further studies because it showed good electrical conductivity and uniform dispersion of AmG/PANI along the PMMA nanofibers. The AmG/PANI sensor that was fabricated revealed good CO_2 sensing properties, fast response (10 s) and recovery times (20 s) along with good stability for one month at RT. The superior CO_2 sensing properties of the AmG/PANI nanofibers are attributed to the presence of primary amine functional group, p-n junction between p-type PANI and n-type AmG which was discussed further in Chapter 6. Despite the superior CO_2 sensing properties, the sensor nanofibers exhibited less flexibility which could be attributed to the long-time exposure to the UV-radiation and polymerization as well as washing several times with DI water and ethanol to remove the residual oxidant.

Therefore, considering the outcome above, the BC nanofibers were selected as a substrate to deposit the active sensing materials onto its surfaces due to its mechanical robustness, high surface area, permeability to liquid and gases, and elevated water uptake capacity. As well as, the abundant functional groups of BC the AmG and PANI composites can strongly bind with BC nanofibers via covalent bonding or electrostatic interactions. The third part was to design a flexible freestanding sensor using BC as a flexible substrate and AmG/PANI as active materials for detecting CO_2 at RT. The facile process for the covalent intercalation of AmG with BC nanofibers via one-step esterification between the COOH groups of AmG and OH of BC was prepared. Raman spectra of CLBC-AmG displayed a higher I_D/I_G intensity ratio (1.1) than the AmG (0.97), which is ascribed to BC nanofibers intercalating between the AmG sheets which resulted in increased disorder in the graphene sheets. Furthermore, the SEM cross sectional images of CLBC-AmG/PANI compared with BC/PANI confirmed that the PANI and AmG distributed into the BC and formed many channels to provide effective electrolyte transport. The sensing properties of CLBC-AmG/PANI for detecting CO_2 gas at RT showed high flexibility, manageability, fast response (20 s), excellent selectivity, and an accurate detection of CO_2 concentrations ranging from 50 to 2000 ppm. Nevertheless, the sensor is not reversible nor reusable at RT, which was not as expected for CLBC-AmG/PANI sensors. Yet, since the preparation process for the CLBC-AmG/PANI sensors was easy and the sensing performance reliable, we believe it has great potential for the sensitive

detection of CO_2 gas in many environmental and industrial applications. However, more investigation is still needed to understand and improve the recovery time and stability of the CLBC-AmG/PANI sensor.

CHAPTER 9 CONCLUSIONS AND RECOMMENDATIONS

9.1 Conclusions

The current research work focuses on developing a lightweight, room temperature sensor by using AmG with PANI as an innovative sensing material to detect toxic gases such as CO_2. To do so, the first part of this research identified the primary materials and process factors necessary to fabricate amino-functionalized graphene and then examine the morphology and microstructure of the AmG, including characterizing the morphology and properties of the AmG/PANI/PMMA nanofiber composites. The following conclusions can be drawn from the results:

1. The Amino-functionalized graphene was successfully prepared with less damage to the graphitic structure of the graphene.
2. The functionalized graphene with amino groups lead to stabilizing graphene dispersion in the electrospinning solution of $CHCl_3$/DMF.
3. Optimal processing conditions included pumping of AmG/PANI/PMMA solutions through a 18 G needle, at a flow rate of 0.3 mL/h, a voltage of 18-20 kV and a distance of 15 cm from the needle tip to collector plate.
4. Ultrafine electrospun nanofibers of PANI/PMMA with AmG were obtained with a diameter ranging between 35 and 133 nm.
5. The thermal stability of AmG/PANI/PMMA nanofibers increased by 90°C after the addition of AmG in comparison with neat PANI/PMMA.

The second part of this research focused on the fabrication AmG/PANI nanofiber nanocomposites for room temperature CO_2 sensing. The following conclusions can be drawn from the results:

1. An effective, and facile method used to fabricate nanofiber composites of AmG/PANI sensor for sensing CO_2 gas.
2. The AmG/PANI nanofiber composite materials were synthesized successfully by *in-situ* chemical oxidative polymerization of aniline containing well-dispersed AmG on the surface of electrospun PMMA nanofibers.

3. High sensitivity (20 ppm), fast response (10 s) and recovery time (20 s) for CO_2 sensor based AmG/PANI nanofibers with constant stability for 30 days at RT was obtained.
4. Excellent selectivity of the AmG/PANI sensor toward CO_2 when compared with any other gas used for testing under the same conditions.

The third part of this research focused on designing a flexible freestanding sensor using BC as a flexible substrate and AmG/PANI as an active material for detecting CO_2 at RT. The following conclusions can be drawn from the results:

1. The CLBC-AmG nanofiber nanocomposites were synthesized successfully via one-step esterification.
2. The CLBC-AmG/PANI flexible freestanding electrode was fabricated successfully.
3. Room temperature CO_2 gas sensing with superior flexibility, manageability, higher accuracy, fast response (20 s) and high selectivity was designed.

9.2 Recommendations

The following aspects are recommended for future exploration:

1. Investigate amino functionalized graphene for pathogen detection such as with bacteria antibodies or aptamers (i.e. *E. Coli* antibodies/ aptamers)
2. Study the application of the AmG based polymer nanofibers for antimicrobial activity in food packaging.
3. Optimize the minimum concentration of ammonium peroxydisulfate (APS) as an oxidant to polymerize the aniline on PMMA nanofibers leading to excellent conductivity and less damage on PMMA nanofibers.
4. Study the use of other oxidant agents in the oxidative polymerization of aniline on the PMMA nanofibers.
5. Investigate the usage of plasma treatment on PMMA nanofibers to improve their wettability and polymerization.

6. Study the utilization of other electrospun polymers in this system such as polycaprolactone (PCL) to improve the flexibility of the nanofiber sensor.
7. Investigate the usage of CLBC-AmG nanofibers in supercapacitors application.
8. Evaluate the application of CLBC-AmG/PANI nanofibers for biosensors in pathogen detection.

BIBLIOGRAPHY

1. Muzikante, I., et al., *A novel gas sensor transducer based on phthalocyanine heterojunction devices.* Sensors, 2007. **7**(11): p. 2984-2996.
2. Baha, H. and Z. Dibi, *A novel neural network-based technique for smart gas sensors operating in a dynamic environment.* Sensors, 2009. **9**(11): p. 8944-8960.
3. Wang, L.-C., et al., *A single-walled carbon nanotube network gas sensing device.* Sensors, 2011. **11**(8): p. 7763-7772.
4. Abadi, M., et al., *Characterization of mixed xWO3 (1-x) Y2O3 Nanoparticle thick film for gas sensing application.* Sensors, 2010. **10**(5): p. 5074-5089.
5. Liu, X., et al., *A survey on gas sensing technology.* Sensors, 2012. **12**(7): p. 9635-9665.
6. Herrán, J., G.G. Mandayo, and E. Castano, *Solid state gas sensor for fast carbon dioxide detection.* Sensors and Actuators B: Chemical, 2008. **129**(2): p. 705-709.
7. Mandayo, G.G., et al., *Performance of a CO2 impedimetric sensor prototype for air quality monitoring.* Sensors, 2011. **11**(5): p. 5047-5057.
8. Irimia-Vladu, M. and J.W. Fergus, *Suitability of emeraldine base polyaniline-PVA composite film for carbon dioxide sensing.* Synthetic metals, 2006. **156**(21-24): p. 1401-1407.
9. Chiang, C.-J., et al., *In situ fabrication of conducting polymer composite film as a chemical resistive CO2 gas sensor.* Microelectronic Engineering, 2013. **111**: p. 409-415.
10. Nemade, K. and S. Waghuley, *Role of defects concentration on optical and carbon dioxide gas sensing properties of Sb2O3/graphene composites.* Optical Materials, 2014. **36**(3): p. 712-716.
11. Srinives, S., et al., *A miniature chemiresistor sensor for carbon dioxide.* Analytica chimica acta, 2015. **874**: p. 54-58.
12. Yong, Y., et al., *Adsorption of gas molecules on a graphitic GaN sheet and its implications for molecule sensors.* RSC Advances, 2017. **7**(80): p. 51027-51035.
13. Donarelli, M. and L. Ottaviano, *2D materials for gas sensing applications: A review on graphene oxide, MoS2, WS2 and phosphorene.* Sensors, 2018. **18**(11): p. 3638.
14. Hafiz, S.M., et al., *A practical carbon dioxide gas sensor using room-temperature hydrogen plasma reduced graphene oxide.* Sensors and Actuators B: Chemical, 2014. **193**: p. 692-700.
15. Novoselov, K.S., et al., *Two-dimensional gas of massless Dirac fermions in graphene.* nature, 2005. **438**(7065): p. 197.
16. Lee, C., et al., *Measurement of the elastic properties and intrinsic strength of monolayer graphene.* science, 2008. **321**(5887): p. 385-388.
17. Kuila, T., et al., *Chemical functionalization of graphene and its applications.* Progress in Materials Science, 2012. **57**(7): p. 1061-1105.
18. Gao, W., *The chemistry of graphene oxide*, in *Graphene oxide*. 2015, Springer. p. 61-95.

19. Doan, T.C., et al., *Carbon dioxide detection with polyethylenimine blended with polyelectrolytes.* Sensors and Actuators B: Chemical, 2014. **201**: p. 452-459.

20. Hong, H.S., et al., *Selective detection of carbon dioxide using LaOCl-functionalized SnO2 nanowires for air-quality monitoring.* Talanta, 2012. **88**: p. 152-159.

21. Nemade, K. and S. Waghuley, *Highly responsive carbon dioxide sensing by graphene/Al 2 O 3 quantum dots composites at low operable temperature.* Indian Journal of Physics, 2014. **88**(6): p. 577-583.

22. Ding, B., et al., *Gas sensors based on electrospun nanofibers.* Sensors, 2009. **9**(3): p. 1609-1624.

23. McGrath, M.J. and C.N. Scanaill, *Sensing and sensor fundamentals*, in *Sensor Technologies*. 2013, Springer. p. 15-50.

24. Awang, Z., *Gas sensors: a review.* Sens. Transducers, 2014. **168**: p. 61-75.

25. Capone, S., et al., *Solid state gas sensors: state of the art and future activities.* Journal of Optoelectronics and Advanced Materials, 2003. **5**(5): p. 1335-1348.

26. Bakker, E. and M. Telting-Diaz, *Electrochemical sensors.* Analytical chemistry, 2002. **74**(12): p. 2781-2800.

27. Gan, T. and S. Hu, *Electrochemical sensors based on graphene materials.* Microchimica Acta, 2011. **175**(1-2): p. 1-19.

28. Yu, X., et al., *Fabrication technologies and sensing applications of graphene-based composite films: advances and challenges.* Biosensors and Bioelectronics, 2017. **89**: p. 72-84.

29. Haynes, A.S., *Electrospun conducting polymer composites for chemo-resistive environmental and health monitoring applications*. 2008, The Graduate School, Stony Brook University: Stony Brook, NY.

30. Chen, D., S. Lei, and Y. Chen, *A single polyaniline nanofiber field effect transistor and its gas sensing mechanisms.* Sensors, 2011. **11**(7): p. 6509-6516.

31. Qu, J., Y. Chai, and S. Yang, *A real-time de-noising algorithm for e-noses in a wireless sensor network.* Sensors, 2009. **9**(2): p. 895-908.

32. Vink, J., H. Verhoeven, and J. Huijsing. *Response speed optimization of thermal gas-flow sensors for medical application*. in *Proceedings of the International Solid-State Sensors and Actuators Conference-TRANSDUCERS'95*. 1995. IEEE.

33. Hulko, M., et al., *Cytochrome C biosensor—A model for gas sensing.* Sensors, 2011. **11**(6): p. 5968-5980.

34. Refaat, T.F., et al., *Backscatter 2-μm lidar validation for atmospheric CO_2 differential absorption lidar applications.* IEEE Transactions on Geoscience and Remote Sensing, 2010. **49**(1): p. 572-580.

35. Ke, M.-T., et al., *A MEMS-based benzene gas sensor with a self-heating WO_3 sensing layer*. Sensors, 2009. **9**(4): p. 2895-2906.

36. Kwon, J., et al. *A study on NDIR-based CO_2 sensor to apply remote air quality monitoring system*. in *2009 Iccas-Sice*. 2009. IEEE.

37. Tamaekong, N., et al., *Flame-spray-made undoped zinc oxide films for gas sensing applications.* Sensors, 2010. **10**(8): p. 7863-7873.

38. Belov, I., et al. *Thermal and flow analysis of SiC-based gas sensors for automotive applications*. in *5th International Conference on Thermal and Mechanical Simulation and Experiments in Microelectronics and Microsystems, 2004. EuroSimE 2004. Proceedings of the*. 2004. IEEE.

39. Jimenez-Cadena, G., J. Riu, and F.X. Rius, *Gas sensors based on nanostructured materials.* Analyst, 2007. **132**(11): p. 1083-1099.

40. Wang, C., et al., *Metal oxide gas sensors: sensitivity and influencing factors.* Sensors, 2010. **10**(3): p. 2088-2106.

41. Abideen, Z.U., et al., *Electrospun metal oxide composite nanofibers gas sensors: A review.* Journal of the Korean Ceramic Society, 2017. **54**(5): p. 366-379.

42. Dey, A., *Semiconductor metal oxide gas sensors: A review.* Materials Science and Engineering: B, 2018. **229**: p. 206-217.

43. Yoon, H. and J. Jang, *Conducting ‐polymer nanomaterials for high ‐performance sensor applications: issues and challenges.* Advanced Functional Materials, 2009. **19**(10): p. 1567-1576.

44. Yoon, H., *Current trends in sensors based on conducting polymer nanomaterials.* Nanomaterials, 2013. **3**(3): p. 524-549.

45. Llobet, E., *Gas sensors using carbon nanomaterials: A review.* Sensors and Actuators B: Chemical, 2013. **179**: p. 32-45.

46. Pumera, M., *The electrochemistry of carbon nanotubes: fundamentals and applications.* Chemistry–A European Journal, 2009. **15**(20): p. 4970-4978.

47. Latif, U. and F.L. Dickert, *Graphene hybrid materials in gas sensing applications.* Sensors, 2015. **15**(12): p. 30504-30524.

48. Geim, A.K. and K.S. Novoselov, *The rise of graphene*, in *Nanoscience and Technology: A Collection of Reviews from Nature Journals*. 2010, World Scientific. p. 11-19.

49. Singh, V., et al., *Graphene based materials: past, present and future.* Progress in materials science, 2011. **56**(8): p. 1178-1271.

50. Hamzah, A.A., R.S. Selvarajan, and B.Y. Majlis, *Graphene for biomedical applications: a review.* Sains Malaysiana, 2017. **46**(7): p. 1125-1139.

51. Soldano, C., A. Mahmood, and E. Dujardin, *Production, properties and potential of graphene.* carbon, 2010. **48**(8): p. 2127-2150.

52. Balandin, A.A., et al., *Superior thermal conductivity of single-layer graphene.* Nano letters, 2008. **8**(3): p. 902-907.

53. Bolotin, K.I., et al., *Ultrahigh electron mobility in suspended graphene.* Solid State Communications, 2008. **146**(9-10): p. 351-355.

54. Stoller, M.D., et al., *Graphene-based ultracapacitors.* Nano letters, 2008. **8**(10): p. 3498-3502.

55. Kuilla, T., et al., *Recent advances in graphene based polymer composites.* Progress in polymer science, 2010. **35**(11): p. 1350-1375.

56. Stankovich, S., et al., *Graphene-based composite materials.* nature, 2006. **442**(7100): p. 282.

57. Nethravathi, C., et al., *Graphite oxide-intercalated anionic clay and its decomposition to graphene− inorganic material nanocomposites.* Langmuir, 2008. **24**(15): p. 8240-8244.

58. Szabó, T., A. Szeri, and I. Dékány, *Composite graphitic nanolayers prepared by self-assembly between finely dispersed graphite oxide and a cationic polymer.* Carbon, 2005. **43**(1): p. 87-94.

59. Wong, C.H.A. and M. Pumera, *Stripping voltammetry at chemically modified graphenes.* RSC Advances, 2012. **2**(14): p. 6068-6072.

60. Szabó, T., et al., *Evolution of surface functional groups in a series of progressively oxidized graphite oxides.* Chemistry of materials, 2006. **18**(11): p. 2740-2749.

61. Stankovich, S., et al., *Synthesis of graphene-based nanosheets via chemical reduction of exfoliated graphite oxide.* carbon, 2007. **45**(7): p. 1558-1565.

62. Tung, V.C., et al., *High-throughput solution processing of large-scale graphene.* Nature nanotechnology, 2009. **4**(1): p. 25.

63. Wang, H., et al., *Solvothermal reduction of chemically exfoliated graphene sheets.* Journal of the American Chemical Society, 2009. **131**(29): p. 9910-9911.

64. Si, Y. and E.T. Samulski, *Synthesis of water soluble graphene.* Nano letters, 2008. **8**(6): p. 1679-1682.

65. Wang, G., et al., *Facile synthesis and characterization of graphene nanosheets.* The Journal of Physical Chemistry C, 2008. **112**(22): p. 8192-8195.

66. Zhang, J., et al., *Reduction of graphene oxide via L-ascorbic acid.* Chemical Communications, 2010. **46**(7): p. 1112-1114.

67. Kim, H., A.A. Abdala, and C.W. Macosko, *Graphene/polymer nanocomposites.* Macromolecules, 2010. **43**(16): p. 6515-6530.

68. Schniepp, H.C., et al., *Functionalized single graphene sheets derived from splitting graphite oxide.* The Journal of Physical Chemistry B, 2006. **110**(17): p. 8535-8539.

69. McAllister, M.J., et al., *Single sheet functionalized graphene by oxidation and thermal expansion of graphite.* Chemistry of materials, 2007. **19**(18): p. 4396-4404.

70. Steurer, P., et al., *Functionalized graphenes and thermoplastic nanocomposites based upon expanded graphite oxide.* Macromolecular rapid communications, 2009. **30**(4‐5): p. 316-327.

71. Park, S. and R.S. Ruoff, *Chemical methods for the production of graphenes.* Nature nanotechnology, 2009. **4**(4): p. 217.

72. Salavagione, H.J., M.A. Gomez, and G. Martinez, *Polymeric modification of graphene through esterification of graphite oxide and poly (vinyl alcohol).* Macromolecules, 2009. **42**(17): p. 6331-6334.

73. Liu, Z., et al., *PEGylated nanographene oxide for delivery of water-insoluble cancer drugs.* Journal of the American Chemical Society, 2008. **130**(33): p. 10876-10877.

74. Dong, X., W. Huang, and P. Chen, *In situ synthesis of reduced graphene oxide and gold nanocomposites for nanoelectronics and biosensing.* Nanoscale Res Lett, 2011. **6**(1): p. 60.

75. Zhou, X., et al., *In situ synthesis of metal nanoparticles on single-layer graphene oxide and reduced graphene oxide surfaces.* The Journal of Physical Chemistry C, 2009. **113**(25): p. 10842-10846.

76. Mao, S., et al., *Specific protein detection using thermally reduced graphene oxide sheet decorated with gold nanoparticle‐antibody conjugates.* Advanced materials, 2010. **22**(32): p. 3521-3526.

77. Vadukumpully, S., et al., *Functionalization of surfactant wrapped graphene nanosheets with alkylazides for enhanced dispersibility.* Nanoscale, 2011. **3**(1): p. 303-308.

78. Liu, Y., et al., *Biocompatible graphene oxide-based glucose biosensors.* Langmuir, 2010. **26**(9): p. 6158-6160.

79. Stankovich, S., et al., *Stable aqueous dispersions of graphitic nanoplatelets via the reduction of exfoliated graphite oxide in the presence of poly (sodium 4-styrenesulfonate).* Journal of Materials Chemistry, 2006. **16**(2): p. 155-158.

80. Su, P.-G. and Z.-M. Lu, *Flexibility and electrical and humidity-sensing properties of diamine-functionalized graphene oxide films.* Sensors and Actuators B: Chemical, 2015. **211**: p. 157-163.

81. Su, Q., et al., *Composites of graphene with large aromatic molecules.* Advanced materials, 2009. **21**(31): p. 3191-3195.

82. Moayeri, A. and A. Ajji, *Fabrication of polyaniline/poly (ethylene oxide)/non-covalently functionalized graphene nanofibers via electrospinning.* Synthetic Metals, 2015. **200**: p. 7-15.

83. Xu, Y., et al., *Three-dimensional self-assembly of graphene oxide and DNA into multifunctional hydrogels.* ACS nano, 2010. **4**(12): p. 7358-7362.

84. Potts, J.R., et al., *Graphene-based polymer nanocomposites.* Polymer, 2011. **52**(1): p. 5-25.

85. Chatterjee, S., F. Nüesch, and B. Chu, *Crystalline and tensile properties of carbon nanotube and graphene reinforced polyamide 12 fibers.* Chemical Physics Letters, 2013. **557**: p. 92-96.

86. Du, J. and H.M. Cheng, *The fabrication, properties, and uses of graphene/polymer composites.* Macromolecular Chemistry and Physics, 2012. **213**(10‐11): p. 1060-1077.

87. Rafiee, M.A., et al., *Fracture and fatigue in graphene nanocomposites.* small, 2010. **6**(2): p. 179-183.

88. He, H. and C. Gao, *General approach to individually dispersed, highly soluble, and conductive graphene nanosheets functionalized by nitrene chemistry.* Chemistry of Materials, 2010. **22**(17): p. 5054-5064.

89. Ji, X., et al., *Review of functionalization, structure and properties of graphene/polymer composite fibers.* Composites Part A: Applied Science and Manufacturing, 2016. **87**: p. 29-45.

90. Lim, C.T., *Nanofiber technology: current status and emerging developments.* Progress in Polymer Science, 2017. **70**: p. 1-17.

91. Zheng, W., X. Lu, and S.C. Wong, *Electrical and mechanical properties of expanded graphite‐reinforced high‐density polyethylene.* Journal of Applied Polymer Science, 2004. **91**(5): p. 2781-2788.

92. Hou, W., et al., *Preparation and physico-mechanical properties of amine-functionalized graphene/polyamide 6 nanocomposite fiber as a high performance material.* Rsc Advances, 2014. **4**(10): p. 4848-4855.

93. Huang, X., et al., *Graphene-based composites.* Chemical Society Reviews, 2012. **41**(2): p. 666-686.

94. Ye, L., et al., *Synthesis and characterization of expandable graphite–poly (methyl methacrylate) composite particles and their application to flame retardation of rigid polyurethane foams.* Polymer Degradation and Stability, 2009. **94**(6): p. 971-979.

95. Hassan, M.A., et al., *Fabrication of nanofiber meltblown membranes and their filtration properties.* Journal of membrane science, 2013. **427**: p. 336-344.

96. Martin, C.R., *Membrane-based synthesis of nanomaterials.* Chemistry of Materials, 1996. **8**(8): p. 1739-1746.

97. Nakata, K., et al., *Poly (ethylene terephthalate) Nanofibers Made by Sea‐Island‐Type Conjugated Melt Spinning and Laser‐Heated Flow Drawing.* Macromolecular rapid communications, 2007. **28**(6): p. 792-795.

98. Garg, K. and G.L. Bowlin, *Electrospinning jets and nanofibrous structures.* Biomicrofluidics, 2011. **5**(1): p. 013403.

99. Khoshaman, A.H., *Application of electrospun thin films for supra-molecule based gas sensing*, in *Master of Applied Sciences Thesis*,. 2011, Simon Fraser University

100. Chinnappan, A., et al., *An overview of electrospun nanofibers and their application in energy storage, sensors and wearable/flexible electronics.* Journal of Materials Chemistry C, 2017. **5**(48): p. 12657-12673.

101. Reneker, D.H. and I. Chun, *Nanometre diameter fibres of polymer, produced by electrospinning.* Nanotechnology, 1996. **7**(3): p. 216.

102. Doshi, J. and D.H. Reneker, *Electrospinning process and applications of electrospun fibers.* Journal of electrostatics, 1995. **35**(2-3): p. 151-160.

103. Feng, L., N. Xie, and J. Zhong, *Carbon nanofibers and their composites: a review of synthesizing, properties and applications.* Materials, 2014. **7**(5): p. 3919-3945.

104. Nyangasi, L., et al., *Processing parameters for electrospinning poly (methyl methacrylate)(PMMA)/titanium isopropoxide composite in a pump-free setup.* AAS Open Research, 2018. **1**.

105. Mohammad Khanlou, H., et al., *Electrospinning of polymethyl methacrylate nanofibers: optimization of processing parameters using the Taguchi design of experiments.* Textile Research Journal, 2015. **85**(4): p. 356-368.

106. Koysuren, O. and H.N. Koysuren, *Characterization of poly (methyl methacrylate) nanofiber mats by electrospinning process.* Journal of Macromolecular Science, Part A, 2016. **53**(11): p. 691-698.

107. Kim, B., et al., *Poly (acrylic acid) nanofibers by electrospinning.* Materials letters, 2005. **59**(7): p. 829-832.

108. Zeng, J., et al., *Poly-L-lactide nanofibers by electrospinning–influence of solution viscosity and electrical conductivity on fiber diameter and fiber morphology.* e-Polymers, 2003. **3**(1).

109. Zhao, Z., et al., *Preparation and properties of electrospun poly (vinylidene fluoride) membranes.* Journal of applied polymer science, 2005. **97**(2): p. 466-474.

110. Zhang, C., et al., *Study on morphology of electrospun poly (vinyl alcohol) mats.* European polymer journal, 2005. **41**(3): p. 423-432.

111. Mit‐uppatham, C., M. Nithitanakul, and P. Supaphol, *Ultrafine electrospun polyamide‐6 fibers: effect of solution conditions on morphology and average fiber diameter.* Macromolecular Chemistry and Physics, 2004. **205**(17): p. 2327-2338.

112. Hohman, M.M., et al., *Electrospinning and electrically forced jets. I. Stability theory.* Physics of fluids, 2001. **13**(8): p. 2201-2220.

113. Jiang, H., et al., *Optimization and characterization of dextran membranes prepared by electrospinning.* Biomacromolecules, 2004. **5**(2): p. 326-333.

114. Chen, V.J. and P.X. Ma, *Nano-fibrous poly (L-lactic acid) scaffolds with interconnected spherical macropores.* Biomaterials, 2004. **25**(11): p. 2065-2073.

115. Demir, M.M., et al., *Electrospinning of polyurethane fibers.* Polymer, 2002. **43**(11): p. 3303-3309.

116. Sill, T.J. and H.A. von Recum, *Electrospinning: applications in drug delivery and tissue engineering.* Biomaterials, 2008. **29**(13): p. 1989-2006.

117. Casper, C.L., et al., *Controlling surface morphology of electrospun polystyrene fibers: effect of humidity and molecular weight in the electrospinning process.* Macromolecules, 2004. **37**(2): p. 573-578.

118. Li, D. and Y. Xia, *Electrospinning of nanofibers: reinventing the wheel?* Advanced materials, 2004. **16**(14): p. 1151-1170.

119. Golmohammadi, H., et al., *Nanocellulose in sensing and biosensing.* Chemistry of Materials, 2017. **29**(13): p. 5426-5446.

120. Klemm, D., et al., *Cellulose: fascinating biopolymer and sustainable raw material.* Angewandte chemie international edition, 2005. **44**(22): p. 3358-3393.

121. Lin, N. and A. Dufresne, *Nanocellulose in biomedicine: Current status and future prospect.* European Polymer Journal, 2014. **59**: p. 302-325.

122. Nery, E.W. and L.T. Kubota, *Sensing approaches on paper-based devices: a review.* Analytical and bioanalytical chemistry, 2013. **405**(24): p. 7573-7595.

123. Moon, R.J., et al., *Cellulose nanomaterials review: structure, properties and nanocomposites.* Chemical Society Reviews, 2011. **40**(7): p. 3941-3994.

124. Wei, H., et al., *Environmental science and engineering applications of nanocellulose-based nanocomposites.* Environmental Science: Nano, 2014. **1**(4): p. 302-316.

125. Fontana, J., et al., *Acetobacter cellulose pellicle as a temporary skin substitute.* Applied biochemistry and biotechnology, 1990. **24**(1): p. 253-264.

126. Svensson, A., et al., *Bacterial cellulose as a potential scaffold for tissue engineering of cartilage.* Biomaterials, 2005. **26**(4): p. 419-431.

127. Bodin, A., et al., *Influence of cultivation conditions on mechanical and morphological properties of bacterial cellulose tubes.* Biotechnology and bioengineering, 2007. **97**(2): p. 425-434.

128. Eichhorn, S., et al., *Current international research into cellulosic fibres and composites.* Journal of materials Science, 2001. **36**(9): p. 2107-2131.

129. Wu, J., et al., *Silver nanoparticle/bacterial cellulose gel membranes for antibacterial wound dressing: investigation in vitro and in vivo.* Biomedical materials, 2014. **9**(3): p. 035005.

130. Gutierrez, J., et al., *Conductive properties of TiO2/bacterial cellulose hybrid fibres.* Journal of colloid and interface science, 2012. **377**(1): p. 88-93.

131. Yang, J., et al., *In situ deposition of platinum nanoparticles on bacterial cellulose membranes and evaluation of PEM fuel cell performance.* Electrochimica Acta, 2009. **54**(26): p. 6300-6305.

132. Varaprasad, K., et al., *Nano zinc oxide–sodium alginate antibacterial cellulose fibres.* Carbohydrate polymers, 2016. **135**: p. 349-355.

133. Kiziltas, E.E., et al., *Electrically conductive nano graphite-filled bacterial cellulose composites.* Carbohydrate polymers, 2016. **136**: p. 1144-1151.

134. Müller, D., et al., *Chemical in situ polymerization of polypyrrole on bacterial cellulose nanofibers.* Synthetic Metals, 2011. **161**(1-2): p. 106-111.

135. Shi, Z., et al., *In situ nano-assembly of bacterial cellulose–polyaniline composites.* Rsc Advances, 2012. **2**(3): p. 1040-1046.

136. Yue, L., et al., *Preparation of a carboxymethylated bacterial cellulose/polyaniline composite gel membrane and its characterization.* Rsc Advances, 2016. **6**(73): p. 68599-68605.

137. Núñez-Carmona, E., et al., *BC-MOS: The novel bacterial cellulose based MOS gas sensors.* Materials Letters, 2019. **237**: p. 69-71.

138. Park, S., C. Park, and H. Yoon, *Chemo-electrical gas sensors based on conducting polymer hybrids.* Polymers, 2017. **9**(5): p. 155.

139. Stenger-Smith, J.D., *Intrinsically electrically conducting polymers. Synthesis, characterization, and their applications.* Progress in Polymer Science, 1998. **23**(1): p. 57-79.

140. Tran, H.D., et al., *The oxidation of aniline to produce "polyaniline": a process yielding many different nanoscale structures.* Journal of Materials Chemistry, 2011. **21**(11): p. 3534-3550.

141. Abu-Thabit, N.Y., *Chemical oxidative polymerization of polyaniline: A practical approach for preparation of smart conductive textiles.* Journal of Chemical Education, 2016. **93**(9): p. 1606-1611.

142. Wang, B., J. Tang, and F. Wang, *Electrochemical polymerization of aniline.* Synthetic Metals, 1987. **18**(1-3): p. 323-328.

143. Hangarter, C.M., et al., *Hybridized conducting polymer chemiresistive nano-sensors.* Nano Today, 2013. **8**(1): p. 39-55.

144. Park, S., et al., *Conducting polymer-based nanohybrid transducers: A potential route to high sensitivity and selectivity sensors.* Sensors, 2014. **14**(2): p. 3604-3630.

145. Gao, Y., et al., *Polyaniline nanotubes prepared using fiber mats membrane as the template and their gas-response behavior.* The Journal of Physical Chemistry C, 2008. **112**(22): p. 8215-8222.

146. Zhang, Y., et al., *Electrospun polyaniline fibers as highly sensitive room temperature chemiresistive sensors for ammonia and nitrogen dioxide gases.* Advanced Functional Materials, 2014. **24**(25): p. 4005-4014.

147. Ji, S., Y. Li, and M. Yang, *Gas sensing properties of a composite composed of electrospun poly (methyl methacrylate) nanofibers and in situ polymerized polyaniline.* Sensors and Actuators B: Chemical, 2008. **133**(2): p. 644-649.

148. Bishop-Haynes, A. and P. Gouma, *Electrospun polyaniline composites for NO2 detection.* Materials and manufacturing processes, 2007. **22**(6): p. 764-767.

149. Dixit, V., S. Misra, and B. Sharma, *Carbon monoxide sensitivity of vacuum deposited polyaniline semiconducting thin films.* Sensors and Actuators B: Chemical, 2005. **104**(1): p. 90-93.

150. Li, Y., et al., *Composites of Fe2O3 nanosheets with polyaniline: Preparation, gas sensing properties and sensing mechanism.* Sensors and Actuators B: Chemical, 2017. **245**: p. 34-43.

151. Huang, X., et al., *Reduced graphene oxide–polyaniline hybrid: preparation, characterization and its applications for ammonia gas sensing.* Journal of Materials Chemistry, 2012. **22**(42): p. 22488-22495.

152. Liu, C., K. Hayashi, and K. Toko, *Au nanoparticles decorated polyaniline nanofiber sensor for detecting volatile sulfur compounds in expired breath.* Sensors and Actuators B: Chemical, 2012. **161**(1): p. 504-509.

153. Li, Y., et al., *Fabrication of polyaniline/titanium dioxide composite nanofibers for gas sensing application.* Materials Chemistry and Physics, 2011. **129**(1-2): p. 477-482.

154. Zhang, T., et al., *Electrochemically functionalized single‐walled carbon nanotube gas sensor*. Electroanalysis: An International Journal Devoted to Fundamental and Practical Aspects of Electroanalysis, 2006. **18**(12): p. 1153-1158.

155. Wanna, Y., et al. *Development of nanofibers composite Polyaniine/CNT fabricated by Electro spinning Technique for CO Gas Sensor*. in *SENSORS, 2006 IEEE*. 2006. IEEE.

APPENDIX A BOOK CHAPTER: FUNCTIONALIZED GRAPHENE/POLYMER NANOFIBER COMPOSITES AND THEIR FUNCTIONAL APPLICATIONS

Hanan Abdali[1,2], and Abdellah Ajji[1]

[1]CREPEC, Department of Chemical Engineering, Polytechnique Montréal, P.O. Box 6079, Station Centre-Ville, Montreal, QC H3C 3A7, Canada

[2]Ministry of Education, P.O. Box 225085, Riyadh 11153, Saudi Arabia

hanan.abdali@polymtl.ca

Tel. 1-514-340-4711 ext. 4781,

abdellah.ajji@polymtl.ca

Tel. 1-514-340-4711 ext. 3703, fax. 1-514-340-4159

(This work was published in Springerlink on October 18th, 2019)

Abstract

Nanofiber composites materials produced by electrospinning may have a very high specific surface area owing to their small diameters, and nanofiber mats can be highly porous with excellent pore interconnection. However, applications using nanofiber composites also require specific properties such as good electrical conductivity, are flame retardant, anti-static and anti-radiative as well. Over the past few decades, the carbon nanomaterial, graphene has been researched widely owing to its intrinsic properties such as large surface area, excellent thermal, electrical, and optical properties in addition to superior chemical and mechanical characteristics needed in specific applications. The chemical functionalization of graphene nanosheet improved its dispersibility in common organic solvents, which is important when developing novel graphene-based nanocomposites. Moreover, graphene may also be functionalized in order to modify its intrinsic characteristics, for example, its electronic properties can be modified to control the conductivity and band gap in nano-electronic devices. Functionalized graphene-based polymer nanofiber composites exhibit a variety of improved, or even new properties such as adsorption performance, anti-bacterial, hydrophobicity and conductivity valued across a wide range of applications in sensors, biosensors, transparent conductive films, high-frequency circuits, toxic material removal, capacitors, spintronic devices,

fuel cells, touch screens, flexible electronics and batteries. This book chapter summarizes the recent progress in functionalized graphene-based polymer nanofibers composites, with an emphasis on their applications.

Keywords: Functionalized graphene, Nanofibers, Nanocomposite, Electrospinning, Electrospun polymers, Applications.

A.1 Introduction

Materials with nanoscale dimensions, occur in zero, one, two or three dimensions. One dimensional (1D) fibrous nanostructures can be fabricated by various methods such as self-assembly [1, 2], template synthesis [3], phase separation [4], and electrospinning [5-7] (see Figure A-1). Among these methods, electrospinning is a cost-effective, user-friendly and extremely versatile technique, allowing the manufacture of macro/nanofibers in a continuous process and at longer-length scales. There are three phases in the electrospinning process: jet initiation, jet elongation with or without branching, and/or splitting, followed by the solidification of the jet solution into nanofibers [6-8]. Hitherto, more than 100 polymers and numerous inorganic materials haven been electrospun into nanofibers. The flexible nature of the electrospinning process allows for easily modifying hierarchical features such as; nonwoven, aligned or patterned fibers, nanoribbons, nanorods, random three-dimensional structures, sub-micron spring and convoluted fibers with controlled diameters when preparing complex nanostructures by changing the solution and processing parameters [6-9] and/or set-up geometries [10-12]. Moreover, electrospinning nanofibers of mixed polymers and carbon particles enhance the mechanical properties of the resultant nanofiber mats and presents structural advantages as it constitutes a nonwoven mesh characterized by large surface area, unit mass and interconnected porosity [13-15]. In particular, graphene is composed of single layers of aromatic carbons and is considered a suitable prospect in the production of functionalized electrospun fibers owing to its remarkable physical and chemical properties, including high fracture strength (~125 GPa), high Young's modulus (~1100 thermal conductivity (~5000 W/mK), rapid mobility of charge carriers (~200,000 cm_2/Vs GPa), excellent electrical (~106 S/cm) and large specific surface area (theoretically calculated value, 2630 m^2/g) [13-16]. The unique features of graphene surfaces enable easy suspension and mixture with the polymers in powder form for electrospinning solutions. These composites are suitable for producing architectured, nanofiber

materials for tissue engineering, drug release, sensors, biosensors, batteries and supercapacitors, dye-sensitised solar cells, fuel cells, catalysts, filters, memory devices, and in food applications [14-17]. However, graphene's low dispersibility in common organic and inorganic solutions necessary in such applications, poses a significant challenge that needs to be addressed. In particular, a proficient dispersion of graphene in common solvents is key toward forming homogeneous nanocomposites. Therefore, modifying graphene by tailoring its solubility remains crucial in a multitude of commercial applications. Covalent and noncovalent methods are usually used to modify the surface of graphene. Often, these modification techniques were commonly performed to enhance the dispersion of graphene in a polymer matrix to attain the greatest impact on the fiber materials and correlate the introduced graphene properties to enrich the performance of fibers [13, 18].

In this chapter, the preparation of nanofibers with functionalized graphene and the corresponding effects on the nanofiber composites, while exploring recent research in relevant applications is also discussed. The strategies to functionalize graphene surfaces are also briefly highlighted.

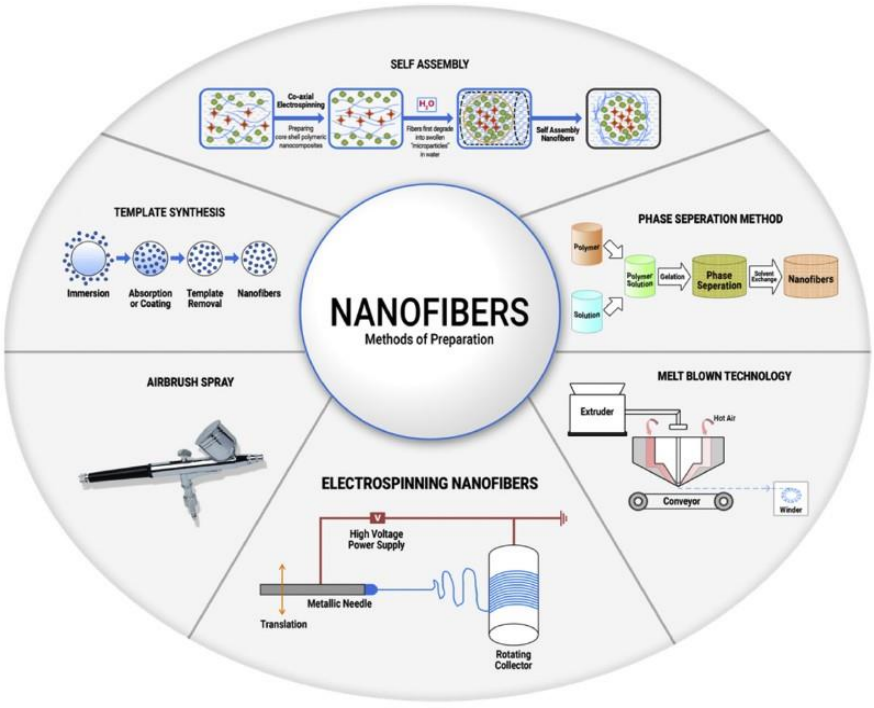

Figure A-1 Various methods for preparation of nanofibers. With permission from [6]. Copyright©2017 Elsevier B.V. All rights reserved.

A.2 Chemical Functionalization of Graphene

Graphene, consisting of a single-layer sp^2-hybridized carbon atom network, is the most intensively studied material in nanotechnology owing to its properties and features. This single-atom-thick sheet of carbon atoms arranged in a honeycomb pattern is the world's thinnest, strongest, and stiffest material, also boasts excellent conductivity, thus graphene is being studied in almost all fields of science, medicine and engineering [19-21]. Despite its potential in various applications, it is also noteworthy that graphene itself possesses a zero band gap including inertness to reaction, that weakens its competitiveness in the field of semiconductors and sensors. Consequently, this remains a significant reason for research in this material paying special attention to its functionalization, reaction with organic and inorganic substances, as well as the chemical modifications of graphene surfaces including the intensity of covalent and noncovalent interactions with graphene [18-23].

As, the most current and lucrative method for large scale production of graphene-based materials is centered around the oxidation of graphite to graphene oxide (GO) and then reducing the GO to graphene by either thermal, chemical, or electrochemical methods [18, 20] (see Figure A-2). The GO surfaces are highly oxygenated, and carboxyl, diol, ketone, epoxide, and hydroxyl functional groups can alter the van der Waals interactions significantly and enable greater solubility in water and some organic solvents. Yet, owing to the presence of the oxygen functional groups in its structure, GO is electronically insulating and thermally unstable as it undergoes pyrolysis at elevated temperatures [19-21]. Therefore, reducing GO removes most but not all of the hydroxyl, carboxylic acid and epoxy functional groups [19-21].

Usually variations on the Staudenmaier [24] or Hummers [25] methods are used to obtain GO in which graphite is oxidized using strong oxidants such as $KMnO_4$, $KClO_3$, and $NaNO_2$ in the presence of nitric acid or its mixture with sulfuric acid [25]. Gao *et al.* [26] used a K_2FeO_4-based oxidation approach instead of $KMnO_4$ to obtained a single-layer GO at room temperature. Recently, using the Hummers method, Yu *et al.* [27] have obtained GO that is free of $NaNO_3$ by partly replacing $KMnO_4$ with K_2FeO_4 and controlling the amount of concentrated sulfuric acid. The chemical reduction of GO by using reducing agents for example; hydrazine [28, 29], sodium borohydride followed by hydrazine [30], hydroquinone [31], dimethylhydrazine [32], and ascorbic acid [33], etc., provides a streamlined technique for the production of graphene, nevertheless, the

cost and hazardous nature of these chemicals utilized during the reduction may limit its application [34]. Conversely, thermally reducing graphene oxide (RGO) is produced by heating dry GO under inert gas and high temperature [34-37], for instance, heating GO in an inert environment at 1000 °C for 30 s results in the reduction and exfoliation of GO generating RGO layers. As such, the thermal reduction produces chemically modified graphene layers without the need for dispersion in a solvent compared with other chemical reduction methods [34]. Accordingly, to obtain functionalized graphene, the chemical modification of graphene oxide followed by reduction was used. It has been demonstrated that both modification techniques are excellent for the preparation of processable graphene, preventing agglomeration and enabling the formation of stable dispersions and was utilized for the fabrication of polymer nanofiber composites in numerous applications [13, 18, 37].

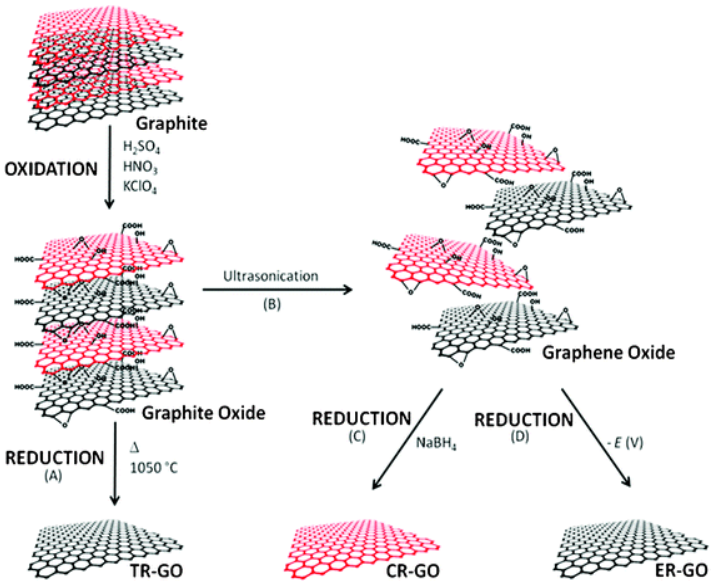

Figure A-2 Schematic of the production of CMGs from graphite. Graphite was first oxidized to graphite oxide. Thermal reduction and exfoliation (A) of graphite oxide led directly to TR-GO. Graphite oxide was ultrasonicated (B) to generate graphene oxide, following which the chemical reduction (C) of graphene oxide yielded CR-GO. Alternatively, graphene oxide was electrochemically reduced (D) to afford ER-GO. With permission from [20].

A.2.1 Non-covalent Functionalization

The non-covalent functionalization, which relies on the van der Waals force, electrostatic interaction or π-π stacking [38, 39], is easier to undertake without changing the chemical structure of the graphene sheets. Consequently, this is the most effective way of customizing the electronic/optical property and solubility of the nanosheets [40], because, without affecting the electronic network, it offers the possibility of attaching functional groups to graphene [41, 42]. Noncovalent modification is attained by the interaction with polymers, such as poly(3-hexylthiophene) (P3HT), porphyrin, pyren, cellulose derivatives, polyaniline (PANi), poly(sodium 4-styrenesulfonate) (PSS), and porphyrins or biomolecules such as deoxyribonucleic acid (DNA) and peptides, as well as adsorption of surfactants or small aromatic molecules.

The first example of non-covalent functionalization of graphene nanosheets using PSS was published by Stankovich *et al.* [39]. It was found that exfoliation and in situ reduction of GO in the presence of PSS could form non-covalently-functionalized graphitic nanosheets that were extremely stable and dispersible in water (1 mg/ml). It is possible to achieve a stable dispersion of reduced graphene in different organic solvents with amine-terminated polymers through non-covalent functionalization [43]. In this technique, the reduction of GO is first undertaken in an aqueous medium using an ammonia-hydrazine mixture, this is then followed by washing and the removal of aggregated graphene sheets. The amine-terminated polymer is dissolved in organic solvents for non-covalent functionalization of RGO. Next, the aqueous dispersion of RGO is added to the organic polymer solution. The phial including phase-separated organic and aqueous phases then undergoes a 5 h sonication for the non-covalent functionalization of graphene. Here, the functionalized graphene can easily be dispersed in a variety of solvents and is shown to exhibit electrical conductivity [43]. Liu *et al.* [44] have successfully functionalized the graphene surfaces with a pyrene-terminated positive charged polymer, poly(2-N,N‘-(dimethyl amino ethyl acrylate)) (PDMAEA), and a negatively charged polymer, polyacrylic acid (PAA) via π-π stacking. The functionalized graphene polymer composites indicated that the phase transfer behavior between aqueous and organic media occurs at different pH values. The remarkable electrical conductivity of graphene with an extremely high surface area (theoretically 2630 m^2/g), is combined with the graphene nanosheets is used to construct nanodevices specifically when developing high capacity cathode materials for Li-ion batteries [44]. In other research, gold nanoparticles were deposited on

DNA-functionalized graphene presented by Liu *et al.* [45] (see Figure A-3), where thiolated DNA oligonucleotides were prepared to adsorb on to the GO nanosheets resulting in the DNA-coated GO being reduced by hydrazine to DNA-RGO. Gold nanoparticles were then mixed in aqueous solutions of DNA-RGO and DNA-GO composites respectively. These gold-arrayed DNA-functionalized graphene nanosheets have considerable potential not only in the field of bio detection but also for use in optoelectronics, battery materials, magnetism catalysis, field effect devices [45]. In a subsequent study, Choi *et al.* [46] have described the functionalization of graphene through self-assembly of a hydrophobic backbone of Nafion (see Figure A-4). The result indicated that the graphene nanosheets were easily dispersible and presented with biosensing properties of good conductivity and electrochemical characteristics for organophosphates.

Functionalization can be used to maximally retain the natural structure of graphene, yet, it must be also be noted that interactions between functionalities and graphene surfaces remain weak and therefore unsuitable applications requiring strong interactions.

A.2.2 Covalent Functionalization

Reaction between the functional groups of the molecules and the oxygenated groups on GO or reduced GO (RGO) surfaces is the foundation for covalent functionalization of graphene [47, 48], for example, carboxyls on the edges with epoxides and hydroxyls on their basal planes [49]. The abundant surface chemistry of GO/RGO enables a myriad of possibilities during the covalent functionalization of graphene-based sheets when compared with non-covalent functionalization. Covalent techniques are employed to generate composites that have strong interactions between graphene and the modifier [49]. GO or RGO can be grafted onto polymeric chains that have reactive groups like hydroxyls and amines, such as, poly(ethylene glycol), polylysine, polyallylamine, and poly(vinyl alcohol). These materials are combined together and promise the desired properties of their individual parts, for example; the polymeric part offers dispersibility in certain solvents, mechanical strengthening, and many morphological properties, while the graphene nanosheets exhibits characteristics such as chemical reactivity, electrical conductivity, and reinforcement of the mechanical properties. The poly-L-lysine (PLL) was covalently grafted to RGO through the reaction of epoxy groups on graphene oxides and amino groups on PLL in the presence of potassium hydroxide (KOH) [50] (see Figure A-5). PLL-functionalized graphene is

water-soluble and biocompatible, which makes it a novel material promising in biological applications. In an analogous approach, Salavagione *et al.* [47] successfully prepared the PVA covalently grafted onto GO nanosheets via ester bonds between the carboxylic groups of GO and the hydroxyl groups of PVA. These chemical bonds can be created either by direct formation or after the transformation of carboxylates to the more reactive acyl chlorides. It was shown that the PVA/RGO composite was generated after partial reduction by hydrazine [47]. Lee *et al.* [51] have also presented an easily obtained method for covalent attachment of polymer brushes to GO surface utilizing initiated atom transfer radical polymerization (ATRP). The hydroxyl groups formed on the surface of GO were initially functionalized with a common ATRP initiator (a-bromoisobutyryl bromide), and next polymers of styrene, butyl acrylate, or methyl methacrylate were grown directly through a surface-initiated polymerization (SIP).

Moreover, Lee *et al.* [51] presented two primary conclusions in their investigation of polystyrene (PS). First, it was suggested that by altering the ratio of initiator modified GO and monomer it was possible to adjust the polymer chain length. Second, it was discovered that the monomer loading changes the molecular weight of the grafted PS, this was produced by gel permeation chromatography (GPC) after detaching by saponification, and it was noted that the polydispersity was low. As such, the authors suggest that the polymerization proceeded in a controlled way. Furthermore, the PS-functionalized GO was shown to increase the solubility in N,N-dimethylformamide (DMF), toluene, chloroform, and dichloromethane significantly, further enhancing the processing capacity of PS-functionalized GO for applications in polymer-based composites [51]. It was found that heating a diazonium salt, resulted in an extremely reactive free radical, which attacks the sp^2 carbon atoms of graphene forming a covalent bond. This reaction has been applied by Niyogi *et al*. [52] the covalent attachment of nitrophenyls to graphene sheets introduces a band gap, which can be controlled, making the functionalized graphene potentially useful as semiconducting nanomaterials. Furthermore, the addition of an alternative free radical includes the reaction of benzoyl peroxide with graphene sheets [53]. In another study, Vadukumpully *et al.* [54] developed a basic yet flexible method for the covalent functionalization of graphene with alkylazides, where the alkyl chains incorporated various functional groups such as hydroxylundecanyl, dodecyl, hexyl and carboxy-undecanyl resulting in improved dispersibility that helped facilitate composite fabrication. This strategy provides a useful platform for the synthesis of functional graphene nanocomposites using gold nanoparticles (the carboxyl groups

can trap and immobilize the gold nanoparticles in a selective manner). Moreover, GO could be used as a support for enzyme immobilization in the preparation of biosensing devices. The immobilization of glucose oxidase (GOx) onto GO nanosheets was attained via amide bonding [55].

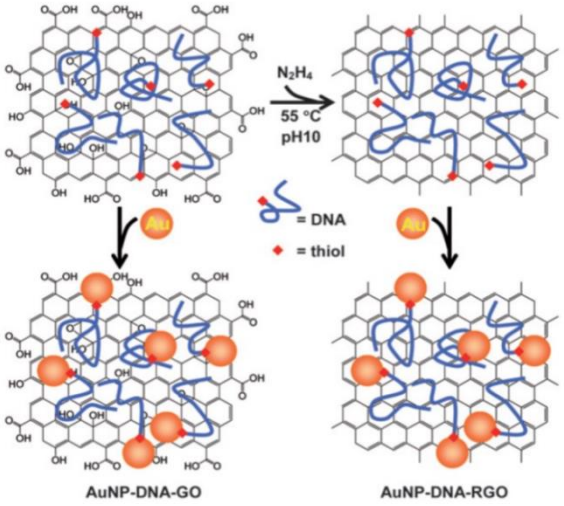

Figure A-3 DNA coating and aqueous dispersion of GO and RGO, which were then used as two-dimensional bio-nano-interfaces for homogeneous assembly of metal carbon heteronanostructures. With permission from [45]. Copyright @2010, Royal Society Chemistry.

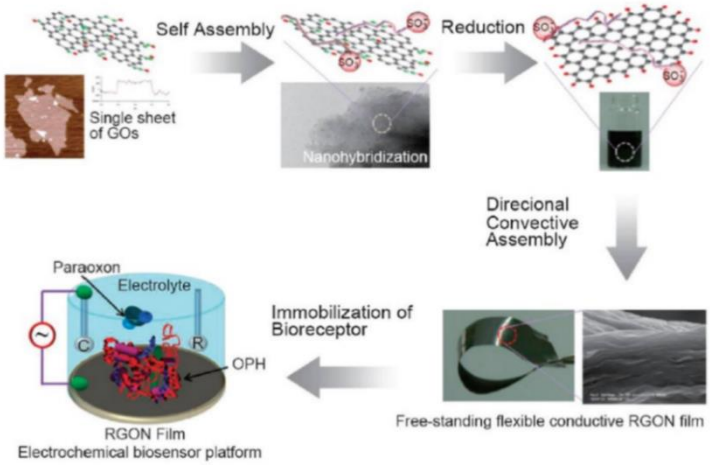

Figure A-4 Illustration of a procedure to design RGON hybrids and the RGON platform used as an electrochemical biosensor. With permission from [46]. Copyright @2010, American Chemical Society.

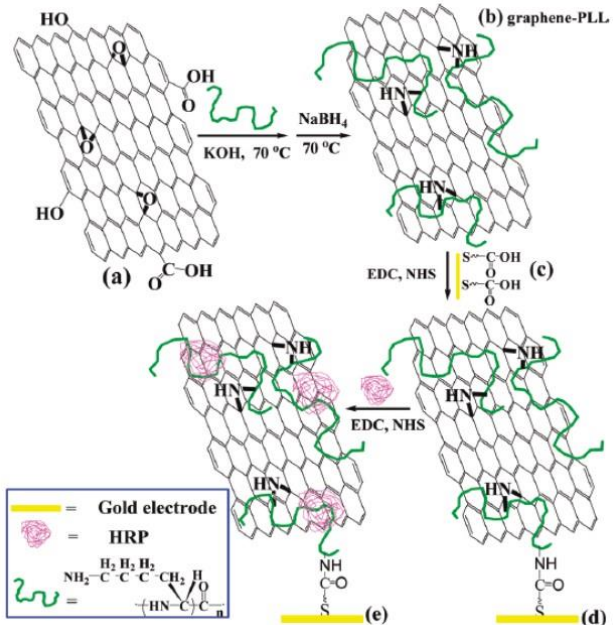

Figure A-5 Schematic diagram of graphene-PLL synthesis and assembly process of graphene-PLL and HRP at a gold electrode. With permission from [50]. Copyright @2009, American Chemical Society.

A.3 Preparation of Functionalized Graphene based Polymer Nanofiber Composites

Graphene's unique electronic, mechanical and thermal properties [14, 15] ensure its role as a promising filling agent for nanofibers composite applications [14]. Graphene has the ability to function as a nanofiller that can potentially enhance the characteristics of polymer-based nanofiber composites at a very low loading. However, several factors can control the characteristics and uses of graphene/polymer nanofiber composites such as the type of graphene utilized, its inherent properties, the manner of dispersion of graphene in the polymeric matrix, its interfacial interaction, the state of wrinkling in the graphene, and the structure of its network in the matrix [13, 56]. Therefore, the functionalization of graphene by covalent and noncovalent modifications promotes

the dispersion of graphene in various organic solvents, and this aqueous dispersibility is greatly beneficial for producing graphene sheets, films, fibers composites, etc. Hence, many studies have shown that the chemical modification of graphene alters the graphene microstructure, producing graphene with various functional groups, electrical conductivity, carbon to oxygen atomic ratio (C/O ratio), and solubility in solvents, etc. [13, 43, 57-59]. He and Gao reported a simple and efficient strategy for grafting different functional groups or polymeric chains onto graphene nanosheets using nitrene cycloaddition. This method produced single- layered, functionalized graphene with a variety of functional groups (e.g., hydroxyl, carboxyl, amino, bromine, long alkyl chain, etc.) or polymers (e.g., poly(ethylene glycol), polystyrene) to covalently attach onto the graphene, in a one-step reaction (see Figure A-6) [58]. The modified graphene nanosheets produced are electrically conductive, and have good dispersibility and processability in organic solvents, which advocates their properties as potential contenders not only in future modifications but also in various applications of polymer nanofiber composites. Similarly, Moayeri and Ajji [60] have successfully fabricated a conductive polymer nanofiber composite of 1-pyrenebutanoic acid, succinimidyl ester functionalized graphene/polyaniline/poly(ethylene oxide) (G-PBASE/PANi/PEO). This unique nanostructured composite of PANi/PEO/G-PBASE with small loading of G-PBASE (5 wt.% relative to PANi) exhibited increased improvement in the electrical conductivity and good thermal stability in comparison to PANi/PEO nanofibers owing to the homogenous distribution of the functionalized graphene in the polymeric matrix [60]. Moreover, Rafiee *et al.* [61] have reported that the modified graphene nanosheets are notably effective at intensifying the energy, fracture toughness, fatigue resistance, strength, and stiffness of epoxy polymers at significantly lower loading fractions upon comparison with other additives such as nanoclay, carbon nanotubes (CNTs), and nanoparticles additives. At 0.125% weight of functionalized graphene sheets was remarked to have improved the fracture toughness ≈ 65% and the fracture energy by ≈115% [61].

The composite fibers are prepared using the two main processes of mixing and spinning. The modified graphene sheets can be dispersed and incorporated in the mixing process in three different ways: melt blending, in situ polymerization, or solution mixing (see Figure A-7). Moreover, other research has coated functionalized graphene onto the fiber surface after spinning [13, 56].

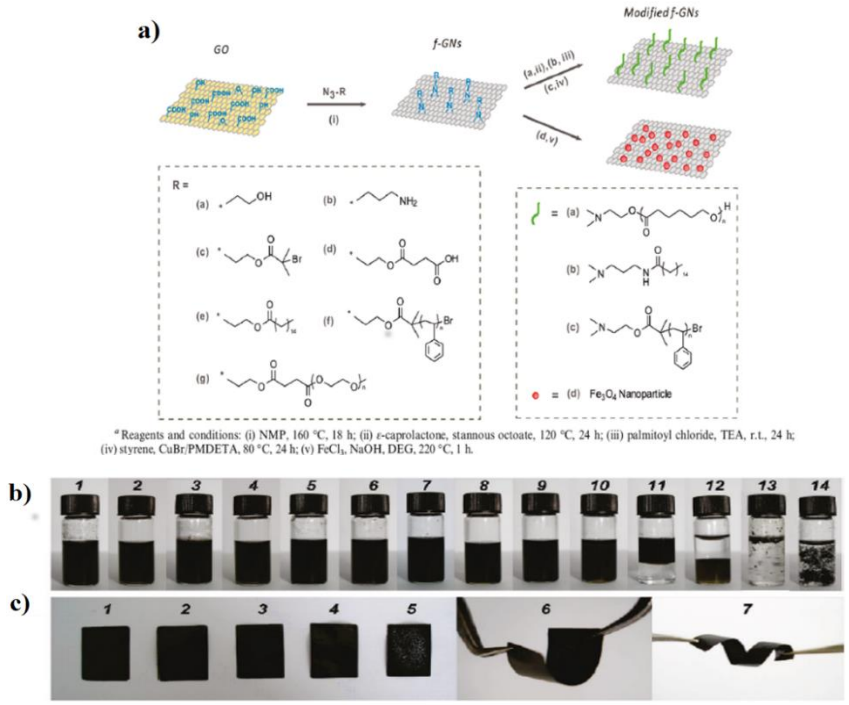

Figure A-6 (a) General Strategy for the Preparation of Functionalized Graphene Nanosheets **(**f-GNs**)** by Nitrene Chemistry and the Further Chemical Modifications[a]. (b) Photographs of f-GNs dispersion in solvents after sonication: G-N-OH in water (1) and DMF (2), G-N-COOH in water (3) and DMF (4), G-N-PEG1900 in water (5) and DMF (6), G-N-C_{16} in chloroform (7) and toluene (8), G-N-PS in chloroform (9) and toluene (10), G-N-NH_2 in water/ chloroform (11), G-N-NH_2-g-C_{16} in water/chloroform (12), GO in chloroform (13), and reduced GO in DMF (14). (c) Photographs of 10 wt%f-GNs/ polyurethane composites: (1) G-N-OH, (2) G-N-COOH, (3) G-N-NH_2, (4) G-N-Br, (5) reduced GO, (6) G-N-OH, and (7) G-N-COOH. With permission from [58]. Copyright©2010, American Chemical Society.

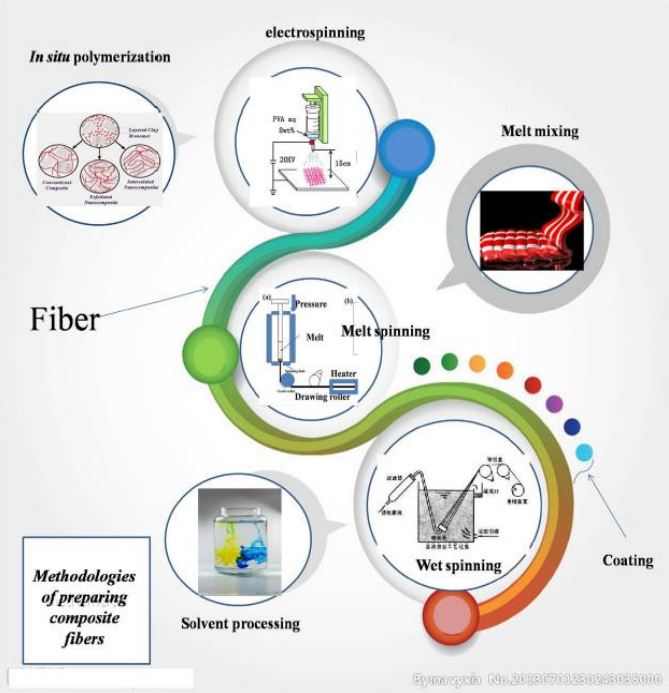

Figure A-7 Schematic illustration of the methods for preparation of fiber composite materials. With permission from [13]. Copyright©2016, Elsevier Ltd. All rights reserved.

Melt blending uses a twin-screw extruder to produce fibers via melt-spinning under specific conditions after the direct addition of the functionalized graphene into the melted polymer in a Brabender mixing chamber, for example; screw speed, temperature and time. This method is commercially preferred to the two others due to its versatility, environmentally friendly nature, economic suitability in mass production [14]. However, in melt processing, dispersing the graphene in the polymer matrix remains a considerable challenge as it does in both in situ polymerization and solvent processing [62]. Chatterjee *et al.* [63] have studied the influence of graphene nanosheets on the structure and mechanical properties of polyamide 12 (PA12) fibers. The PA12 and graphene composite fibers that were fabricated via melt processing were found to help in breaking the agglomerates present in the PA12 and graphene composite fibers during the melt compounding in the micro extruder due to the shear high forces. Although the composite fibers exhibited improved elasticity, yield and tensile strength, the melt spinning process also revealed that there is a high risk of agglomeration [63].

***In situ* polymerization** provides strong interaction between the functionalized graphene and the polymeric matrix and enables an outstanding, homogeneous dispersion. Generally, functionalized graphene is mixed with prepolymers or monomers where heat or radiation is then used to initiate the polymerization process [64]. As functionalized graphene can be further functionalized by grafting polymer chains through atom transfer radical polymerization (ATRP) resulting in covalent bonding. Generally, for *in situ* polymerized nanocomposites, melt spinning which is conducted in a piston spinning machine and hot-roller drawing machine, is commonly used. The research on *in situ* polymerization of nanocomposites studies not only the effect of the nanofillers on the morphology of the polymer matrix and its final characteristics but also includes the polymerization reaction. Hou *et al.* [65] successfully prepared nanocomposites of functionalized graphene grafted by polyamide 6 (PA6) by *in situ* polycondensation of caprolactam (CPL), using the melt spinning and drawing process to produce the nanocomposite fibers. It was established that due to the good distribution of functionalized graphene (0.1 wt%) in the PA6 matrix, the tensile strength of the fibers increased dramatically. Yet, when the functionalized graphene is 0.5 wt% or higher, the graphene agglomerates in the nanocomposite fibers resulting in a reduced tensile strength (see Figure A-8) [65].

Solution processing is widely used to produce polymer nanofiber composites with uniform graphene dispersion effectively. In this method, functionalized graphene is mixed with a polymer solution after first dispersing in a solvent by using techniques such as magnetic agitation, mechanical mixing, or high-energy sonication [56]. Next, by vaporizing the solvent a a composite is produced. Many types of polymer nanofibers have been reinforced by graphene, for instance poly(vinyl alchohol) (PVA) [66-68], polystyrene (PS) [32], Polyethylene (PE) [69], polyvinyl fluoride (PVF) [70], polymethyl methacrylate (PMMA) [57, 60,71], nylon 6 [72], and chitosan [73-75], etc. However, the specific surface area of the 2D fillers could decrease considerably due to the re-stacking, aggregation and folding techniques of the graphene-based nanosheets. As such, surface functionalization of graphene-based fillers before solution mixing is undertaken to overcome this problem.

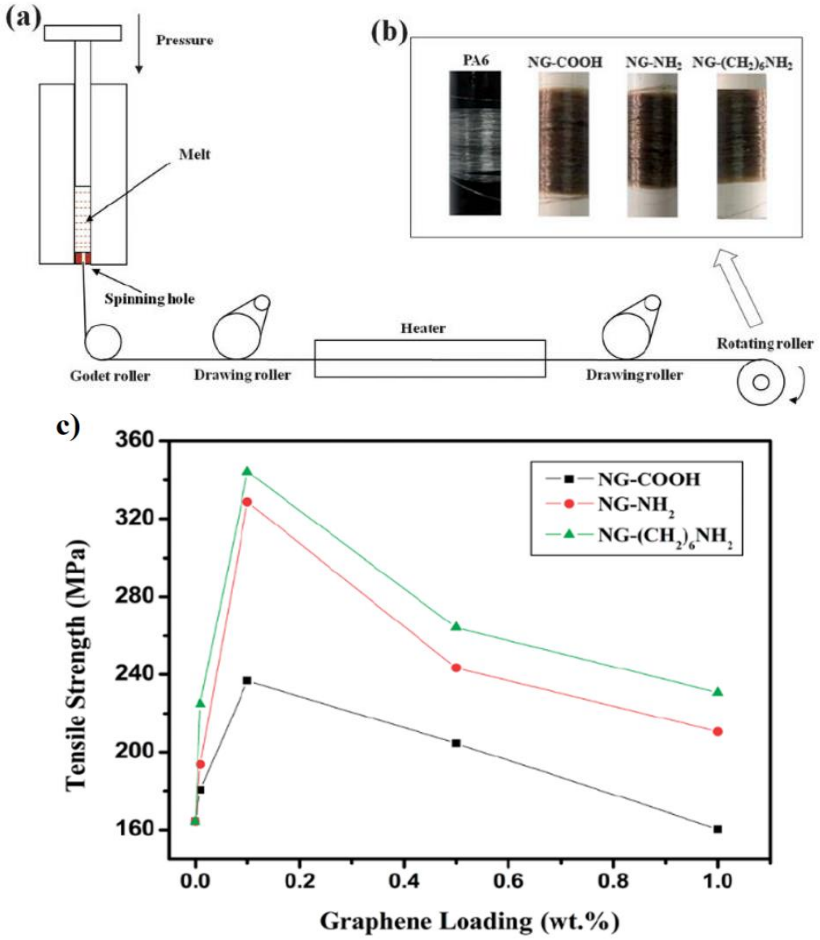

Figure A-8 (a) Melt spinning apparatus used for preparing nanocomposite fibers. (b) Photographs of neat PA6 and 0.1 NG fibers. (c) Tensile strength of NG nanocomposite fibers with different loadings of graphene. With permission from [65]. Copyright©2014, The Royal Society of Chemistry.

Usually, there are three types of spinning techniques to fabricate modified graphene-based polymer nanofiber composites: melt-spinning, wet-spinning and electrospinning. We mainly discuss below the electrospinning technique to fabricate functionalized graphene-based polymer nanofiber composites.

A.4 Principle of Electrospinning

Recently, interest in nanoscale properties and technologies have increased the use of electrospinning technology, owing to its efficient, relatively simple and cost-effective process for producing ultrafine nanofibers or fibrous structures of many polymers with a range of diameters from sub-microns to nanometers [7, 76, 77]. The nanofibers structures obtained using this process result in unique advantages for example, the flexible porosity of the electrospun structure, high surface to volume ration and the ability to spin into different shapes and sizes. These characteristics exemplified by the nanofibers qualifies their candidacy for applications in filtrations, tissue engineering scaffolds, wound healing, energy storage, sensors, catalyst and enzyme carriers [7]. Technically, electrospinning is a method that employs a strong electric field to draw liquid polymer into fine filaments [12, 78, 79]. The simple electrospinning apparatus made up of a micro-syringe with a needle of small diameter, a nozzle, a high voltage supplier, and an electrode collector, (see Figure A-9) The collector can be fashioned into any shape according to the specified product requirements for example; a flat plate, rotating drum, or patterned collector. In most cases, the collector is simply grounded. When a high voltage solution is charged, and the repulsive force within the charged solution is larger than its surface tension and a jet erupts from the tip of the spinneret. This electrified jet then moves counterclockwise towards the electrode, forming a long and thin thread. Subsequently, as the liquid jet is continuously elongated and the solvent is evaporated, randomly oriented, nonwoven mat nanofibers with small diameters (micro to nanometers) are deposited on the collector [12, 78, 79].

Electrospinning deals with several conditions that can influence the transformation of polymer solutions into nanofibers through its process. These include; i) the intrinsic properties of the solution, such as viscosity, elasticity, conductivity, and surface tension. ii) the processing parameters for example; the electric potential at the needle, the feeding rate for the polymer solution, and the distance between the syringe and the collector screen [78, 79], iii) ambient conditions such as temperature, humidity and air velocity in the electrospinning chamber [78, 79]. Proper control of these parameters can be tailored to fiber morphologies and diameters of the electrospun fibers. However, researchers usually elect to keep ambient conditions constant in their research.

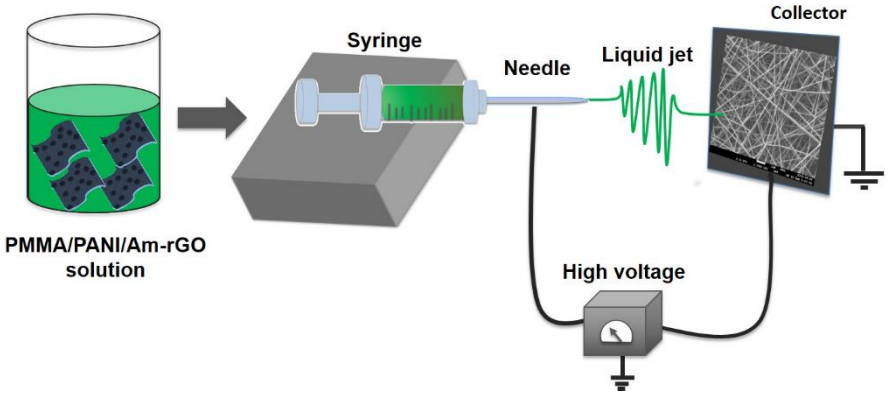

Figure A-9 Schematic illustration of the electrospinning setup. With permission from [57]. Copyright© 2017, Polymers

Zong *et al.* [80] studied the effects of varying the processing parameters and solution properties on the structure and morphology of the electrospun fibers. It was discovered that the effect of solution conductivity on the fiber diameter are inversely related, for example, the lower solution conductivity resulted in a larger fiber diameter. Zong *et al.* reported that the addition of different salts to the polymer spinning solutions, resulted in a higher charge density on the surface of the ejected jet exhibiting more electric charges carried by the jet [80]. The results also demonstrated that salts with smaller ionic radii formed fibers with smaller diameters and vice versa. Mainly, it indicated that greater charge densities led to greater mobility of ions with smaller radii which generated increased elongation forces exerted on the polymer jet creating a smaller fiber (see Figure A-10) [80]. Moreover, they reported that different fiber morphologies can also be obtained by altering the solution feed rate at a given electric field. They concluded that the droplet suspension at the end of the spinneret is larger with a higher feed rate so the jet of the solution could carry the fluid away at faster velocity. Therefore, this can lead to large beaded fibers as the polymer is not completely dry upon reaching the collector (see Figure A-11) [80]. Additionally, it was demonstrated that higher concentrations and the corresponding higher charge densities of the solution produced uniform fibers with no bead-like textures.

In another study, Ramazani and Karimi investigated the presence of varying amounts of graphene oxide (GO) with different oxidation levels on the morphological appearance, fiber diameter, and structure of poly(ε-caprolactone) (PCL) nanofibers fabricated by the electrospinning method

[81]. It was observed that parameters such as GO dispersibility, charge relaxation time, polarity and wettability all of which are used to measure the fiber diameter, improves with oxidation. The surface tension of PCL solution is unchangeable in the presence of GO with different loading and level of oxidation, resulting in diameter variations in the electrospun fibers. Moreover, they reported that the average fiber diameter decreases in the presence of GO with different loading, owing to the reduction of solution viscosity and increase in the conductivity [81]. Accordingly, researchers have also shown that after GO surfaces were functionalized with poly(ethylene glycol) (PEG), the poly(lactic acid) (PLA)/GO-g-PEG nanocomposite nanofibers exhibited a decrease in diameters when comparing with pure PLA [82]. The plasticizing effect of the grafted PEG molecules on the surface of GO attributed to the decrease in viscosity for PLA/GO-g-PEG electrospinning suspensions, indicating strong interfacial adhesion between GO-g-PEG and PLA and was responsible for the reduction in the average diameter from PLA to PLA/GO-g-PEG [82]. Das *et al.* [83] indicated that the addition of noncovalently functionalized graphene to the PVA fibers increased the effective fluid charge density, therefore it was necessary to change the flow rate from 0.3 to 15 mL/h. It was shown that a reduction in bead formation resulted with an increase in applied voltage from 10 to 15 kV. An increase in voltage is necessary as the conductivity of the graphene increases the surface charge of the fiber, perpetuating natural bead formation. Furthermore, a higher voltage is required as the elasticity of the jet is increased due to the addition of graphene when compared with the baseline experiment. Increasing the voltage amplifies the repulsive electrostatic force and favors the formation of fibers with smaller diameters [83].

Overall, it was considered that preparing an optimized suspension of functionalized graphene in the solution improved the applicability of the resulting nanofibers. Therefore, many experiments are still needed to produce electrospun functionalized graphene/polymer nanofibers for morphological modification, necessary to meet specific requirements for applications.

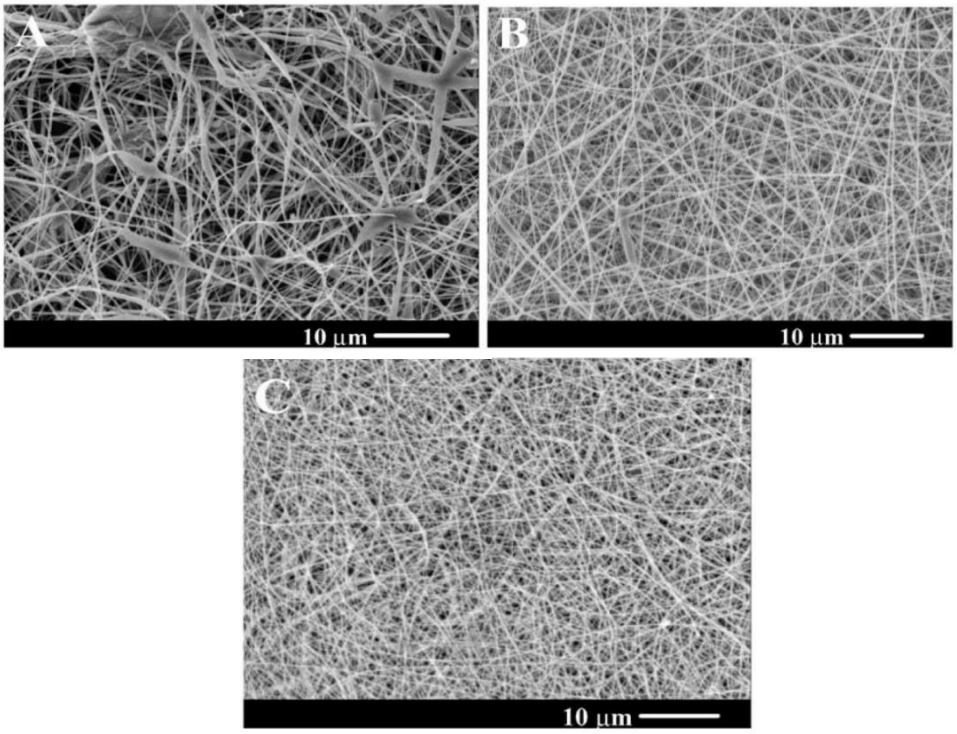

Figure A-10 SEM images of PDLA membranes fabricated by electrospinning of a 30 wt% solution at voltage of 20 kV, feeding rate of 20 ml/min and with 1 wt% of (A) KH_2PO_4; (B) NaH_2PO_4 and (C) NaCl. With permission from [80].

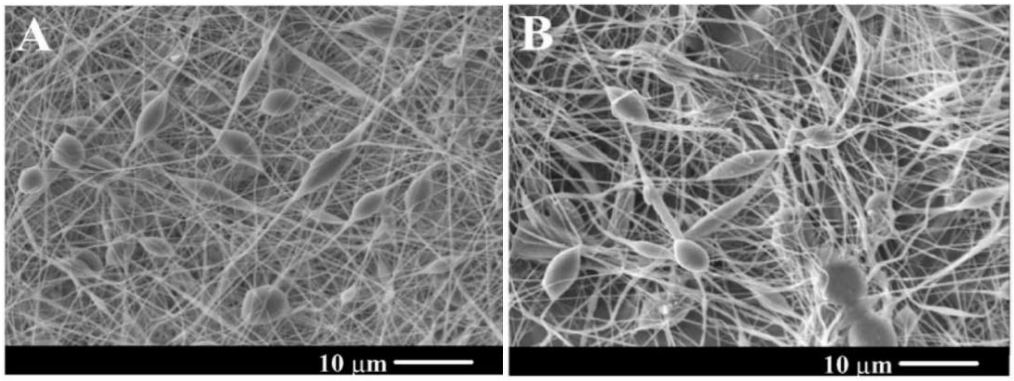

Figure A-11 SEM images showing the variation of beaded fibers at different feeding rates: (A) 20 ml/min; (B) 75 ml/min. The applied voltage was 20 kV and concentration was 25 wt% with 1 wt% KH_2PO_4. With permission from [80].

A.5 Properties of Functionalized Graphene based Polymer Nanofibers Composite

Surface functionalization of graphene showed significant improvement in dispersibility/processability in solvents, as well as in polymer matrices [49, 56, 84]. These in turn, exhibit excellent enhancement in mechanical, electrical, optical and thermal properties of host polymers at very low loading levels. Numerous studies on the properties of functionalized graphene based polymer nanofiber composites have been reported [14, 56, 84]. For instance, Young's modulus, tensile strength, thermal stability, conductivity, and hydrophobicity. Hsiao *et al.* [85] advocated a basic yet effective method to decorate silver nanoparticles (AgNPs) and reduced graphene oxide (RGO) on the surface of polyurethane (PU) fibers to fabricate AgNP@RGO/PU fiber composites. This technique provided an effective way of producing lightweight, highly flexible electronic products that have excellent electrical properties. The surface of PU fiber mat was decorated with GO by dipping the PU fiber mats into the GO aqueous solution (GO/PU) and then the GO/PU fiber composite was reduced in hydriodic acid (HI). After that, the AgNPs were deposited on RGO/PU to fabricate AgNP@RGO/PU fiber composites (see Figure A-12a) [85]. They found that the decorated AgNP@RGO restricts the PU fiber mat from thermal decomposition resulting in a notable improvement in thermal stability of composite (see Figure A-12b). Moreover, the AgNP@RGO/PU fiber composites showed superior improvement in electrical properties (<10 U/sq), because the deposited m-AgNPs effectively facilitate the charge transfer ability of RGO [85].

Chee *et al*. [86] reported a new, non-covalent surface functionalization technique of GO via a UV-sensitive initiator embedded via π-π interactions on the graphene nanosheets, followed by the polymerization of hydrophobic polymeric chains along the surface of the graphene. Thereafter, the functionalized GO/Polyacrylonitrile (PAN) nanofibers were produced by the electrospinning technique and then the nanofibers underwent thermal treatments that converted the polymeric chains into a CNF structure as shown in Figure A-13a. The results revealed that functionalized GO was readily dispersed in different solvents, and in the hydrophobic polymeric solution. Furthermore, the functionalized, GO-reinforced, CNF exhibited an extraordinary ability by showing a specific capacitance of 140.10 F/g, approximately three times higher than that of neat

CNF, coupled with a high stability capacitance retention of 96.2% after 1000 times of charge/discharge cycles at 1 A/g (see Figure A-13b and c) [86].

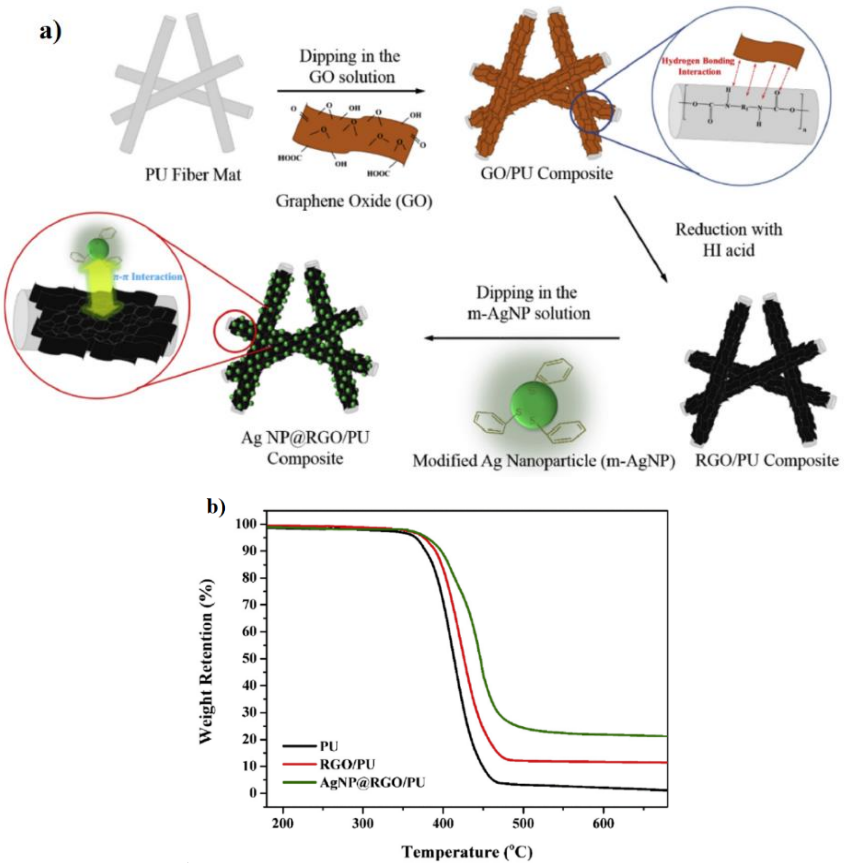

Figure A-12 (a) Schematic representation of the procedure for preparing the AgNP@RGO/WPU composites; (b) The TGA curves for PU, RGO/PU and AgNP@RGO/PU. With permission from [85]. Copyright © 2015, Elsevier Ltd. All rights reserved.

In a further study, Moayeri and Ajji [87, 44] have produced core-shell structured CNF embedded with non-covalently modified graphene by single-nozzle electrospinning setup utilizing phase separated solutions of PAN and polyvinylpyrrolidone (PVP) in DMF solution, followed by the calcination and carbonization processes. Electrochemical assessment of CNF/graphene (G) nanofibers revealed a maximum specific capacitance of 265 F/g after addition of 10 wt. % graphene nanosheets. Furthermore, based on the Brunauer-Emmett-Teller (BET) results, the specific surface

area and pore volume were increased, directly proportional from CNF/G0 to CNF/G10 samples and then showed a decreased amount for CNF/G15 sample, which further supports the outcomes generated from the electrochemical tests. The larger pore volume and surface area can be attributed for affecting ion diffusion with high speed at high loading current density and allows for more efficient utilization of specific surface area [87]. Scaffaro *et al*. [88] investigated the reaction of GO-g-PEG on the mechanical and wettability characteristics of polycaprolactone (PCL) electrospun scaffolds. The contact water angle measurements of PCL/GO-g-PEG composite nanofiber showed better performance with lower water contact angles. The Young moduli of the composite nanofiber mats were significantly improved by adding a low concentration of GO-g-PEG, owing to the grafted PEG chains, which enhanced the filler dispersion. Additionally, the primary proliferation rate results were studied, to examine the capability of MC3T3-E1 osteoblastic cells to proliferate on the surfaces of PCL and PCL/GO-g-PEG nanocomposite scaffolds. The preliminary biological assay indicated that PCL/GO-g-PEG improved the ability of cell growth and attachment, owing to the increased hydrophilicity and the resulting degree of cell affinity for the substrate, when compared with the electrospun PCL scaffold [88]. Other research showed significant improvements in thermal, mechanical, and wettability properties of PLA electrospun nanofibers upon addition of GO-g-PEG was published [82]. These studies found that the PLA/GO-g-PEG demonstrated better wettability with lower water contact angles than PLA and PLA/GO as well as the TGA results, that exhibited the GO-g-PEG had a prominent influence than GO in enhancing the thermal stability of PLA electrospun nanofibers. Besides, a significant enhancement of tensile strength of PLA/GO-g-PEG composite nanofibers was reported [82]. In addition, the initial tests of cytocompatibility with Swiss mouse NIH 3T3 cells of PLA, PLA/GO, and PLA/GO-g-PEG nanofibers, were examined. The results indicated the PLA/GO and PLA/GO-g-PEG composite nanofiber scaffolds were non-toxic to NIH 3T3 cells and able to support cell attachment and growth [82, 88].

It can be generally regarded that these electrospun functionalized graphene/polymer nanofibers are capable of supporting various applications in different fields such as sensors, biosensors, electrodes, energy storage or conversion (supercapacitors, fuel cells, solar cells, and batteries), conductive wires, and biomedical materials.

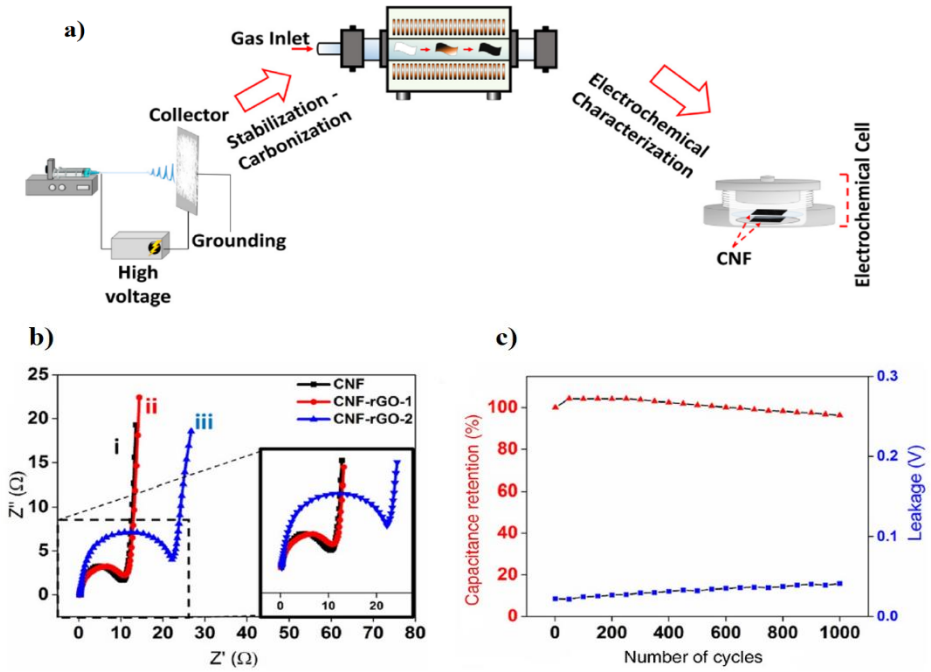

Figure A-13 (a) Schematic diagram illustrates the synthesis of functionalized CNF/fGO for electrochemical measurement in a two-electrode configuration; (b) Nyquist plots of pure (i) CNF, (ii) CNF/fGO-1, and (iii) CNF/fGO-2. The inset magnified the high frequency region of the spectra; (c) capacitance retention and voltage drop of CNF/fGO-2 as the function of continuous charge/discharge cycles. With permission from [86].

A.6 Application of Functionalized Graphene-based Polymer Nanofiber Composites

Various applications can be designed using functionalized graphene/ polymer composite nanofibers. For instance, the produced polymer/GO-g-PEG composite nanofiber scaffolds have good cytocompatibility, noncytotoxicity characteristics, superior mechanical, thermal, and electrical properties, which have broad applications in tissue engineering [82, 88]. It was observed that a small amount of GO-g-PEG did not prevent the proliferation and viability of cells, which indicates the high cell affinity of GO-g-PEG. It is expected that the cells will spread on the

composite scaffolds and in some cases improve cell growth by having similar rate of cell proliferation to that of tissue culture plates [82, 88].

Advances in sensor technology are in constant demand because of their wide use in various industries, environmental monitoring, space exploration, biomedicine, and pharmaceutics. Therefore, improving Gas/chemical sensors and biosensors with faster response times, higher accuracies, increased sensitivities and other properties is an important area of research.

The desired features of sensors include small sizes, quicker response times, small sample volumes, selectivity or specificity, stability, longevity, and low costs. Therefore, owing to the unique electronic structures, remarkable mechanical, optical, electrochemical, thermal, magnetic properties, and ease of functionalization with antibodies and other bioreceptors, functionalized graphene has been extensively used in ultrasensitive sensors and biosensor applications [89, 90]. Abideen *et al*. [91] examined the gas sensing characteristics of gold (Au) or palladium (Pd) functionalized RGO-loaded ZnO nanofibers. The gas sensing tests were carried out at varying temperatures and in the presence of varying concentrations of specific gases (see Figure A-14). It was found that the Au-functionalized RGO-loaded ZnO nanofibers showed higher sensitivity toward 1 ppm of carbon monoxide (CO) gas in the air, while the Pd-functionalized sensors exhibited good performance for 1 ppm of benzene (C_6H_6) gas. The high sensing properties of the Au or Pd functionalized RGO loaded ZnO nanofibers was attributed to the RGO/ZnO heterointerfaces, the catalytic effect of Au and Pd nanoparticles, and the large surface area of nanofibers [91]. Li *et al.* [92] developed a sensor of N-doped, graphene quantum dots decorated with N-doped, carbon nanofibers (NGQDs@NCNFs) composites. The electrochemical sensors for the detection of nitrites found in sausage, pickle, lake water and tap water showed wide linear ranges (5-300 µM, R^2= 0.999; 400-3000 µM, R^2= 0.997), low detection limit (3 µM), superior reproducibility and selectivity, and good testing recoveries. In another work, Ali *et al.* [93] reported the fabrication of a microfluidic electrochemical sensor for the detection and immunodiagnosis of breast cancer biomarkers using a new three-dimensional (3D) immunoelectrodes produced by hierarchical graphene foam (GF) functionalized with electrospun carbon-doped titanium dioxide nanofibers ($nTiO_2$) and anti-ErbB2 molecules (see Figure A-15). Blending GF with functional $nTiO_2$ yields high charge transfer resistance, high surface area, and absorption to the sensor's surface by the analyte, resulting in sensor with remarkable detection of breast cancer biomarkers.

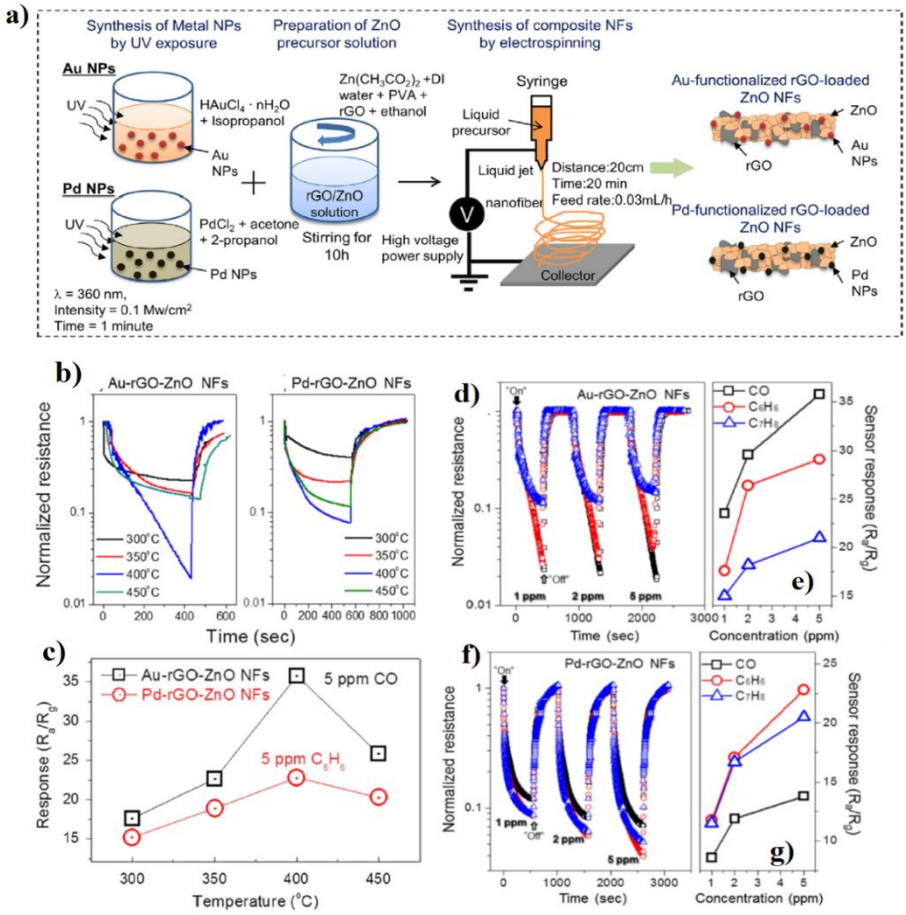

Figure A-14 (a) Schematic illustration of the synthesis procedure for Au- or Pd-functionalized rGO-loaded ZnO NF; (b) Dynamic normalized resistances of the Au-functionalized rGO-loadedZnO NFs sensor to 5 ppm CO gas at different temperatures and dynamic normalized resistances of the Pd-functionalized rGO-loaded ZnO NFs sensor to 5 ppm C_6H_6 gas at different temperatures; (c) Temperature dependence of the response of the Au-functionalized rGO-loaded ZnO NF sensor and the Pd-functionalized rGO-loaded ZnO NFs sensor to CO and C_6H_6 gases; (d) Dynamic normalized resistances of the Au-functionalized rGO-loaded ZnO NFs sensor to different concentrations of CO, C_6H_6 and C_7H_8 gases; (e) Corresponding calibration curves; (f) Dynamic normalized resistances of the Pd-functionalized rGO-loaded ZnO NFs sensor to different concentrations of CO, C_6H_6 and C_7H_8 gases; (g) Corresponding calibration curves. With permission from [91].

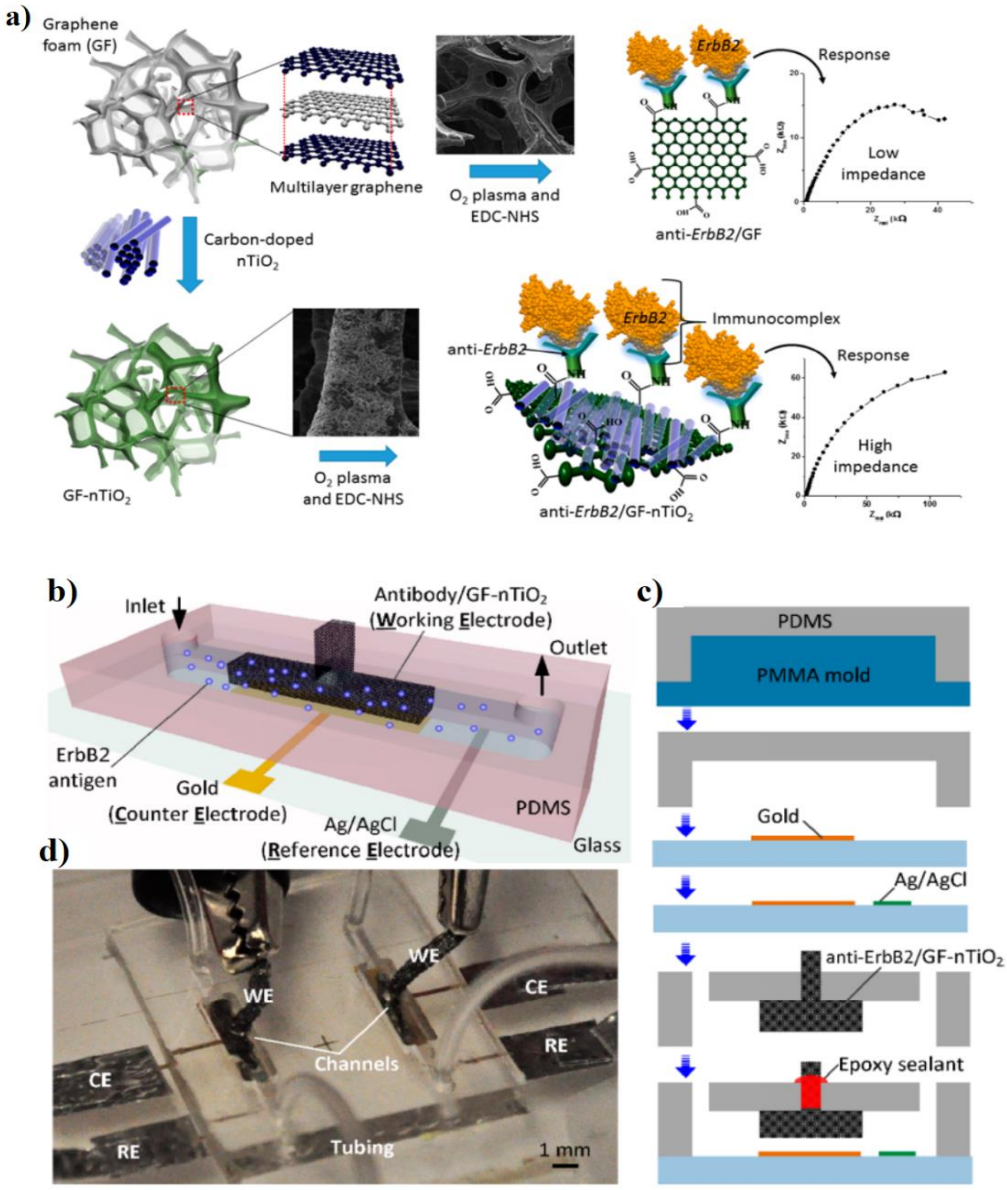

Figure A-15 (a) Functionalization of anti-ErbB2 molecules on the surface of GF and GF −$nTiO_2$ electrodes using EDC-NHS chemistry followed by oxygen plasma treatment; (b) Schematic of the microfluidic immunosensor with 3D porous GF electrode modified with carbon-doped TiO_2 nanofibers for the detection of breast cancer biomarkers; (c) Schematic representation of the fabrication of the microfluidic sensor; (d) Photo of two microfluidic immunosensors. With permission from [93]. Copyright © 2016, American Chemical Society.

Moreover, functionalized graphene nanosheets are a promising material for flexible, transparent, conductive, thin films, and electronic devices, such as transistors [94], solar cells [95], and field emission displays [95], due to their remarkable, mechanical strength and flexibility. Huang *et al.* [97] presented a simple yet effective technique to synthesize large silver nanoparticles (AgNps)-graphene nanosheet (GNS) films onto a polyethylene terephthalate (PET), a flexible substrate, by decorating AgNps on GNS surface and enhancing self-assembly of AgNps-GNSs onto the surface of PU nanofibers. They found that the AgNp-GNS (5:1)/PU thin film revealed a considerable rising in transmittance after melting, resulting in a thin film with surface resistance of 150 Ω/sq and transmittance of 85% at 550 nm [97]. It has been also reported that the decoration of TiO_2 with metals such as Pd, Nickel (Ni) and Au with graphene, improve the catalytic and photocatalytic characteristics of TiO_2 [98-100]. The fabrication of Pd-functionalized graphene nanoparticles merged with TiO_2 composite nanofibers displayed good photocatalysis to methylene blue [101].

Graphene quantum dots (GQDs) have extraordinary electrical conductivity, good dispersion in various solvents, tunable photoluminescence, high specific surface area, and exhibit low toxicity and good biocompatibility, thus having contributed to energy storage devices applications [102]. For example, the electropolymerization of poly(3,4-ethylenedioxythiophene) (PEDOT) onto polyvinyl alcohol-graphene quantum dot-cobalt oxide (PVA-GQD-Co_3O_4), (PVA-GQD-Co_3O_4/PEDOT) nanofiber composite showed a specific capacitance of 361.97 F/g, low equivalent series resistance (ESR) and good stability with retention of 96% after 1000 cycles. The results also inducted a high specific energy and exceptional power ranging from 16.51 to 19.98 W/kg and 496.10 to 2396.99 W/kg, as the current density increased from 1.0 to 5.0 A/g [102]. In another example, GQD/PANi (GQDP) nanofiber exhibited an excellent specific capacitance value of ∼1044 F/g at a current density of 1 A/g as well as moderate cyclic stability with a retention of life time of 80.1% after 3000 cycles [103].

Contaminants such as dyes that contribute to water pollution crisis that has affected agriculture, industries and inevitably economic growth has generated interest in solving this problem. Consequently, the process of adsorption is a commonly used technique owing to its relative easy operation, good performance and cost effectiveness when compared with other approaches. Water-dispersible amine-functionalized graphene (G-NH_2) nanosheets, were blended directly into the PVA/ glutaraldehyde (GA) aqueous solution for crystal violet (CV) adsorption, deemed hazardous to cells and tissues of living organisms and could possibly be cancer-causing upon prolonged

exposure in concentrated amounts [68]. The study indicated that the G-NH_2 is a desirable reinforcing filler to promote higher adsorption sites for the PVA fibers, and by that means an greater adsorption of the CV dye from water in composite mats (removal efficiency of 80.85% compared to 66.24% for crosslinked PVA/GA mats) [68].

Additionally, several other studies have concentrated on the application in areas such as antimicrobial agents in food applications, dentistry, drug release, catalysts, recovery of metal ions, medical implants and enzyme carriers [72, 104-106]. Current research and focus on functionalized graphene/polymer nanofiber composites seem to indicate that their use in a variety of industries will be proliferate and long lasting.

A.7 Conclusions and Future Scope

The functionalization of graphene by covalent and noncovalent methods has been discussed briefly in this chapter. The electrospinning process to prepare modified, graphene based polymer nanofiber composites, their properties and applications were also discussed. It has been proven that these modification techniques are extremely successful when preparing processable graphene. However, it must be remarked that a suitable technique for mass producing functionalized graphene has not yet been discovered. In conclusion, it is important that future research in this field concentrate on realizing grand-scale production of functionalized graphene if science and technology in this area remain relevant when concerning environmental safety and security standards, health, and energy production. Numerous researchers have indicated that the functionalized graphene is a suitable and desirable choice as multifunctional nanofiller, which will encourage many industry developments and forge our steps into a new energy and material world. The use of electrospinning to develop functionalized graphene polymer nanofiber composites is an effective choice when obtaining high, specific surface area, fibers at a nanoscale level. Moreover, this method offers appreciable improvements in maximizing specific properties out of the electrospun composites. However, research towards commercializing functionalized graphene polymer electrospun nanofibers in applications as well as the refinement of electrospinning machines needs to be further investigated, so that their advantages can be fully realized to a greater extent. Finally, further investigation on fundamental issues such as the homogeneous distribution of individual functionalized graphene

nanofillers, their orientation, connectivity, and interface bonding with the polymer matrix are required.

Acknowledgments

The authors would like to thank the NSERC (Natural Science and Engineering Research Council of Canada), and ProAmpac, for their support. We are also sincerely grateful to the Saudi Ministry of Education for their financial support to Hanan Abdali.

A.8 Reference

1. Hassan, M.A., et al., *Fabrication of nanofiber meltblown membranes and their filtration properties.* Journal of membrane science, 2013. **427**: p. 336-344.
2. Ma, P.X. and R. Zhang, *Synthetic nano-scale fibrous extracellular matrix.* Journal of Biomedical Materials Research: An Official Journal of The Society for Biomaterials, The Japanese Society for Biomaterials, and The Australian Society for Biomaterials, 1999. **46**(1): p. 60-72.
3. Martin, C.R., *Membrane-based synthesis of nanomaterials.* Chemistry of Materials, 1996. **8**(8): p. 1739-1746.
4. Nakata, K., et al., *Poly (ethylene terephthalate) Nanofibers Made by Sea–Island-Type Conjugated Melt Spinning and Laser-Heated Flow Drawing.* Macromolecular rapid communications, 2007. **28**(6): p. 792-795.
5. Drosou, C., M. Krokida, and C.G. Biliaderis, *Composite pullulan-whey protein nanofibers made by electrospinning: Impact of process parameters on fiber morphology and physical properties.* Food Hydrocolloids, 2018. **77**: p. 726-735.
6. Kamble, P., et al., *Nanofiber based drug delivery systems for skin: A promising therapeutic approach.* Journal of Drug Delivery Science and Technology, 2017. **41**: p. 124-133.
7. Garg, K. and G.L. Bowlin, *Electrospinning jets and nanofibrous structures.* Biomicrofluidics, 2011. **5**(1): p. 013403.
8. Theron, S., E. Zussman, and A. Yarin, *Experimental investigation of the governing parameters in the electrospinning of polymer solutions.* Polymer, 2004. **45**(6): p. 2017-2030.
9. Bhardwaj, N. and S.C. Kundu, *Electrospinning: a fascinating fiber fabrication technique.* Biotechnology advances, 2010. **28**(3): p. 325-347.
10. Teo, W.E. and S. Ramakrishna, *A review on electrospinning design and nanofibre assemblies.* Nanotechnology, 2006. **17**(14): p. R89.
11. Cavaliere, S., et al., *Electrospinning: designed architectures for energy conversion and storage devices.* Energy & Environmental Science, 2011. **4**(12): p. 4761-4785.

12. Reneker, D.H. and I. Chun, *Nanometre diameter fibres of polymer, produced by electrospinning.* Nanotechnology, 1996. **7**(3): p. 216.

13. Ji, X., et al., *Review of functionalization, structure and properties of graphene/polymer composite fibers.* Composites Part A: Applied Science and Manufacturing, 2016. **87**: p. 29-45.

14. Kuilla, T., et al., *Recent advances in graphene based polymer composites.* Progress in polymer science, 2010. **35**(11): p. 1350-1375.

15. Geim, A.K. and K.S. Novoselov, *The rise of graphene*, in *Nanoscience and Technology: A Collection of Reviews from Nature Journals*. 2010, World Scientific. p. 11-19.

16. Service, R.F., *Materials science. Carbon sheets an atom thick give rise to graphene dreams.* Science (New York, NY), 2009. **324**(5929): p. 875.

17. Pan, Y., N.G. Sahoo, and L. Li, *The application of graphene oxide in drug delivery.* Expert opinion on drug delivery, 2012. **9**(11): p. 1365-1376.

18. Kuila, T., et al., *Chemical functionalization of graphene and its applications.* Progress in Materials Science, 2012. **57**(7): p. 1061-1105.

19. Gao, W., *The chemistry of graphene oxide*, in *Graphene oxide*. 2015, Springer. p. 61-95.

20. Wong, C.H.A. and M. Pumera, *Stripping voltammetry at chemically modified graphenes.* RSC Advances, 2012. **2**(14): p. 6068-6072.

21. Szabó, T., et al., *Evolution of surface functional groups in a series of progressively oxidized graphite oxides.* Chemistry of materials, 2006. **18**(11): p. 2740-2749.

22. Nethravathi, C., et al., *Graphite oxide-intercalated anionic clay and its decomposition to graphene− inorganic material nanocomposites.* Langmuir, 2008. **24**(15): p. 8240-8244.

23. Tung, V.C., et al., *High-throughput solution processing of large-scale graphene.* Nature nanotechnology, 2009. **4**(1): p. 25.

24. Staudenmaier, L., *Verfahren zur darstellung der graphitsäure.* Berichte der deutschen chemischen Gesellschaft, 1898. **31**(2): p. 1481-1487.

25. Hummers Jr, W.S. and R.E. Offeman, *Preparation of graphitic oxide.* Journal of the american chemical society, 1958. **80**(6): p. 1339-1339.

26. Gao, C.e.a., *A green method to fast prepare single-layer graphene oxide.* China patent, JAN 28 2015. **CN104310385A in Chinese**

27. Yu, H., et al., *High-efficient synthesis of graphene oxide based on improved hummers method.* Scientific reports, 2016. **6**: p. 36143.

28. Stankovich, S., et al., *Synthesis of graphene-based nanosheets via chemical reduction of exfoliated graphite oxide.* carbon, 2007. **45**(7): p. 1558-1565.

29. Wang, H., et al., *Solvothermal reduction of chemically exfoliated graphene sheets.* Journal of the American Chemical Society, 2009. **131**(29): p. 9910-9911.

30. Si, Y. and E.T. Samulski, *Synthesis of water soluble graphene.* Nano letters, 2008. **8**(6): p. 1679-1682.

31. Wang, G., et al., *Facile synthesis and characterization of graphene nanosheets.* The Journal of Physical Chemistry C, 2008. **112**(22): p. 8192-8195.

32. Stankovich, S., et al., *Graphene-based composite materials.* nature, 2006. **442**(7100): p. 282.

33. Zhang, J., et al., *Reduction of graphene oxide via L-ascorbic acid.* Chemical Communications, 2010. **46**(7): p. 1112-1114.

34. Kim, H., A.A. Abdala, and C.W. Macosko, *Graphene/polymer nanocomposites.* Macromolecules, 2010. **43**(16): p. 6515-6530.

35. Schniepp, H.C., et al., *Functionalized single graphene sheets derived from splitting graphite oxide.* The Journal of Physical Chemistry B, 2006. **110**(17): p. 8535-8539.

36. McAllister, M.J., et al., *Single sheet functionalized graphene by oxidation and thermal expansion of graphite.* Chemistry of materials, 2007. **19**(18): p. 4396-4404.

37. Steurer, P., et al., *Functionalized graphenes and thermoplastic nanocomposites based upon expanded graphite oxide.* Macromolecular rapid communications, 2009. **30**(4-5): p. 316-327.

38. Shen, B., et al., *Melt blending in situ enhances the interaction between polystyrene and graphene through π–π stacking.* ACS applied materials & interfaces, 2011. **3**(8): p. 3103-3109.

39. Stankovich, S., et al., *Stable aqueous dispersions of graphitic nanoplatelets via the reduction of exfoliated graphite oxide in the presence of poly (sodium 4-styrenesulfonate).* Journal of Materials Chemistry, 2006. **16**(2): p. 155-158.

40. Huang, X., et al., *Graphene-based composites.* Chemical Society Reviews, 2012. **41**(2): p. 666-686.

41. Karousis, N., N. Tagmatarchis, and D. Tasis, *Current progress on the chemical modification of carbon nanotubes.* Chemical Reviews, 2010. **110**(9): p. 5366-5397.

42. Tasis, D., et al., *Chemistry of carbon nanotubes.* Chemical reviews, 2006. **106**(3): p. 1105-1136.

43. Choi, E.-Y., et al., *Noncovalent functionalization of graphene with end-functional polymers.* Journal of Materials Chemistry, 2010. **20**(10): p. 1907-1912.

44. Liu, J., et al., *Synthesis, characterization, and multilayer assembly of pH sensitive graphene− polymer nanocomposites.* Langmuir, 2010. **26**(12): p. 10068-10075.

45. Liu, J., et al., *Noncovalent DNA decorations of graphene oxide and reduced graphene oxide toward water-soluble metal–carbon hybrid nanostructures via self-assembly.* Journal of Materials Chemistry, 2010. **20**(5): p. 900-906.

46. Choi, B.G., et al., *Solution chemistry of self-assembled graphene nanohybrids for high-performance flexible biosensors.* ACS nano, 2010. **4**(5): p. 2910-2918.

47. Salavagione, H.J., M.A. Gomez, and G. Martinez, *Polymeric modification of graphene through esterification of graphite oxide and poly (vinyl alcohol).* Macromolecules, 2009. **42**(17): p. 6331-6334.

48. Liu, Z., et al., *PEGylated nanographene oxide for delivery of water-insoluble cancer drugs.* Journal of the American Chemical Society, 2008. **130**(33): p. 10876-10877.

49. Park, S. and R.S. Ruoff, *Chemical methods for the production of graphenes.* Nature nanotechnology, 2009. **4**(4): p. 217.

50. Shan, C., et al., *Water-soluble graphene covalently functionalized by biocompatible poly-L-lysine.* Langmuir, 2009. **25**(20): p. 12030-12033.

51. Lee, S.H., et al., *Polymer brushes via controlled, surface-initiated atom transfer radical polymerization (ATRP) from graphene oxide.* Macromolecular Rapid Communications, 2010. **31**(3): p. 281-288.

52. Niyogi, S., et al., *Spectroscopy of covalently functionalized graphene.* Nano letters, 2010. **10**(10): p. 4061-4066.

53. Liu, H., et al., *Photochemical reactivity of graphene.* Journal of the American Chemical Society, 2009. **131**(47): p. 17099-17101.

54. Vadukumpully, S., et al., *Functionalization of surfactant wrapped graphene nanosheets with alkylazides for enhanced dispersibility.* Nanoscale, 2011. **3**(1): p. 303-308.

55. Liu, Y., et al., *Biocompatible graphene oxide-based glucose biosensors.* Langmuir, 2010. **26**(9): p. 6158-6160.

56. Du, J. and H.M. Cheng, *The fabrication, properties, and uses of graphene/polymer composites.* Macromolecular Chemistry and Physics, 2012. **213**(10-11): p. 1060-1077.

57. Abdali, H. and A. Ajji, *Preparation of Electrospun Nanocomposite Nanofibers of Polyaniline/Poly(methyl methacrylate) with Amino-Functionalized Graphene.* Polymers, 2017. **9**(9): p. 453.

58. He, H. and C. Gao, *General approach to individually dispersed, highly soluble, and conductive graphene nanosheets functionalized by nitrene chemistry.* Chemistry of Materials, 2010. **22**(17): p. 5054-5064.

59. Jia, L., J. Liu, and H. Wang, *Preparation of poly (diallyldimethylammonium chloride)-functionalized graphene and its applications for H2O2 and glucose sensing.* Electrochimica Acta, 2013. **111**: p. 411-418.

60. Moayeri, A. and A. Ajji, *Fabrication of polyaniline/poly (ethylene oxide)/non-covalently functionalized graphene nanofibers via electrospinning.* Synthetic Metals, 2015. **200**: p. 7-15.

61. Rafiee, M.A., et al., *Fracture and fatigue in graphene nanocomposites.* small, 2010. **6**(2): p. 179-183.

62. Dasari, A., Z.-Z. Yu, and Y.-W. Mai, *Electrically conductive and super-tough polyamide-based nanocomposites.* Polymer, 2009. **50**(16): p. 4112-4121.

63. Chatterjee, S., F. Nüesch, and B. Chu, *Crystalline and tensile properties of carbon nanotube and graphene reinforced polyamide 12 fibers.* Chemical Physics Letters, 2013. **557**: p. 92-96.

64. Zheng, W., X. Lu, and S.C. Wong, *Electrical and mechanical properties of expanded graphite-reinforced high-density polyethylene.* Journal of Applied Polymer Science, 2004. **91**(5): p. 2781-2788.

65. Hou, W., et al., *Preparation and physico-mechanical properties of amine-functionalized graphene/polyamide 6 nanocomposite fiber as a high performance material.* Rsc Advances, 2014. **4**(10): p. 4848-4855.

66. Jiang, L., et al., *Preparation and characterization of graphene/poly (vinyl alcohol) nanocomposites.* Journal of Applied Polymer Science, 2010. **118**(1): p. 275-279.

67. Liang, J., et al., *Molecular-level dispersion of graphene into poly (vinyl alcohol) and effective reinforcement of their nanocomposites.* Advanced Functional Materials, 2009. **19**(14): p. 2297-2302.

68. Chailek, N., et al., *Crosslinking assisted fabrication of ultrafine poly (vinyl alcohol)/functionalized graphene electrospun nanofibers for crystal violet adsorption.* Journal of Applied Polymer Science, 2018. **135**(22): p. 46318.

69. Chen, Y., et al., *Preparation, mechanical properties and biocompatibility of graphene oxide/ultrahigh molecular weight polyethylene composites.* European Polymer Journal, 2012. **48**(6): p. 1026-1033.

70. Yu, J., et al., *Permittivity, thermal conductivity and thermal stability of poly (vinylidene fluoride)/graphene nanocomposites.* IEEE Transactions on Dielectrics and Electrical Insulation, 2011. **18**(2): p. 478-484.

71. Zhang, H.-B., et al., *The effect of surface chemistry of graphene on rheological and electrical properties of polymethylmethacrylate composites.* Carbon, 2012. **50**(14): p. 5117-5125.

72. Leyva-Porras, C., et al., *EELS analysis of Nylon 6 nanofibers reinforced with nitroxide-functionalized graphene oxide.* Carbon, 2014. **70**: p. 164-172.

73. Cao, L., et al., *Fabrication of chitosan/graphene oxide polymer nanofiber and its biocompatibility for cartilage tissue engineering.* Materials Science and Engineering: C, 2017. **79**: p. 697-701.

74. Hong-Pei, L., et al., *Electrospinning gelatin/chitosan/hydroxyapatite/graphene oxide composite nanofibers with antibacterial properties.* JOURNAL OF INORGANIC MATERIALS, 2015. **30**(5): p. 516-522.

75. Ardeshirzadeh, B., et al., *Controlled release of doxorubicin from electrospun PEO/chitosan/graphene oxide nanocomposite nanofibrous scaffolds.* Materials Science and Engineering: C, 2015. **48**: p. 384-390.

76. Bao, Q., et al., *Graphene–polymer nanofiber membrane for ultrafast photonics.* Advanced functional materials, 2010. **20**(5): p. 782-791.

77. Ding, B., et al., *Gas sensors based on electrospun nanofibers.* Sensors, 2009. **9**(3): p. 1609-1624.

78. Doshi, J. and D.H. Reneker, *Electrospinning process and applications of electrospun fibers.* Journal of electrostatics, 1995. **35**(2-3): p. 151-160.

79. Feng, L., N. Xie, and J. Zhong, *Carbon nanofibers and their composites: a review of synthesizing, properties and applications.* Materials, 2014. **7**(5): p. 3919-3945.

80. Zong, X., et al., *Structure and process relationship of electrospun bioabsorbable nanofiber membranes.* Polymer, 2002. **43**(16): p. 4403-4412.

81. Ramazani, S. and M. Karimi, *Electrospinning of poly (ε-caprolactone) solutions containing graphene oxide: Effects of graphene oxide content and oxidation level.* Polymer Composites, 2016. **37**(1): p. 131-140.

82. Zhang, C., et al., *The surface grafting of graphene oxide with poly (ethylene glycol) as a reinforcement for poly (lactic acid) nanocomposite scaffolds for potential tissue engineering applications.* Journal of the mechanical behavior of biomedical materials, 2016. **53**: p. 403-413.

83. Das, S., et al., *Electrospinning of polymer nanofibers loaded with noncovalently functionalized graphene.* Journal of Applied Polymer Science, 2013. **128**(6): p. 4040-4046.

84. Georgakilas, V., et al., *Noncovalent functionalization of graphene and graphene oxide for energy materials, biosensing, catalytic, and biomedical applications.* Chemical reviews, 2016. **116**(9): p. 5464-5519.

85. Hsiao, S.-T., et al., *Preparation and characterization of silver nanoparticle-reduced graphene oxide decorated electrospun polyurethane fiber composites with an improved electrical property.* Composites Science and Technology, 2015. **118**: p. 171-177.

86. Chee, W., et al., *Functionalized graphene oxide-reinforced electrospun carbon nanofibers as ultrathin supercapacitor electrode.* Journal of energy chemistry, 2017. **26**(4): p. 790-798.

87. Moayeri, A. and A. Ajji, *High Capacitance Carbon Nanofibers from Poly (acrylonitrile) and Poly (vinylpyrrolidone)-Functionalized Graphene by Electrospinning.* Journal of Nanoscience and Nanotechnology, 2017. **17**(3): p. 1820-1829.

88. Scaffaro, R., et al., *Electrospun PCL/GO-g-PEG structures: Processing-morphology-properties relationships.* Composites Part A: Applied Science and Manufacturing, 2017. **92**: p. 97-107.

89. Latif, U. and F.L. Dickert, *Graphene hybrid materials in gas sensing applications.* Sensors, 2015. **15**(12): p. 30504-30524.

90. Llobet, E., *Gas sensors using carbon nanomaterials: A review.* Sensors and Actuators B: Chemical, 2013. **179**: p. 32-45.

91. Abideen, Z.U., et al., *Sensing behavior to ppm-level gases and synergistic sensing mechanism in metal-functionalized rGO-loaded ZnO nanofibers.* Sensors and Actuators B: Chemical, 2018. **255**: p. 1884-1896.

92. Li, L., et al., *Quantitative detection of nitrite with N-doped graphene quantum dots decorated N-doped carbon nanofibers composite-based electrochemical sensor.* Sensors and Actuators B: Chemical, 2017. **252**: p. 17-23.

93. Ali, M.A., et al., *Microfluidic immuno-biochip for detection of breast cancer biomarkers using hierarchical composite of porous graphene and titanium dioxide nanofibers.* ACS applied materials & interfaces, 2016. **8**(32): p. 20570-20582.

94. Sun, Q., et al., *Characteristics of a pentacene thin film transistor with periodic groove patterned poly (methylmethacrylate) dielectrics.* Applied Physics Letters, 2010. **96**(10): p. 41.

95. Ratcliff, E.L., P.A. Lee, and N.R. Armstrong, *Work function control of hole-selective polymer/ITO anode contacts: an electrochemical doping study.* Journal of Materials Chemistry, 2010. **20**(13): p. 2672-2679.

96. Yoon, B.-J., et al., *Fabrication of flexible carbon nanotube field emitter arrays by direct microwave irradiation on organic polymer substrate.* Journal of the American Chemical Society, 2005. **127**(23): p. 8234-8235.

97. Huang, Y.-L., et al., *Self-assembly of silver–graphene hybrid on electrospun polyurethane nanofibers as flexible transparent conductive thin films.* Carbon, 2012. **50**(10): p. 3473-3481.

98. Zhang, L., et al., *Electrospun titania nanofibers segregated by graphene oxide for improved visible light photocatalysis.* Applied Catalysis B: Environmental, 2017. **201**: p. 470-478.

99. Zhang, H., et al., *P25-Graphene Composite as a High Performance Photocatalyst.* ACS Nano, 2010. **4**(1): p. 380-386.

100. Wu, M.-C., et al., *Enhanced photocatalytic activity of TiO2 nanofibers and their flexible composite films: Decomposition of organic dyes and efficient H2 generation from ethanol-water mixtures.* Nano Research, 2011. **4**(4): p. 360-369.

101. Lee, H.-G., et al., *Facile synthesis of functionalized graphene-palladium nanoparticle incorporated multicomponent TiO2 composite nanofibers.* Materials Chemistry and Physics, 2015. **154**: p. 125-136.

102. Abidin, S.N.J.S.Z., et al., *Electropolymerization of poly (3, 4-ethylenedioxythiophene) onto polyvinyl alcohol-graphene quantum dot-cobalt oxide nanofiber composite for high-performance supercapacitor.* Electrochimica Acta, 2017.

103. Mondal, S., U. Rana, and S. Malik, *Graphene quantum dot-doped polyaniline nanofiber as high performance supercapacitor electrode materials.* Chemical Communications, 2015. **51**(62): p. 12365-12368.

104. De Faria, A.F., et al., *Antimicrobial electrospun biopolymer nanofiber mats functionalized with graphene oxide–silver nanocomposites.* ACS applied materials & interfaces, 2015. **7**(23): p. 12751-12759.

105. Ding, X., et al., *Spinning fabrication of graphene/polypyrrole composite fibers for all-solid-state, flexible fibriform supercapacitors.* Journal of Materials Chemistry A, 2014. **2**(31): p. 12355-12360.

106. Li, S., et al., *One-step synthesis of graphene/polypyrrole nanofiber composites as cathode material for a biocompatible zinc/polymer battery.* ACS applied materials & interfaces, 2014. **6**(19): p. 16679-16686